EXPLORING THE ROLE OF AMPK SIGNALING AND HPV ONCOPROTEINS IN REGULATION OF TUMOR METABOLISM AND GROWTH

Thesis submitted to

Jawaharlal Nehru University

For the award of the degree of

DOCTOR OF PHILOSOPHY

Submitted by

GOPINATH PRAKASAM

SCHOOL OF LIFE SCIENCES

JAWAHARLAL NEHRU UNIVERSITY

NEW DELHI-110067

INDIA

(March - 2017)

SCHOOL OF LIFE SCIENCES
JAWAHARLAL NEHRU UNIVERSITY
NEW DELHI-110067
INDIA

CERTIFICATE

This is to certify that this thesis entitled, **"Exploring the role of AMPK signaling and HPV oncoproteins in regulation of tumor metabolism and growth"** submitted for the award of the degree of Doctor of Philosophy (Ph.D.) embodies original research work carried out by **Mr. Gopinath Prakasam** under the guidance and supervision of **Prof. R.N.K. Bamezai** and co-supervision of **Dr. Ashu Bhan Tiku,** carried out in School of Life Sciences, Jawaharlal Nehru University, New Delhi, India. The work is original and has not been submitted in part or full for any degree or diploma in this or any other university or institute.

R. Bamezai

Prof. R.N.K. Bamezai
(Supervisor)

P. Gopinath

Mr. Gopinath Prakasam
(Candidate)

Dr. Ashu Bhan Tiku
(Co-supervisor)

29.3.17

Prof. S. K. Goswami
(Dean- School of Life Sciences)

Contents

Figures and Tables

Chapter-1

Chapter-3

Chapter-4

Dedicated to…

My Mom, Dad and Motherland

Words of Gratitude

I would like to begin this acknowledgment by thanking the God Almighty for providing me with my beloved parents, who always gave me unconditional love and stood by my side like a pillar of strength. I would say, they are the best thing that I would ever get in my lifetime, who sacrificed their own dreams for my comfort and wellbeing. They always respected my decision and applauded smallest of my achievements. Their only vision and lifetime accomplishment was my career success. Without their support, this accomplishment would not have been possible. I bow to the almighty and pray to Him to maintain this cherished soul bonding till eternity.

I should thank the God Almighty again in providing me with the right mentor, Prof. R.N.K. Bamezai, to enlighten me in all aspects. For who I am writing these words, deserves much more than this. I would like to express my sincere gratitude to him for creating opportunities and provide the right platform to pursue my doctoral degree; and in exploring the unmet horizons in science. Besides science, I was always fascinated by his morals, the attitude in confronting the real-life problems and an ever smiling face. Needless to mention, I thank him for bearing with my mistakes, giving me freedom, having faith in me, motivating and supporting me during difficult times. He has been a teacher beyond the definition of a Ph.D. supervisor with whom I learnt hard work and determination in the real sense. I owe him my indebtedness till eternity.

I want to express my deep regards for Dr. Ashu Bhan Tiku for co-supervising this thesis work and for her valuable suggestions and support throughout the tenure. I want to extend my gratitude to former deans, Prof. Rentala Madhubala, Prof. Neera Bhalla-Sarin, Prof. Birendra Nath Mallick, Prof. B.C.Tripathy and the current dean, Prof. S.K. Goswami, for being highly co-operative. I would also like to thank Prof. Atul Kumar Johri, Prof. Rana P. Singh, Dr. K. Natarajan and Dr. Rohini Muthuswami and rest of faculties of SLS for their constant support and motivation in numerous ways. I wish to remember and extend my regards to my

beloved teachers, Dr. Saravanamoorthy, Mrs. Ester Ranjeetham Stephen, Prof. Chellam Balasundara, Prof. Akbarsha and Dr. Emmanuvel Rajan Koilmani from my graduation studies, for serving an immense role in expanding my knowledge and wisdom.

My warm and special thanks go to all my all seniors and fellow lab mates; Dr. Niloo, Dr. Ranjana, Dr.Shafat, Dr. Shweta Agarwal, Dr.Rupali, Dr. Amit, Dr.Mamta, Dr.Shweta Singh, Dr.Nabodita, Dr. Yoginder, Dr.Siddhath, Dr. Shazia, Dr. Archana, Mrs. Archita, Mr. Kailash and Mr. Sunil, for their friendly and supportive nature and for creating a friendly and helpful ambience in the lab to carry out my research work. My special thanks to Dr. Askandar, Dr. Rajnish, Dr. Vibhor, Dr. Noor, Dr. Bhupender and Farid for their encouragement and being a supportive team member during my entire period of Ph.D. I extend my heartfelt gratitude to Askandar sir, Rajnish sir, Rita mam, and Sunil for providing their supporting hands during the most challenging period of my life. I earnestly thank them for all their time, help and support. I thank Ghanshyam ji, late kamata nath tripathi, Somnath Dutta, Sonu and Mrs. Rita Raina for their kind help and smoothening the path for my research work. My sincere acknowledgment for the invaluable help and progressive discussions provided by all dissertation students who did their project and summer training work with me, especially Divya Misra, sneha Misra, Avinash Ranjan and Vaibhav Raina.

My sincere thanks and gratitude to SLS staff, especially Mrs. Meenu, Mrs. Sunita, Late Mr. Talwar and Mrs. Shini mam for their help in Ph.D. related official work, processing of my fellowship and contingency. I would like to thank CIF and AIRF staff, especially Mrs. Sarika, Mr. Joginder, Mr. Amar Chand and Mrs. Tripti for their help.

I pay my heartiest regards to all my batchmates, Subash, Manjith, Vineeth, Deepak, Rakesh, Prince, Vipin, buddhi, Sudhaker, sarfraz, Poonam, Saba, ketki, suchismita Roy, pieu, Arun sen, Janesh, sneha singh and pratyusha for being friendly and helping me in hours of need. I am highly grateful to my seniors Dr. Hafiz Ahmad, Dr. Goutam K Tanti, Dr. Alok Kumar Singh, Dr. Deepak Kumar, Dr. Mudasir, Dr.

Bhavan sethulakshmi, and especially Dr. Praveen Kujur for helping me in hours of need and in trouble shootings during the research.

No words can suffice to express my gratitude to Prabu anna, Kalai anna, Yogavel anna Vinoth anna, Chandru anna, Prasanna Venkatesan anna, Dinesh anna and Radha Krishnan for their immense encouragement, understanding, moral support and for all enjoyable moments during my Ph.D. tenure. I would also like to thank my friends and hostel inmates, Manivannan Murugesan, Poonu durai anna, Ramadoss, Raja, Sakthi vel and Amit Kumar Dash for exchange of healthy discussion, advice and jokes which kept me away from my stress at times.

Words fail to express my gratitude for my dearest buddies Vishnu Vivek and Sindhuja from Tapti hostel, for their love, affection, care and moral support which made my every moment cherishable and memorable. I would also like to thank my sister, who always has been my strength and I wish I could show how much I love her.

I would like to remember and thank my grandfather late Tirunanam and Jagannathan uncle for their constant support and their belief in me that I will succeed.

I thank organizers of all national and international scientific meetings who gave an opportunity to present my research work. I acknowledge JNU, DST, ICMR, CSIR, Immunology foundation for the travel grants and UGC for fellowship.

Last but not the least, I would like to thank God Almighty, the one who never failed to prove his omnipresence and in correcting by wrongdoings and always leading me on the right path, giving me the strength and courage all these years and taking care of all my needs.

Abbreviations

ACC	Acetyl-coA Carboxylase
Acetyl CoA	Acetyl Coenzyme A
ADP	Adenosine 5'-diphosphate
AMPK	AMP activated Protein Kinase
APS	Ammonium persulfate
ATP	Adenosine 5'-triphosphate
BCA	Bicinchoninic acid
BSA	Bovine serum albumin
DEPC	Diethyl pyrocarbonate
DMEM	Dulbecco's Modified Eagle's Medium
DNA	Deoxyribonucleic acid
dNTP	Deoxynucleotide triphosphate
DTT	Dithiothreitol
ECL	Enhanced chemiluminescence
EDTA	Ethylenediaminetetraacetic acid
FBP	Fructose 1,6-bisphosphate
HK	Hexokinase
HPV	Human Papilloma Virus
HRPO	Horseradish peroxidase
IPTG	Isopropyl β-D-1-thiogalactopyranoside
ISCD	Inter subunit contact domain
LDH	Lactate dehydrogenase
LKB1	Liver Kinase B1
MG132	Proteasome Inhibitor (Z-Leu-Leu-Leu-al)

NAD (oxidized)	Nicotinamide adenine dinucleotide (oxidized)
NADH	Nicotinamide adenine dinucleotide (reduced form)
PAGE	Polyacrylamide gel electrophoresis
PEP	Phosphoenolpyruvic acid
PFK	Phosphofructokinase
PK	Pyruvate Kinase
PKM1	Pyruvate kinase M1 isoform
PKM2	Pyruvate kinase M2 isoform
PMSF	phenylmethane sulfonyl fluoride
SEM	Standard error of the mean
shRNA	Short hairpin ribonucleic acid
TBE	Tris-Boric acid-EDTA solution
TBS	Tris-buffered saline
TBST	Tris buffer saline with Tween-20 (detergent)
TEMED	N, N, N', N'-tetramethylethylenediamine
V/V	Volume/Volume
W/V	Weight/Volume

Symbols Used:

°C Degree Celsius

μ Micro

λ Wavelength

α Alpha

β Beta

∑ Summation of

Introduction

Introduction

Tumor cells evolve to rewire the expression of metabolic enzymes to compete with their neighboring normal cells in consuming more glucose to metabolize it chiefly into lactate, regardless of the presence of molecular oxygen to support cellular respiration, a phenomenon known as Warburg effect or aerobic glycolysis (Warburg 1956). This shift in glucose metabolism towards aerobic glycolysis from oxidative phosphorylation (Cairns et al. 2011) is the first biochemical hallmark feature of cancer cells, apart from six cardinal alterations in cell physiology that collectively dictate transformation (Hanahan and Weinberg 2000). Till date, the comprehensive understanding and significance of aerobic glycolysis remains unclear and under debate. However, the emerging evidences have more or less established the indispensable role of oncogenic mutations in metabolism reprogramming (Vander Heiden et al. 2009), offering potential benefits to cancer cells by the accrual of metabolic intermediates for macromolecular synthesis, prompt ATP production, retaining balanced redox state, and the ability to tolerate recurrent microenvironmental stresses (hypoxia/hypoglycemia), to support their rapid division and progression (DeBerardinis et al. 2008, Cairns et al. 2011).

Amongst the wide range of oncogenes that involve in cellular transformation, aberrant oncogenic protein kinases involved in pro-growth signaling pathways, such as MAP-Kinase and PI3K-AKT-mTOR, have been shown to constitutively stimulate the downstream transcription networks of HIF and Myc to remodel metabolism (Shackelford and Shaw 2009, Vander Heiden et al. 2009). In particular, the aforementioned aberrant signaling cascades converge to alter the expression of tissue-specific isoforms of glycolytic enzymes, preferentially to HK2 (Isoform 2 of Hexokinase), PKM2 (Isoform M2 of Pyruvate kinase) and LDHA (Lactate dehydrogenase A subunit), to exhibit aerobic glycolysis (Fantin et al. 2006, Christofk et al. 2008, Patra et al. 2013). Besides deregulated oncogenic pathways loss of tumor suppressors, that principally serve as cellular metabolic checkpoint, have been shown to further strengthen the pro-growth metabolism of cancer cells. In the recent past, tumor suppressor *LKB1* (a serine/threonine protein kinase) has gained ample interest, where loss of its function fails to activate its downstream substrate AMP-activated protein kinase (AMPK) to inhibit AKT-mTOR driven HIF and c-Myc transcription activation of pro-

growth metabolism (aerobic glycolysis) in non-small cell lung cancer (Faubert et al. 2014) and cervical adenocarcinomas (Zeng et al. 2016).

With the pouring literature, that has improved our understanding of cancer metabolism, researchers now unequivocally believe that aerobic glycolysis is indispensable on the course of tumorigenesis to meet the demands of its rapid proliferation. However, the key challenges in understanding tumor development and its progression are of, how rapidly dividing cancer cells in solid tumors overcome the checkpoints that maintain tissue homeostasis, including the cellular metabolic checkpoints. Emerging evidences have demonstrated that glucose addicted and rapidly proliferating cancer cells, in comparison to their normal counterparts, are more vulnerable to metabolic stress both *in vitro* and *in vivo* (Jones and Thompson 2009). Owing to the high proliferation rate and poor vasculature, tumor cells frequently outpace the diffusion limits of blood supply; and the intratumoral microenvironment often faces the hypoglycemic challenge. This situation raises an important question of how nutrient insufficiency affects metabolism of the cancer cells. Also, what remains unanswered is, whether these cells rely on aerobic glycolysis, like their richly vascularized counterparts and how do the critical glycolytic enzymes respond to nutrient deprivation? It is of interest to unravel the signaling pathway(s) and its downstream adaptive metabolic phenotype(s) that benefit cancer cells to survive the fluctuations in available nutrient conditions.

The ability of the cellular or tissue organization in physiological conditions to adapt to the dynamic microenvironment with recurrent replete and deplete nutrient supply depends on the energy sensing signaling pathways, which sense and couple the availability of nutrient status with the cell growth and division (Jones and Thompson 2009). During nutrient deprivation and hypoxia, AMPK-a serine/threonine protein kinase is known to get activated by sensing bioenergetic stress of decreasing intracellular ATP and increasing intracellular AMP and ADP (Hardie et al. 2012). AMPK plays a pivotal role in conserving the cellular energetic homeostasis by remodeling the metabolic phenotype to resist nutritional stress. Upon activation, AMPK increases catabolic ATP-generating processes, such as fatty-acid oxidation and inhibits ATP-consuming biosynthetic processes, such as protein, cholesterol and fatty-acid synthesis (Shackelford and Shaw 2009, Hardie et al. 2012). In recent years, extensive studies have appreciated the importance of LKB1-AMPK pathway in tumorigenesis, where the axis of LKB1-AMPK is shown to provide tolerance to nutrient deprivation in cancer cells (Kato et al. 2002, Jeon et al. 2012, Liang and Mills 2013).

However, how AMPK contributes to metabolic phenotype of cancer cells, and the mechanistic link through which AMPK exhibits tolerance to hypoglycemic situation that arises upon tumor progression, remains largely elusive.

Comprehending further the impact of HPV encoded oncoproteins, E6 and E7, on metabolic remodeling within proliferating tumor cells is of utmost importance; but remains ambiguous with special focus on loss of LKB1-AMPK signaling that facilitates metabolic transformation. Based on global cancer incident statistics, HPV accounts for 5% of global cancer burden, and serves as a prime etiological factor of 99% of cervical adenocarcinoma cases (Arbyn et al. 2011, de Martel et al. 2012). Nearly 20% of human papillomavirus (HPV)-driven cervical adenocarcinoma, 30% of lung adenocarcinoma cases, and a substantial number of cases with endometrial and prostate cancers either lack LKB1 expression or harbor a loss of function mutation (Hezel and Bardeesy 2008, Wingo et al. 2009, Marcus and Zhou 2010). Further, a recent study by Zeng et al. reveals that the loss of LKB1 expression facilitates glycolytic reprograming in cervical adenocarcinoma (Zeng et al. 2016). However, the absence of LKB1-AMPK signaling pathway in cervical cancer cells and lung adenocarcinoma make them more prone to cell death in response to limited glucose availability or treatment with 2-deoxy glucose or AMPK activators (Nafz et al. 2007, Inge et al. 2009, Shackelford et al. 2013, Whang et al. 2016). Understanding the mechanisms through which HPV (HPV-16 or HPV-18) facilitates metabolic remodeling to nurture tumor progression provides an experimental model to find out causal association with oncogenesis and allows drawing parallels with metabolic reprogramming in other non-viral human cancers. Evidently, it is pertinent to investigate the role of LKB1-AMPK axis in the regulation of glycolytic enzymes involved in aerobic glycolysis, such as hexokinase (HK), pyruvate kinase (PK) and lactate dehydrogenase (LDH), and to validate their importance in the regulation network in tumor maintenance and progression.

Finally, in view of heterogenic cellular status of the LKB1-AMPK pathway in cancer cells, there is a great scope to understand how tumor cells that fail to activate AMPK, either due to the lack or loss of function of LKB1, tolerate hypoglycemic stress. A deeper insight is expected to rationalize therapeutic strategies based on synthetic lethality approach with reference to the unique glycolytic metabolism of cancer cells in association with the cellular status of the LKB1-AMPK pathway.

CHAPTER-1
Review of Literature

Chapter-1

Review of Literature

1.1. AMP-activated protein kinase, the bio-energetic sensor, and a metabolic checkpoint.

Responding to the dynamic extracellular and intracellular cues are the primary tasks of the cells to coordinate their growth and division with the availability of nutrients to guarantee sustenance of generations. It is not surprising if the cells through the passages of evolution have conserved a special sensor to monitor and alarm the cells about an assault of physiological (Nutritional, Hypoxic, and Genotoxic) stress, critical in establishing the bioenergetic homeostasis within the system. AMPK (5' Adenosine Monophosphate - activated Protein kinase) (EC; 2.7.11.31) is a cellular energy sensor that is activated by increased intracellular levels of AMP or ADP, produced as a result of unrestrained ATP hydrolysis, thus representing scarcity of cellular ATP. AMPK, therefore, allows adaptation to low energy conditions to preserve the cellular energy homeostasis; and in response increases catabolism to generate more ATP. Besides acting as a sensor of intracellular metabolic stress signals, due to nutritional insufficiency and hypoxia, AMPK also gets activated by an array of physiological stimulations, including calcium concentration via calmodulin kinase (CAMKKβ), the action of various hormones and cytokines. Once activated by sensing the falling energy (ATP) status, it reprograms the cellular metabolic pathway by increasing the expression or activity of proteins (enzymes) involved in catabolism; and on the other hand restricts the energy demanding anabolic pathway to conserve ATP (**Fig. 1.1**). AMPK regulates the energy balance at cellular as well as at whole-body (organismal) level. Though the role of AMPK in metabolism regulation is considered central, it has many other functions, including regulation of mitochondrial biogenesis, autophagy, cell polarity, cell growth and proliferation (Shackelford and Shaw 2009).

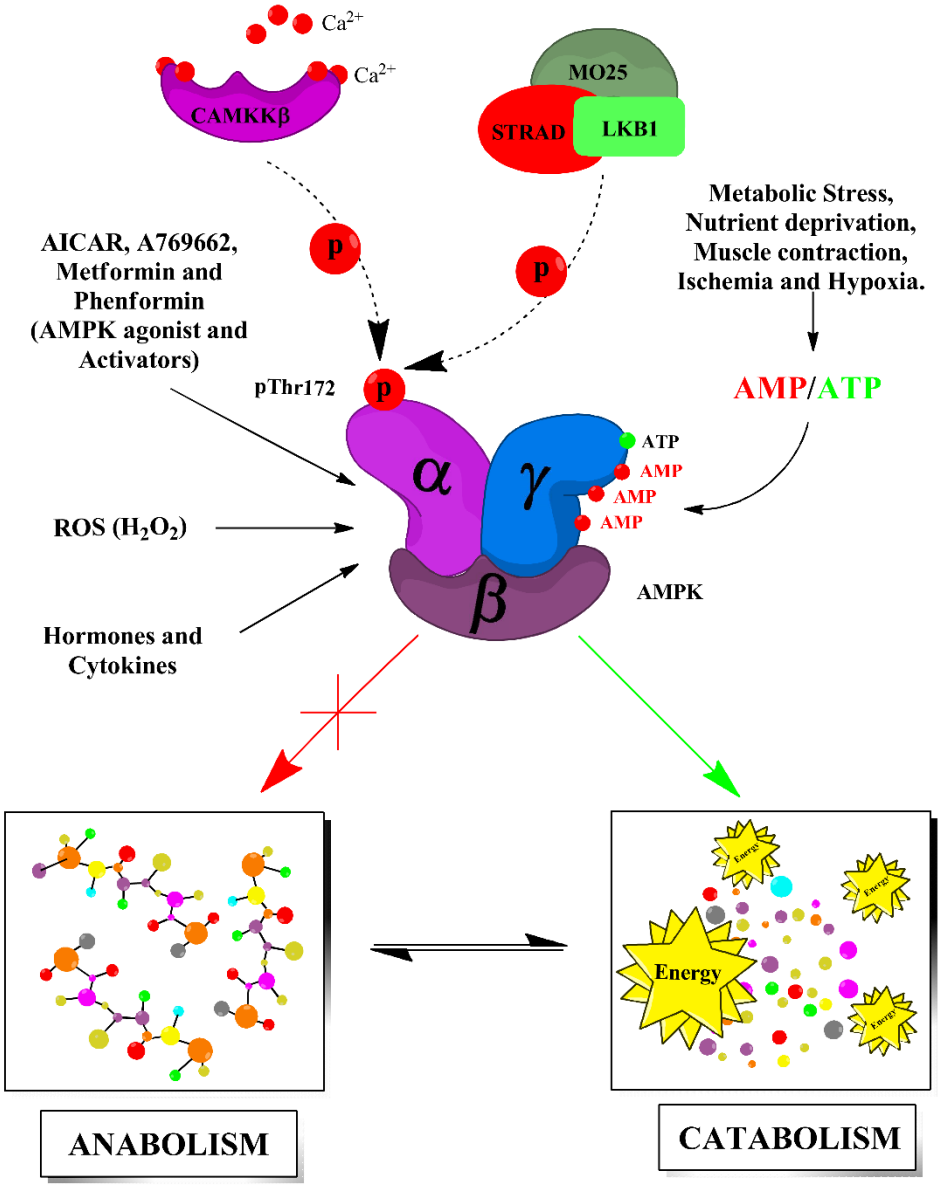

Fig. 1.1. Schematic elucidation of the factors that impact AMPK activation and affect metabolism. *LKB1 and CAMKK are the two distinct protein kinases that activate the bioenergetic sensor, AMPK, by phosphorylating Thr172 residue in response to the surge in AMP/ADP and calcium (Ca2+) concentrations. In addition, AMPK activation is influenced by various stimuli that involve AMPK agonists, activators, hormones, cytokines and reactive oxygen species. The activated AMPK in response to bioenergetic stress reprograms the metabolic phenotype from anabolism to catabolism for rapid energy generation.*

1.1 Features of AMP-activated protein kinase.

The first seminal observation on AMPK (primarily named as HMG-CoA reductase kinase) was made in 1973 when the study emphasized about HMG-CoA reductase kinase and its regulation both *in vivo* and *in-vitro* (Hardie et al. 1994). Shortly after this, researchers realized that the kinase which inactivated HMG-CoA reductase was identical with the one which phosphorylated and inactivated Acetyl-CoA carboxylase (ACC), the key regulatory enzyme that controls fatty acid synthesis (Hardie et al. 1994). The term HMG-CoA reductase was collectively replaced by AMP-activated protein kinase after it was shown that the protein kinase could be allosterically activated by 5'-AMP (Ferrer et al. 1985).

The physiological role of AMPK apart from its role in regulating HMG-CoA reductase and ACC activity (controlling net sterol and fatty acid synthesis pathways) remained unclear for decades. However, with time numerous protein substrates were discovered downstream to AMPK protein kinase, unraveling the unique role of AMPK in sensing and safeguarding cells from environmental stresses and in preserving energy homeostasis. Later findings revealed that AMPK homologs are evolutionarily conserved in all eukaryotes, from yeast to mammals. Snf1 (Sucrose non-fermenting 1), an AMPK homolog in yeast, was shown to serve a pivotal role in maintaining energy homeostasis upon encountering nutritional stress in *Saccharomyces Cerevisiae* (Hardie et al. 1994).

A long search of decades for the upstream kinase that phosphorylates AMPK at the Thr172 residue lead to a landmark finding of the heterotrimeric protein complex, a tumor suppressor kinase-liver kinase B1 (LKB1), the pseudokinase STE20-related adaptor (STRAD), and the scaffold protein mouse protein 25 (MO25) (Hardie and Alessi 2013). Further, studies using LKB1 knockout models and tumor cells lacking LKB1 demonstrated that AMPK could still undergo Thr172 phosphorylation by a secondary kinase known as calmodulin-dependent protein kinase kinase β (CaMKKβ) (Hardie et al. 2012).

1.2.1 Genes that encode AMPK Subunits and its isoforms.

AMPK, a heterotrimeric serine/threonine protein kinase, consists of alpha, beta and gamma subunits. Each of the subunits exists in more than one isoform, encoded by independent genes.

Protein kinase AMP-activated catalytic subunit alpha1 (PRKAA1) (5p12) and alpha2 (PRKAA2) (1p31) genes code for the two isoforms of α subunit (α1 and α2); whereas, PRKAB1 (12q24) and PRKAB2 (1q21) encode the two isoforms of β subunit (β1 and, β2). PRKAG1 (12q12-q14), PRKAG2 (7q36) and PRKAG3 (2q35), however, code for 3 isoforms of the γ subunit (γ1, γ2, and γ3) (See, **Table. 1.1** for more details). The expression of a given subunit isoform and the resultant combination of the heterotrimeric complex is suggested to be cell type and tissue specific. Theoretically, the co-expression of these isoforms could result in 12 combinations of heterotrimeric complexes, though the functional efficiency and relevance of these distinct complexes are unclear (Ross et al. 2016). In the background of distinct heterotrimeric combinations of AMPK in response to diverse stresses, it is interesting to expedite the structural combinations of different isoforms and their cell type or tissue-specific functional implication.

1.2.2 Structural features of Human AMPK Protein.

Within a heterotrimeric complex of AMPK, each subunit performs a distinct function, which includes protein kinase activity, stability and stress sensing (regulation). The alpha subunit of AMPK consists of, a typical serine/threonine kinase domain, where its kinase activity depends on Thr172 phosphorylation at the activation loop by the upstream kinases, an autoinhibitory sequence (AIS) and a C-terminal β-subunit interacting domain (β-SID). The β subunits consist of a conserved carbohydrate binding module (CBM) and a carboxyl-terminal αγ subunit binding sequence (αγ-SBS), the latter serves a pivotal role in connecting α and γ subunits to make the core complex. The γ subunit serves as a regulatory domain and contains four tandem repeats of adenine nucleotide binding sites known as cystathionine beta synthase (CBS) motifs. CBS motifs usually exist as pairs and each pair of CBS motifs is termed as Bateman domain. This regulatory domain of AMPK senses energy status by binding competitively to AMP or ADP during energetic stress; and ATP when there is an adequate quantity of nutrient supply and energy production (**Fig. 1.2**).

Table 1.1: AMPK isoforms and their variants

Subunits of AMPK complex	**Gene name**	**Chromosome loci**	**Alternate variants**	**No. of amino acid**	**Protein size**
AMPKα1	PRKAA1 (Entrez 5562)	5p12	2	559 (Isoform 1) 574 (Isoform 2)	64 kDa (Isoform 1) 65.5 kDa (Isoform 2)
AMPKα2	PRKAA2 (Entrez 5563)	1p31	N.A.	552	62.3 kDa
AMPKβ1	PRKAB1 (Entrez 5564)	12q24-q24.3	N.A.	270	30.3 kDa
AMPKβ2	PRKAB2 (Entrez 5565)	1q21.1	2	272 (Isoform 1) 190 (Isoform 2)	30.3 kDa 21.4 kDa
AMPKγ1	PRKAG1 (Entrez 5571)	12q12-q14	3	331 (Isoform 1) 340 (Isoform 2) 299 (Isoform 3)	37.5 kDa 34.0 kDa 38.5 kDa
AMPKγ 2	PRKAG2 (Entrez 51422)	7q36.1	5	569 328 328 525 444	63.0 kDa 37.5 kDa 37.5 kDa 58.4 kDa 48.8 kDa
AMPKγ 3	PRKAG3 (Entrez 53632)	2q35	1	489	54.2 kDa

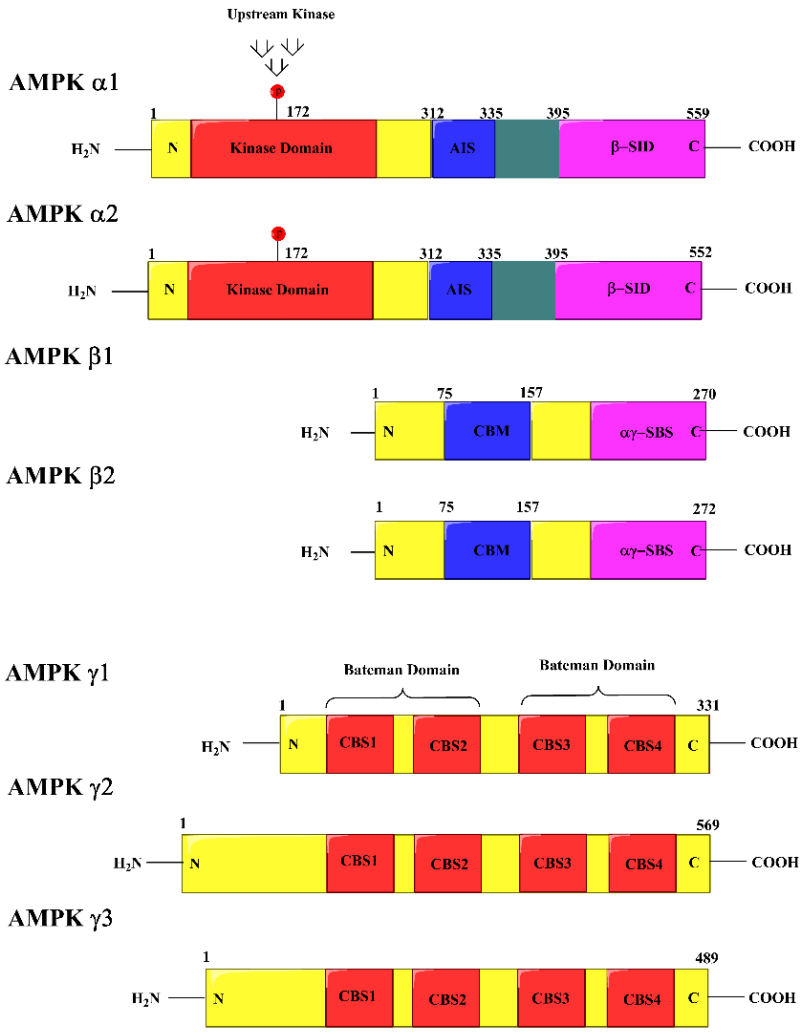

Fig. 1.2. Schematic illustration of the subunits of human AMPK isoforms and their domain organization. *The alpha subunits of AMPK involve N-terminal Serine/Threonine protein kinase domain, followed by an autoinhibitory sequence (AIS) and a C-terminal β-subunit interacting domain (β-SID). Thr-172 phosphorylation of N-terminal kinase domain triggers AMPK activation by an upstream kinase. β subunits of AMPK comprise of a carbohydrate binding module (CBM) at the epicenter and a α-, γ-subunit binding sequence (αγ-SBS) at the C-terminal end. γ subunits of AMPK differ by the length of their amino terminal end and contain four nucleotide binding cystathionine beta synthase (CBS) domains, numbered 1-4; pairs of CBS domains form two Bateman domains, the latter sense energetic stress by binding AMP/ATP and allosterically regulate AMPK complex.*

1.3 Mechanics of AMPK activation and sensing of energy stress

Structural studies have demonstrated that at resting - normoglycemic and normoxic - phase, the regulatory γ subunit shows preferential binding of ATP to CBS-1, CBS-3 and of AMP to CBS-4 **(Fig. 1.1 and 1.2)**. CBS-2 remains unoccupied with adenine nucleotides. While encountering moderate nutritional stress, the ratio of AMP versus ATP within a cell rises gradually and one of the resultant outcomes within the structure of AMPK protein is the replacement of ATP with AMP at CBS-3, which in turn favors phosphorylation of AMP kinase at Thr172 position of the α subunit by AMPKK and protects AMPK from dephosphorylation by phosphatases, stimulating its activity by many folds. However, a severe stress causes replacement of ATP with AMP at CBS-1, resulting in the allosteric activation of AMPK activity.

Once cells recover back from extrinsic and intrinsic stresses and replenish their ATP levels, the bound AMP at CBS sites 1 and 3 of γ subunit are readily replaced with ATP, which in turn promotes dephosphorylation of AMPK at Thr172 and retains its conformation in resting state (Hardie et al. 2012). This mode of AMPK activation in sensing moderate to severe or acute to chronic stress provides graded responses to a wide range of stimuli. Although the allosteric activation of AMPK by cellular AMP has been known for quite some time, the role of ADP in influencing the rate of phosphorylation and dephosphorylation has been identified in the recent past (Oakhill et al. 2011, Xiao et al. 2011). However, with the exception, AMPK in hypothalamic neurons, T cells, and endothelial cells has been shown to be activated predominantly by calcium/calmodulin-dependent kinase kinase2 (CaMKKβ) in response to the rise in cellular Ca^{2+} levels, without influencing AMP or ADP concentrations.

In addition to the above mentioned canonical mechanisms responsible for AMPK activation, involving the cellular increase in the concentration of AMP, ADP, and Ca^{2+}, there are reports which demonstrate that TGF-β-activating kinase 1 (TAK1) and reactive oxygen species (e.g. H_2O_2) could activate AMPK through non-canonical mechanisms. ROS-mediated AMPK activation involves phosphoinositide 3-kinase (PI3K) or Ataxia telangiectasia mutated (ATM) signaling pathway (Hardie et al. 2012). Moreover, ATM-mediated activation of AMPK requires LKB1 presence as reflected from studies where abrogation of LKB1 expression resulted in the loss of H_2O_2 mediated AMPK activation. Conversely, studies using cells exposed to DNA damaging

agents like etoposide, doxorubicin and IR (radiation) have demonstrated that ATM can phosphorylate AMPK independent of LKB1.

1.3.1 Pharmacological agonists that activate AMPK in vitro and in vivo

A variety of natural and synthetic drugs have been shown to differentially activate AMPK. Based upon the mode of AMPK activation, these drugs are categorized in 3 different major classes (Grahame Hardie 2016).

The first category of activators includes drugs, such as (i) glycolysis inhibitor: 2-deoxyglucose (2DG); and (ii) inhibitors of mitochondrial complex I: Metformin and Phenformin; -Complex III: Antimycin A; and -Complex V: F1 ATP synthase, Oligomycin and Resveratrol that activate AMPK by modulating the ratio of AMP and ADP by inhibiting ATP synthesis. The second category involves Pro-drugs: (i) 5-aminoimidazole-4-carboxamide ribonucleoside (AICAR), which is cell permeable and is enzymatically converted into ZMP molecule to activate AMPK; (ii) C2, a potent synthetic allosteric activator of AMPK, produced from its pro-drug C13 (phosphonate diester) by cellular esterases, preferentially binds and activates AMPK complex containing α1 rather than the α2 isoform; and (iii) Cordycepin, a natural compound extracted from the fungus, *Cordyceps militaris*, which is readily permeable in cells and is converted to Cordycepin -5'-monophosphate (AMP analog) by cellular enzymes that bind γ subunit of AMPK to activate the protein kinase. The third category is a class of activators that bind and activate AMPK distinct from AMP binding site, and these are: (i) A-769662 from Abbot Laboratories, which directly binds AMPK in the cleft situated in-between α subunit kinase domain and CBM of β-subunit, although A-769662 binding is distinct from that of AMP, however like AMP, it allosterically activates AMPK and protects it from dephosphorylation of Thr172 (Goransson et al. 2007, Sanders et al. 2007), A-769662 selectively activates AMPK complex that comprises β1 rather than β2 subunit; (ii) two compounds, 991(also known as ex229) and MT 63-78, identified by high-throughput screens, that bind the above-stated region and allosterically activate AMPK; (iii) in addition to the above-mentioned synthetic compounds, salicylate, a plant-derived natural product has also been shown to bind this site and in turn activate AMPK; similar to A-769662, preferentially activating β1 subunit comprising complexes instead of β2 complexes (Hawley et al. 2012).

1.4. Role of AMPK in Metabolism

1.4.1 AMPK in regulation of anabolic pathway to limit energy Consumption

Upon activation, AMPK reversibly inhibits almost all energy demanding pathways, such as biosynthesis of lipids, proteins, carbohydrates, ribosomal RNA transcription and cell division, to preserve ATP **(Fig. 1.3)**. The effect of AMPK activation on its downstream targets is either through direct phosphorylation of protein substrates (that entails highly conserved motif with characteristic sequence features) or through the control of transcriptional programs that modulate the expression status of key regulatory proteins (regulatory enzymes) of anabolic pathways. This includes ACC Ser79 phosphorylation which inhibits its role and attenuates the function of mitochondrial glycerol-3-phosphate acyltransferase (GPAT) (involved in phospholipids and triglycerides synthesis) following phosphorylation by AMPK. The 3-hydroxy-3-methylglutaryl CoA reductase (HMGCR) phosphorylation by AMPK blocks its function in cholesterol biosynthesis; whereas, glycogen synthase (GS) phosphorylation at Ser7 residue inhibits glycogen synthesis. Activation of malonyl-CoA decarboxylase by AMPK decreases fatty acid esterification and increases its oxidation. Muscle contraction-induced AMPK phosphorylates hormone-sensitive lipase (HSL), a neutral lipase, which hydrolyzes variety of esters, breaks diacylglycerides to monoglycerides and free fatty acids **(Fig. 1.4)** (Hardie et al. 2012).

Alternatively, AMPK negatively regulates the expression of lipogenic enzymes FAS (fatty acid synthase) and ACC by downregulating the expression of the key transcription factor, sterol regulatory element-binding transcription factor 1 (SREBP-1), or by preventing SREBP1 nuclear translocation and transactivation of lipogenic enzymes by direct phosphorylation. Likewise, AMPK inhibits gluconeogenesis pathway by phosphorylating transcriptional coactivator, TORC2 (transducer of regulated CREB activity 2; also known as CRTC2), to prevent its nuclear entry and transcriptional activation of gluconeogenesis enzymes (Shackelford and Shaw 2009). In addition, AMPK phosphorylates and prevents class II histone deacetylase family members in activating FOXO family transcription factors to encode gluconeogenesis enzymes.

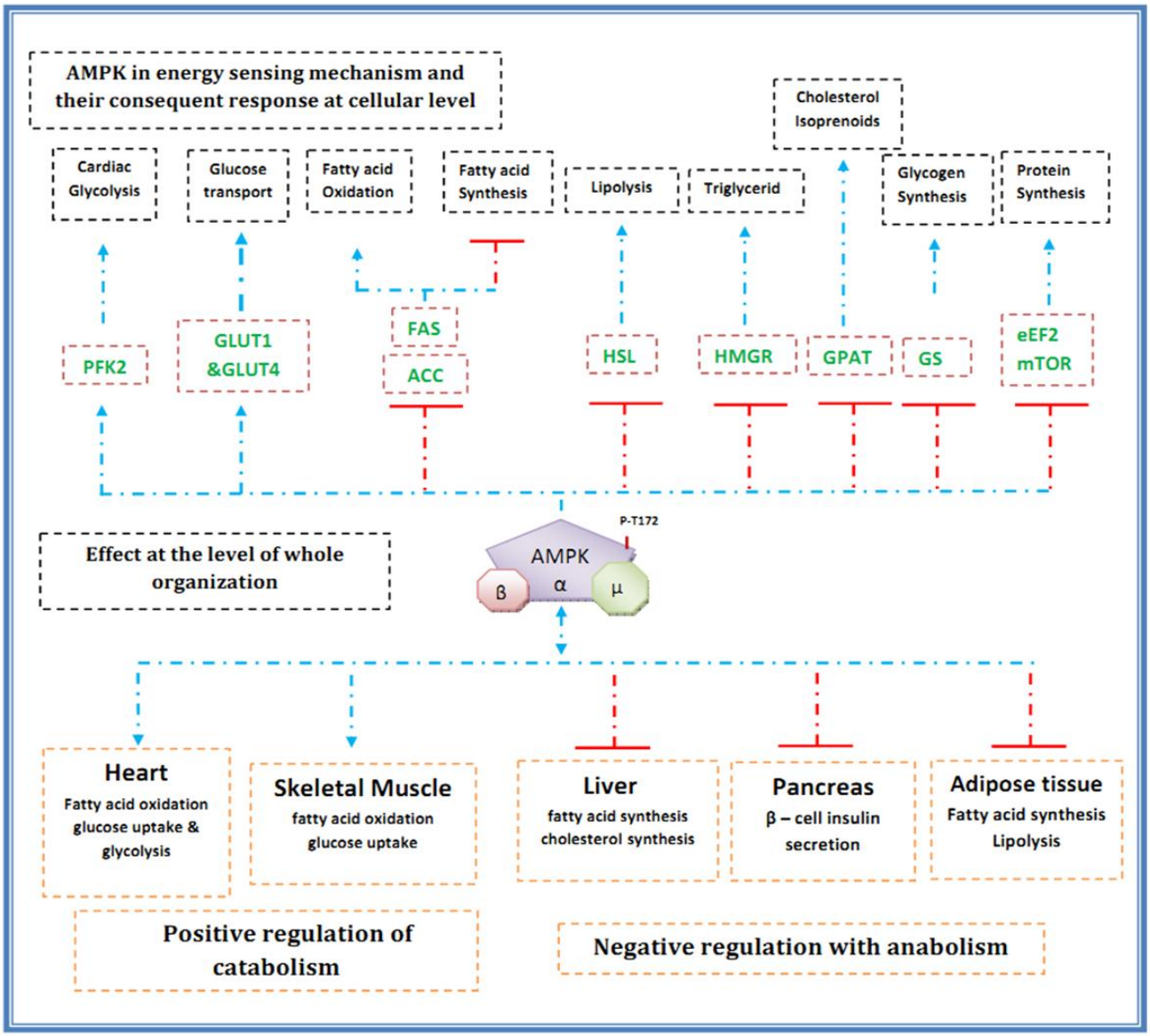

Fig. 1.3. Illustration of the central role of AMPK stress signaling cascade in the regulation of metabolism. *The physiological targets of activated AMPK from carbohydrate, lipid and protein metabolism are depicted. This metabolic regulation by AMPK in diverse organs plays a vital role in maintaining physiological homeostasis. The above artwork was modified from the original source http://themedicalbiochemistrypage.org/ampk.php.*

1.4.2 AMPK regulates catabolism for rapid energy generation

The major contribution of AMPK to glucose metabolism involves enhanced glucose uptake and increased glycolytic flux in order to generate energy (ATP) rapidly. AMPK enables the glucose uptake primarily in contracting muscles by facilitating the translocation of type 4 glucose transporter (GLUT4) to the plasma membrane from intracellular storage vesicles **(Fig. 1.4)**. AMPK is directly involved in the trafficking of membrane-bound vesicle of GLUT4 transporters by phosphorylating RabGAP-TBC1D1 (TBC1 domain family member 1) to relieve the anchored cargo to fuse with the plasma membrane. In addition, AMPK also regulates the translocation of GLUT1. AMPK accelerates the flux of glycolysis by phosphorylating 6-phosphofructo-2-kinase (PFKFB; fructose-2, 6-biphosphatase), in particular, AMPK phosphorylates isoform - PFKFB2 in cardiac myocytes (Marsin et al. 2000) and -PFKFB3 in monocytes and macrophages, on sensing ischemic and hypoxic stresses (Marsin et al. 2002) **(Fig. 1.4)**.

AMPK mediated phosphorylation of dual functional phosphofructokinase-2 (PFK2) promotes its kinase activity while inhibiting its phosphatase activity to accumulate fructose-2, 6-bisphosphate (F26BP), which allosterically activates key rate-limiting glycolytic enzyme phosphofructokinase-1 (PFK1) to accelerate the glycolytic flux for energy generation. On the other hand, F26BP inhibits energy consuming gluconeogenesis by allosteric inhibition of fructose-1, 6-bisphosphatase (F1,-6BPase) enzyme. In cardiomyocytes, AMPK has been shown to promote fatty acid uptake by transporting the membrane-bound vesicles harboring CD36 (Fatty acid transporter) to the plasma membrane, however, the precise mechanism remains obscure. Further, AMPK has been shown to facilitate the export of fatty acid from cytosol to mitochondria for β-oxidation. AMPK achieves this by phosphorylating and inactivating acetyl-CoA carboxylase (isoform ACC1 and ACC2) to synthesize malonyl-CoA, a potent inhibitor of Carnitine O-palmitoyltransferase. Drop in the level of malonyl-CoA sets Carnitine O-palmitoyltransferase free to export fatty acid to mitochondria followed by β-oxidation, an energy generating process (Hardie et al. 2012).

1.4.3 AMPK in mitochondrial biogenesis, autophagy, and mitophagy

The connecting link of AMPK with mitochondrial biogenesis is elucidated from studies on rats fed with AICAR, an AMPK agonist. These rats demonstrated increased mitochondrial gene expression, especially in the cells of muscle origin **(Fig. 1.4)**. Further, extensive studies carried out using double knockout mice models for AMPK-β1 and AMPK-β2 exhibited attenuated AMPK activity in muscle and reduced mitochondrial content or biogenesis. Peroxisome proliferator activated receptor-γ coactivator 1α (PGC1α), the master regulator of mitochondrial biogenesis, plays an indispensable role in regulating the expression of nuclear encoded mitochondrial genes by serving as a transcriptional co-activator. AMPK phosphorylates PGC1α at Thr177 and Ser538 residues to induce the expression of GLUT4, nuclear encoded mitochondrial genes, and self-regulates its own expression through a positive feedback loop. In addition, through a distinct mechanism AMPK enhances mitochondrial biogenesis, which involves deacetylation of PGC1α by NAD-dependent deacetylase, sirtuin I (SIRT1) (Canto, Jiang et al. 2010). Besides mitochondrial biogenesis, AMPK is also involved in the recycling of non-functional mitochondria by selectively targeting them through autophagy known as mitophagy. AMPK executes this function by interacting and phosphorylating master regulator of autophagy, UNC-52-like kinase 1 (ULK1), an orthologue of yeast Atg1 (Behrends et al. 2010, Egan et al. 2011). AMPK and ULK1 axis through mitophagy eliminates aberrant mitochondria which undergo oxidative damage and restores new ones by mitochondrial biogenesis to increase the oxidative catabolic endurance of cells to meet energy paucity.

1.5 Role of AMPK beyond energy Metabolism

1.5.1 AMPK, mTOR and protein synthesis

AMPK controls net protein translation rate under the nutrient deprived circumstances by negatively regulating mammalian target of rapamycin (mTOR). mTOR, a highly conserved Serine/Threonine protein kinase, couples the available growth factor and nutrient signaling to stimulate protein synthesis and cell growth (Guertin and Sabatini 2007) **(Fig. 1.4)**. Active mTOR

complex plays a vital role in controlling the assembly of translation initiation by recruiting and phosphorylating its well-characterized substrates, 4EBP1 and p70 ribosomal S6 kinase (S6K). Active AMPK exerts its inhibitory effects on mTOR and its protein translation mechanism through Tuberous sclerosis complex 2 (TSC2 or tuberin). TSC2 and its obligate partner TSC1 inhibit MTORC1 (mTOR Complex 1) through the regulation of small GTPase Ras homologue enriched in brain (RHEB). Moreover, AMPK has been shown to directly phosphorylate raptor (regulatory associated protein of mTOR) subunit of mTORC1 and promote raptor to bind 14-3-3, thus decreasing the mTOR activity.

1.5.2 AMPK and cell cycle checkpoints

Like protein synthesis, cell division is also a high energy demanding processes. AMPK, in order to conserve energy, creates cell division checkpoints in cells that meet energy deficiency **(Fig. 1.4)**. Studies have demonstrated the characteristic ability of AMPK to directly phosphorylate P53 at Ser15 residue and cyclin-dependent kinase inhibitor P27 at Thr198 residue to block cell cycle upon limited nutrient supply (Jones et al. 2005) **(Fig. 1.5)**. In addition, AMPK phosphorylates Ser36 residue of histone2B (H2B) at the promoter and coding region of stress associated genes, *p21* and *cpt1c*, to regulate their expression for stress adaptation. On the contrary, Banko et al., using chemical genetic screen, has revealed the key role of AMPK in progression of mitosis and cytokinesis, via the phosphorylation of protein phosphatase 1 regulatory subunit 12C (PPP1R12C), suggesting the importance of the energy sensor, AMPK, in the accomplishment of mitosis (Banko et al. 2011).

1.5.3 Control of cell polarity, migration and cytoskeletal dynamics by AMPK

Studies in the recent past have found remarkable interconnecting links of AMPK pathway with cell polarity and cytoskeletal dynamics (Mihaylova and Shaw 2011). Loss of AMPK in drosophila has shown abnormal cell polarity and mitosis. It was anticipated that loss of AMPK abrogates phosphorylation on myosin light Chain (MLC), a key event that regulates cell polarity and mitotic cell division. The involvement of activated AMPK following calcium switch and its

role in tight junction formation was reported by using mammalian MDCK cell lines. It has been reported that Afadin, an adherens junction protein, and GBF1 (Golgi-specific brefeldin A resistance factor 1), a guanine nucleotide exchange factor for the ADP-ribosylation factor family, act as putative downstream substrates of AMPK, proposed to be involved in regulating cell polarity.

1.5.4 AMPK and organism physiology

In addition to its confined role at the cellular level, AMPK exerts major biochemical and behavioral changes at a whole-body level to preserve energy homeostasis. For instance, AMPK activity in hypothalamus regulates appetite. The factors that induce appetite, such as ghrelin, adiponectin (adipokine) or cannabinoids, enhance AMPK activity in the hypothalamus. Whereas, hormones that inhibit eating (anorexigenic or appetite suppressant), such as leptin and insulin inhibit AMPKα2 activity in the hypothalamus **(Fig. 1.3)**. Notably, administration of AMPK agonist or AMPK-constitutively-active-mutants in the hypothalamus has shown to induce hunger.

In recent studies it has been shown that ghrelin activates AMPK through Ca^{2+} dependent CaMKKβ kinase in presynaptic neurons upstream of NPY/AgRP neurons in the hypothalamus, which in turn triggers a positive feedback loop of continued neurotransmitter release for an urge to eat. Whereas, leptin after feeding activates pro-opiomelanocortin (POMC) neurons to release opioids, halting the AMPK activation in the presynaptic neurons (Hardie et al. 2012). Emerging evidence states that dietary restriction and well-characterized agonist or activator of AMPK, like resveratrol and metformin, have been shown to enhance the longevity of *C. elegans*. In addition, genetic deletion screens have validated the role played by AMPK orthologues in life-extending effects (Greer and Brunet 2009, Onken and Driscoll 2010).

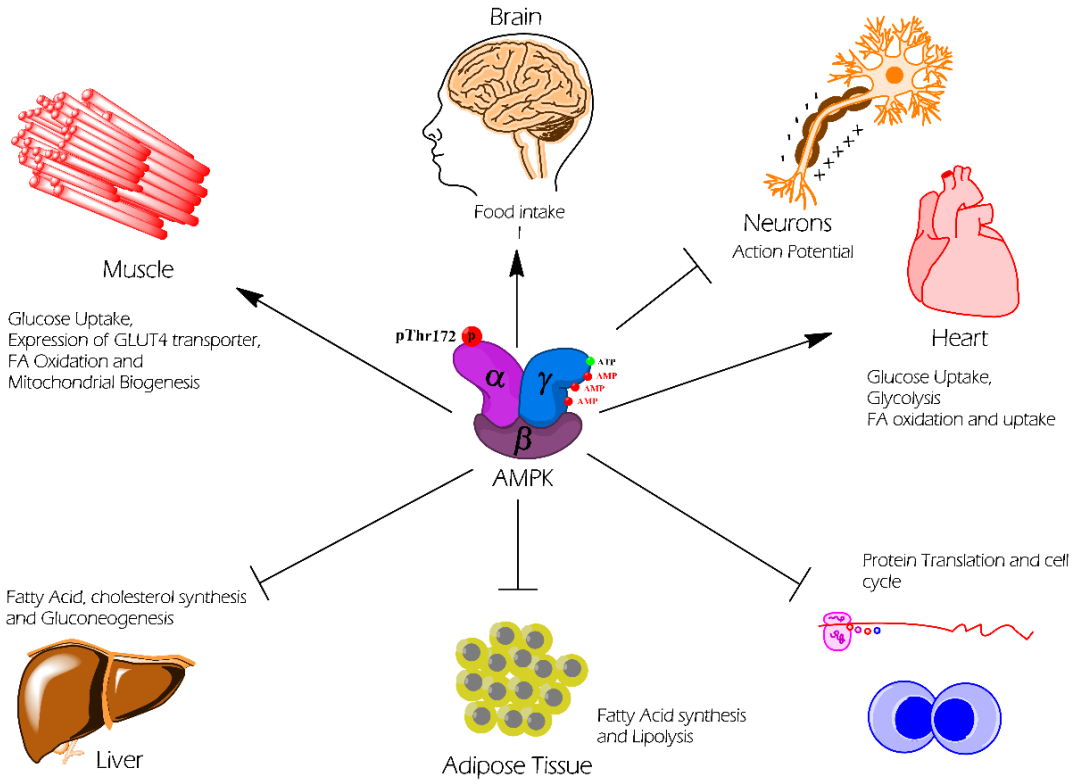

Fig. 1.4. The role of AMPK in cellular and whole body energy metabolism and homeostasis. AMPK following activation exerts its inhibitory effect on the anabolic pathway and promotes catabolic metabolism for energy conservation in tissues of diverse origin. AMPK inhibits the biosynthesis of fatty acid and cholesterol in the liver and adipose tissue. In addition, AMPK inhibits; gluconeogenesis in the liver, lipolysis in adipose tissue, an action potential in neurons, protein synthesis and cell division in cells of multiple tissue origin. Conversely, AMPK stimulates glucose uptake, enhances the rate of glycolysis, fatty acid uptake, fatty acid oxidation and mitochondrial biogenesis in cardiomyocytes and in skeletal muscle cells. AMPK activity in hypothalamus co-ordinates the food intake habit. The above graphics was modified from its original source (Kahn et al. 2005)

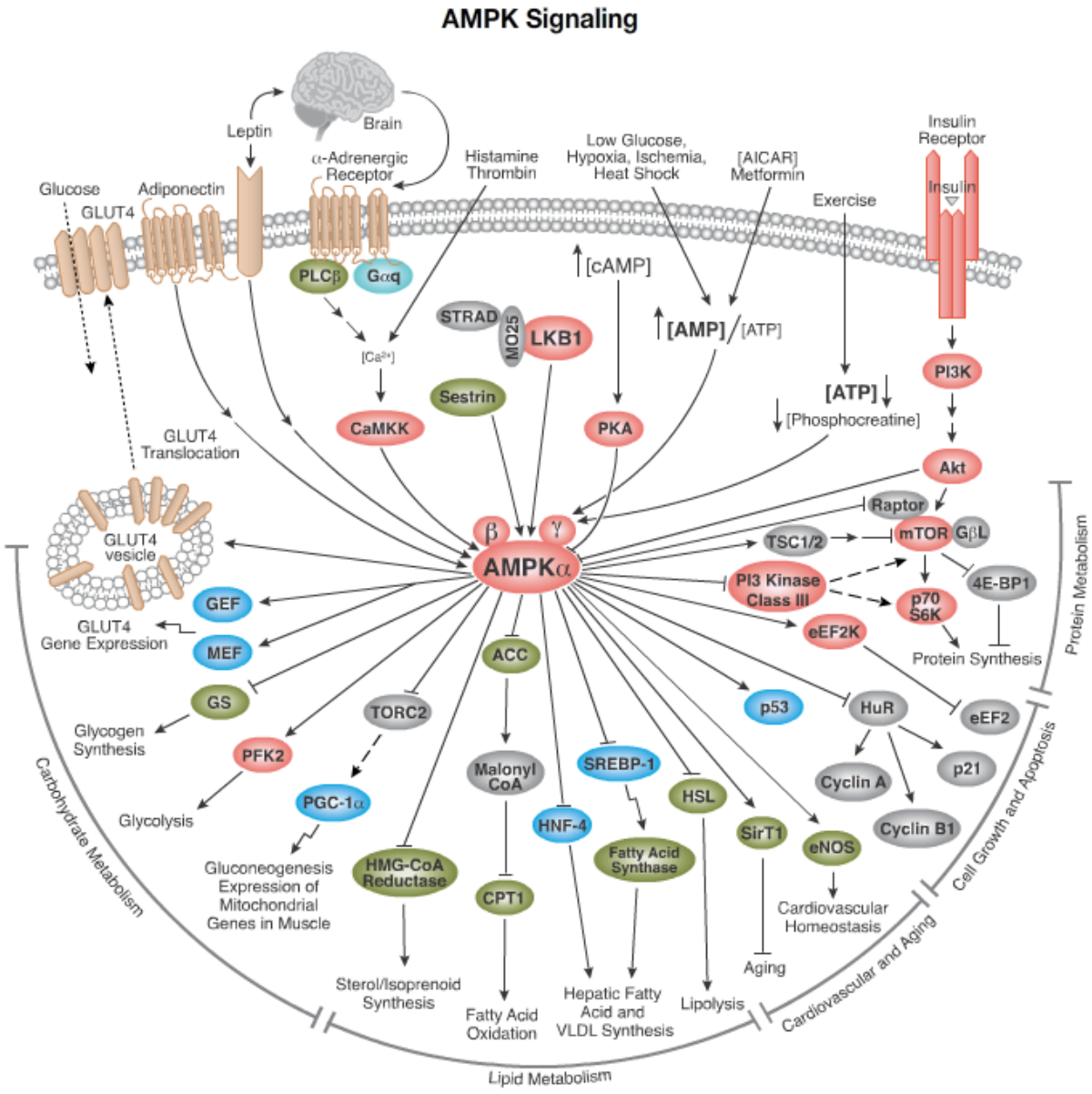

Fig. 1.5. Schematic representation of AMPK signaling cascade with its recognized upstream regulators and downstream effectors. The model demonstrates the energy sensing mechanism of AMP-activated protein kinase and its antagonistic relationship with pro-growth signaling pathway i.e.PI3K-AKT-mTOR to affect the protein translation and cell cycle machinery. The graphics presented here were reused from Cell Signalling Technology®.

1.6 Emerging role of AMPK in cancer: a contextual oncogene or a conditional tumor suppressor.

Evidence from literature suggests that AMPK activation in tumors may exert anti-tumorigenic potential, considering the cellular checkpoint character of AMPK and its association with characterized tumor suppressors including; LKB1, P53, and TSC1/2. As a proof of concept, epidemiological studies in type II diabetes patients supplemented with anti-diabetic biguanide – potent activators of AMPK (metformin, phenformin) has revealed a statistical reduction in tumor incidence (Shaw 2006). Besides, AMPK agonists, as well as glucose withdrawal, has been shown to inhibit tumor cell growth *in vitro* and *in vivo*. However, till date, this area of study lacks a convincing evidence to support the tumor suppressive role of AMPK.

Contrary to the above hypothesis, extensive studies in recent years have emphasized the importance of LKB1-AMPK (Liver Kinase B1, an upstream kinase of AMPK) pathway in tumorigenesis (Jeon and Hay 2012, Liang and Mills 2013, Faubert et al. 2015, Jeon and Hay 2015, Zadra et al. 2015). The lack of LKB1 expression has been shown to result in inhibition of tumorigenesis (Bardeesy et al. 2002). Numerous studies have demonstrated the indispensable role of AMPK in the oncogene-driven tumor propagation, such as oncogene Src which was shown to activate AMPK by regulating PKCα-LKB1 pathway (Rios et al. 2013), oncogene Myc and H-Ras^{V12} in osteosarcoma cell lines and astrocytes to activate AMPK to maintain cancer cell energy homeostasis (Liu et al. 2012, Rios et al. 2013), androgen receptor (AR) in prostate cancer cells to activate AMPK through the upstream CAMKK2 (Frigo et al. 2011, Massie et al. 2011, Tennakoon et al. 2014). Altogether, these studies have highlighted the inherent, context dependent, tumor supportive and tumor suppressive properties of the LKB1-AMPK signaling pathway (Liang and Mills 2013).

1.6.1 AMPK in Cancer metabolism and the unmet challenges.

Ever since AMPK has been shown to regulate lipid, cholesterol and glucose metabolism in specialized metabolic tissues, such as liver, muscle, and adipose tissue, it is considered as a very attractive target for drug discovery in metabolic diseases, like diabetes and cancer. Interestingly, it turns out that AMPK activation is vital for tumor cells to survive the dynamic tumor microenvironment that often encounters recurrent hypoglycemic stress (Kato et al. 2002, Jeon et

al. 2012). However, the mechanistic link through which AMPK exhibits tolerance to hypoglycemic situation and how AMPK contributes to the metabolic phenotype of cancer cells remains largely elusive. Besides, the proven role of AMPK in regulating PFK2 (a rate limiting enzyme of the glycolytic pathway) to facilitate glycolytic flux in cardiomyocytes (Marsin et al. 2002), much work is needed to understand the role of AMPK in adaptive glycolysis metabolism of cancer. It is, therefore, pertinent to investigate the role of LKB1-AMPK axis in the regulation of critical players of aerobic glycolysis, such as hexokinase (HK), pyruvate kinase (PK) and lactate dehydrogenase (LDH). Unraveling a mechanism that couples the AMPK signaling pathways with the downstream adaptive metabolic phenotype(s) that benefit cancer cells to survive the fluctuations under available nutrient conditions may suggest promising targeted therapeutic interventions.

1.7 Oncoviruses and tumor metabolism

Virus-derived malignancies have been shown to account for roughly 11% of global cancer burden (de Martel et al. 2012). The regulation of growth-signaling pathways by oncogenic viruses has been related to its potential in forming neoplastic tumors, however, till date, the precise molecular mechanism through which oncoviruses give rise to cancer remains largely elusive. Intriguingly, in comparison to transformed cells, oncovirus infections in mammalian cells have been shown to alter the central carbon metabolism to support biosynthesis to facilitate uninterrupted viral replication. Emerging evidences have revealed that the onco-modulatory features of viruses in mammalian cells are accomplished by the viral encoded oncoproteins (Noch and Khalili 2012, Levy and Bartosch 2016), which dynamically govern both cellular- and metabolic transformation.

1.7.1 Human Papilloma Virus (HPV) mediated carcinogenesis

Human papillomavirus (HPV) is one among many tumor-causing viruses that has been extensively studied to understand the molecular basis of tumorigenesis by the virally encoded oncoproteins. High-risk type–HPVs serve as a prime etiological agent in cervical carcinoma and account for 5% of global cancer burden (Arbyn et al. 2011). HPV-encoded E6 and E7 viral oncoproteins facilitate cellular transformation by inactivating potent tumor suppressors, P53 and RB; and on the other hand these viral oncoproteins stimulate components of growth signaling pathway, including the protein Kinase B (AKT), and mammalian target of rapamycin (mTOR) **(Fig. 1.6)** (Lu et al. 2004,

Menges et al. 2006, Zheng et al. 2008, Spangle and Munger 2010). The molecular events that follow post-HPV infection, such as HPV E6 oncoprotein dependent proteasomal degradation of tumor suppressor P53, could only immortalize the cancer cells but did not cause cellular transformation (zur Hausen 2009). Extensive studies in this area, however, have postulated an indispensable role of additional aspects in supporting HPV-mediated cellular transformation or carcinogenesis, such as recurring genetic alterations, immune deficiency, hormone imbalance, and adaptive metabolic remodeling (zur Hausen 2009, Moody and Laimins 2010).

1.7.2 HPV encoded oncoproteins in tumor metabolic remodeling and the unmet problems.

Cervical cancer cells have been shown to preferentially depend more on glycolytic metabolism. HPV encoded oncoproteins in cervical cancer cells were suggested to remodel the metabolism by modulating the pro-growth signaling pathways or through their interaction with central carbon metabolism enzymes. In the recent past, the loss of function of LKB1 in cervical cancer has been shown to facilitate the HPV encoded oncoproteins to acquire aerobic glycolysis by up-regulating the expression of glycolytic enzymes, such as Hexokinase 2 (HK2) in a c-Myc dependent manner (Zeng et al. 2016). Ectopic expression of LKB1 in HPV-positive cells was shown to inhibit the growth of cervical cancers by restoring their altered glucose metabolism. Besides, a study using yeast two-hybrid technique uncovered a physical interaction between high-risk type HPV16 encoded E7 oncoprotein and the glycolytic M2 isoform of pyruvate kinase enzyme. The interaction was shown to influence the quaternary structure of PKM2 by stimulating a disassociation of more active tetrameric PKM2 into less active dimeric form (Zwerschke et al. 1999). Tetrameric isoform of PKM2 is known to show a high affinity to substrate phosphoenol pyruvate, PEP, and actively convert PEP into pyruvate; whereas, the dimeric PKM2 that has low affinity to PEP allows accumulation of the upstream glycolytic intermediates, redirecting the reactions towards the biosynthetic pathway, yielding macromolecules that support rapid proliferation (Mazurek 2011). Nevertheless, more studies are required to comprehend the molecular events that regulate the metabolic phenotype of HPV-associated cancer cells (Cervical Carcinomas). Understanding the mechanisms through which HPV facilitates metabolic remodeling to nurture tumor progression is an interesting experimental model to try fathom causal association with oncogenesis and also draw parallels to understand metabolic reprogramming in other non-viral human cancers.

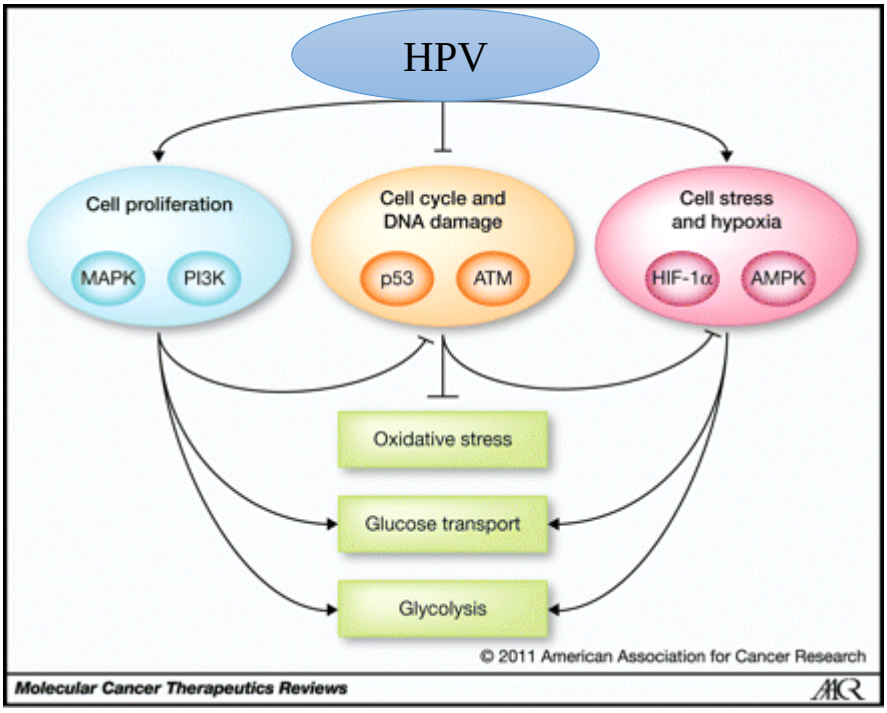

Fig. 1.6. Schematic portrayal of the HPV encoded Oncoprotein driven cell cycle and metabolic control. *HPV encoded oncoproteins accelerate cell proliferation through consecutively stimulating the PI3K and MAPK, pro-growth signaling cascade and prevent cell cycle arrest by negatively regulating p53 and ATM. Conversely, they rearrange the metabolic phenotype of virus-driven cancer cells with the support of HIF-1α and AMPK expression. The graphics was derived and modified from its original source (Noch and Khalili 2012).*

1.8 Cancer metabolism at a glance: Warburg and Beyond.

Cancer cells in contrast to their normal non-transformed counterparts consume a large amount of glucose and preferentially catabolize it into lactate under well-oxygenated conditions, a phenomenon known as aerobic glycolysis or Warburg effect **(Fig. 1.7)** (Warburg 1956). This unique theory was proposed nearly a century ago by Otto Warburg (Warburg 1924), which he later postulated as a shift in glucose metabolism due to the defect in the cellular mitochondrial respiratory pathway, forming a molecular basis for cellular transformation (Warburg 1956). With advances in the field of cancer biology, the importance of the theory weaned due to the lack of concrete support, however, it was later accepted that the altered glucose metabolism in tumors was a result of the consequence of cellular transformation and not a cause of tumorigenesis, as proposed

by Warburg (Seyfried and Shelton 2010). In the past two decades, the theory, however, has regained its significance in mainstream oncology research, ever since aerobic glycolysis was proven to be a hallmark feature of most of the cancer types studied. Further, the mechanism of aerobic glycolysis is considered to hold more promise for discovering novel diagnostic markers and therapeutic targets. Notably, the phenomenon of aerobic glycolysis is clinically exploited in imaging technique of positron emission tomography (PET), using the glucose analogue tracer^{18} fluorodeoxyglucose (FDG) (Weber et al. 2000) to diagnose and precisely locate the site of most primary and metastatic human cancers; as well as in the follow-up studies to monitor the effect of the drugs on tumors (Hsu and Sabatini 2008, Ben-Haim and Ell 2009).

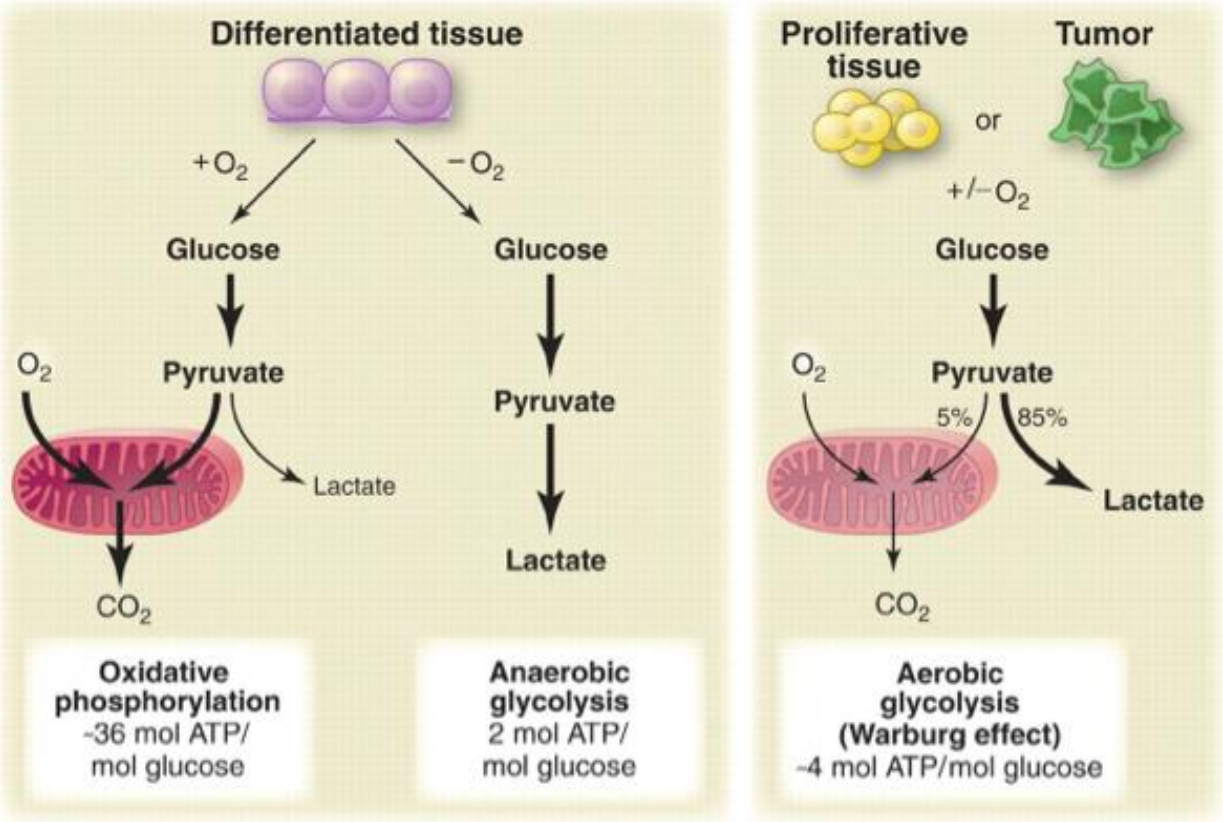

Fig. 1.7. Types of metabolism. *The diagramatic illustration depicts the characteristic differences in the metabolism of the differentiated, and proliferating cancer cells and also highlights the metabolic outcomes from oxidative phosphorylation, anaerobic and aerobic glycolysis (Vander Heiden et al. 2009).*

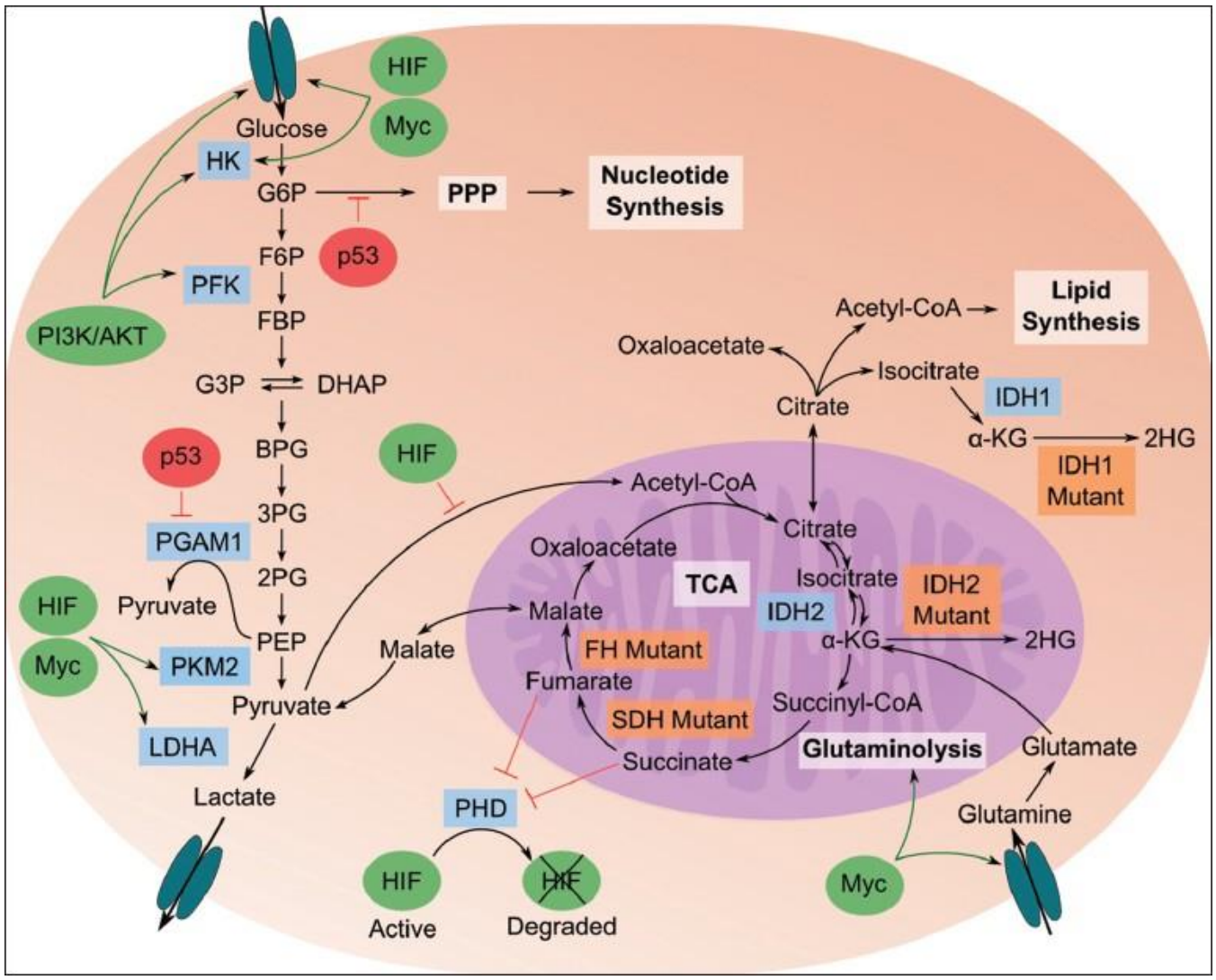

Fig. 1.8. Scheme of metabolic remodeling in cancer cells. *Pro-growth signaling pathway facilitates the HIF and Myc (transcription factors) dependent transcriptional activation of glycolytic enzymes to orchestrate aerobic glycolysis to obtain an enormous amount of ATP and precursors for the biosynthesis of nucleotides, protein, and lipid. Loss of function of tumor suppressors that serve as metabolic checkpoints, such as p53 and LKB1, provide additional benefits of facilitating aerobic glycolysis.*

1.8.1 Dissecting the molecular mechanistic link

Cellular transformation is the outcome of deregulated cell-signaling pathways majorly influenced by aberrant-genetic, -epigenetic, -environmental and/or infectious processes. The fundamental requisite of aerobic glycolysis in cancer cells is still an open debate and provides an adequate scope for active research. Emerging studies widely admit an intricate connecting-link between the oncogenic factors that collectively dictate cellular transformation and the metabolic rewiring of cancer cells that exhibit aerobic glycolysis (**Fig. 1.7 and 1.8)** (DeBerardinis et al. 2008, Hsu and Sabatini 2008, Jones and Thompson 2009, Vander Heiden et al. 2009, Sun et al. 2011, Faubert et al. 2014).

1.8.1.1 Aberrant oncogene signal and the altered metabolism

Among the wide range of oncogenes, aberrant receptor tyrosine kinases (e.g. FGFR, EGFR, PDGFR etc.) or non- receptor tyrosine kinases (e.g. Src, ABL etc.) and their subsidiary pro-growth signaling pathways, such as MAP-Kinase and PI3K-AKT-mTOR and downstream transcription networks, HIF and Myc, have been shown to contribute to the adaptive metabolic remodeling in tumour cells (Shackelford and Shaw 2009, Vander Heiden et al. 2009). The aberrant oncogenic signals in cancer cells remodel the expression of major glycolytic pathway housekeeping genes by switching to the alternate isoforms, such as, HK2 (Isoform 2 of Hexokinase), PKM2 (Isoform M2 of Pyruvate kinase) and LDHA (Lactate dehydrogenase A subunit), which have been proposed as critical regulators of Warburg effect (Fantin et al. 2006, Christofk et al. 2008, Patra et al. 2013) (Fig. 1.7 and 1.8). The preferential expression and oligomeric status of these enzymes are suggested to determine the flux of glycolysis and the fate of glucose. Besides their preferential expression these enzymes also undergo post-translational modifications by the oncogenic stimuli to provide an adaptive sustenance, metabolically and non-metabolically, to encourage proliferation of cancer cells that ultimately develop into a tumor (Hitosugi et al. 2009, Fan et al. 2011, Yang et al. 2012, Roberts et al. 2013).

1.8.1.2 Loss of function of tumor suppressor and metabolism remodeling

Besides deregulated oncogenic pathways, loss of function of many critical tumor suppressors supports the pro-growth metabolic phenotype of cancer cells. In this context, tumor suppressor

p53 and *LKB1* have gained ample interest, where P53 was shown to inhibit the pro-growth metabolism feature (aerobic glycolysis) by hindering PI3K-AKT-mTOR pathway, either through activation of TSC1/TSC2 complex to inhibit mTOR, or phosphate and tensin homolog (PTEN) to inhibit the PI3K pathway (Vousden and Ryan 2009, Berkers et al. 2013). Likewise, the loss of function mutation of LKB1 that fails to activate the bioenergetic sensor, AMPK was shown to reprogram the glycolytic metabolism of cervical adenocarcinoma (Zeng et al. 2016), and non-small cell lung cancer (Faubert et al. 2014).

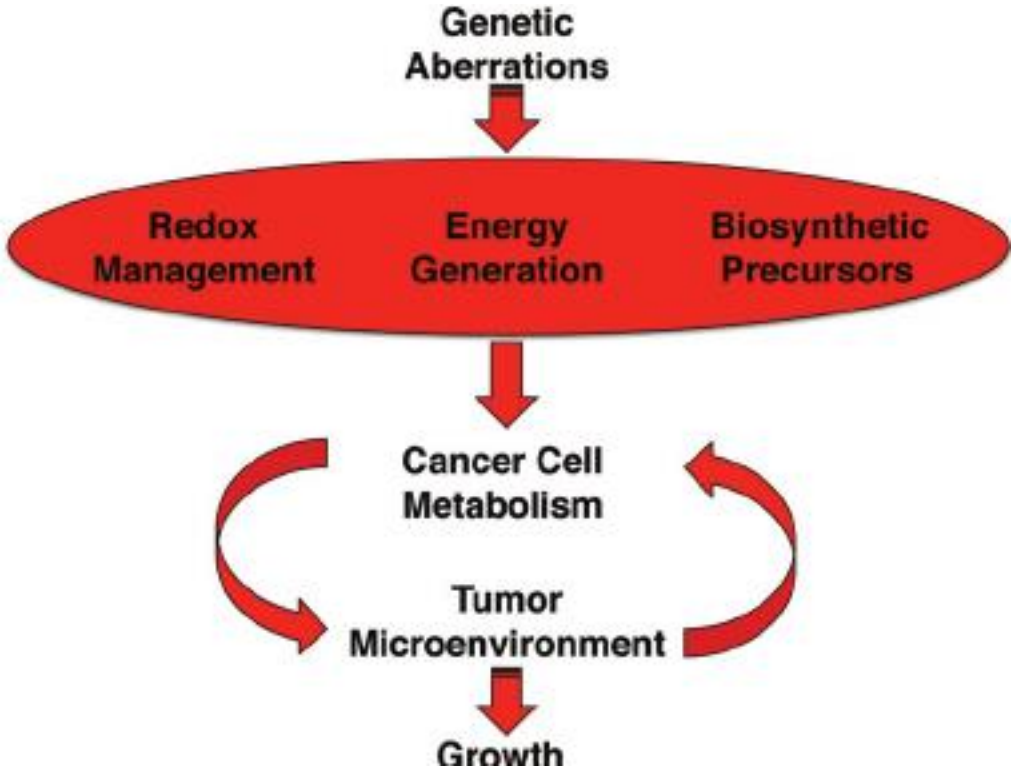

Fig. 1. 9. Schematic presentation of the cause and consequence of cancer cell metabolism. *Driver oncogenic mutations and intratumoral microenvironment principally shape the metabolic phenotype of cancer cells. Such acquired metabolic phenotype support the aggressive proliferation of cancer by providing them a multitude of advantages, such as biosynthetic precursors, rapid energy generation, and redox balance. The ensuing metabolic adaptations also affect the tumor microenvironment, potentially resulting in sporadic hypoxia, acidity, and/or nutrient starvation. Consequently, the tumor microenvironment exerts additional selective pressure on the cancer cells to adapt to the harsh conditions.*

1.8.1.3 Tumor-microenvironment in remodeling cell metabolism

The hostile intratumoral microenvironment faces numerous challenges; and as the primary tumor propagates it outpaces the diffusion limits of blood supply, giving rise to hypoxic (less oxygenated) conditions and hypoglycemia (low blood sugar supply) in the tumor microenvironment. In order to tolerate the hypoxic stress, cancer cells stabilize hypoxia-inducible transcription factor (HIF), which transactivate the early response genes, such as glucose transporters, nearly all glycolytic enzymes, and the inhibitors of mitochondrial oxidative phosphorylation (reviewed in Kaelin and Ratcliffe, 2008). In addition, HIF also stimulates angiogenesis by inducing the expression of delayed response genes, such as vascular endothelial growth factor (VEGF), and erythropoietin (EPO) to evade the hypoxic condition. However, the blood vessels that have been recruited to the site of hypoxia in primary tumors are highly disorganized and fail to deliver efficient blood supply, exposing the tumor mass to recurrent hypoxia (reviewed in Gatenby and Gillies, 2004). Compelling evidences suggest that the cancer cells that encounter recurrent hypoxia within the intratumoral microenvironment undergo a selection pressure to exhibit aerobic glycolysis **(Fig. 1.8)**. Cancer cells by choosing aerobic glycolysis acquire an advantage to survive and proliferate in the dynamic tumor microenvironment with recurrent hypoxia.

However, studies are scanty to understand how cancer cells adapt to the hypoglycemic condition. Further, it is also not clear, how nutrient insufficiency affects the metabolism of these cells, where the outcome of glucose depletion on aerobic glycolysis and associated key glycolytic enzymes remains elusive. Also, what remains unanswered is if these cells rely on glycolysis like their richly vascularized counterparts and how do the critical glycolytic enzymes respond to the condition of nutrient deprivation? Under physiological conditions, during nutrient deprivation, AMP-activated protein kinase (AMPK) - a serine/threonine protein kinase and its orthologues, are known to get activated by sensing bioenergetic stress of decreasing intracellular ATP and increasing intracellular AMP and ADP (Hardie et al. 2012). AMPK plays a pivotal role in conserving the cellular energetic homeostasis by remodeling the metabolic phenotype to resist nutritional stress and in maintaining physiological homeostasis. Consistent with the role of AMPK in a cell metabolic checkpoint, the importance of AMPK pathway in tumor metabolism and tumor progression has remained largely ambiguous.

1.9 Pyruvate kinase (PK) M: key enzyme in cancer cell metabolism

M2 isoform of pyruvate kinase (PKM2), a glycolytic terminal enzyme and one of the two alternate isoforms encoded by PKM gene, has emerged as a key factor that regulates aerobic glycolysis in cancer cells (Christofk et al. 2008, Mazurek 2011). PKM2 (pyruvate kinase muscle isoform 2) is an isoform of pyruvate kinase (PK; ATP-pyruvate 2-*O*-phosphotranferase, EC 2.7.1.40); catalyzes an irreversible rate limiting transphosphorylation reaction between phosphoenolpyruvate (PEP) and adenosine diphosphate (ADP) to generate pyruvate and ATP, accounting for net glycolytic energy (ATP) generation (Mazurek 2011). The expression of PKM isoforms has been assumed as mutually exclusive in nature, where out of 12 exons that PKM gene harbors, a primary transcript that retains exon 9 and skips exon 10 is PKM1 and the one that retains exon 10 is PKM2 (Noguchi et al. 1986, Noguchi et al. 1986). A preferential expression of PKM2 over other tissue-specific PK isoforms has been proposed as one of the metabolic hallmarks of cancer (Cairns et al. 2011, Chaneton and Gottlieb 2012), where preferential expression of PKM2 and its enzymatically inactive dimeric state serves a pivotal role in cancer growth by governing aerobic glycolysis (Mazurek et al. 2005, Gupta et al. 2010, Mazurek 2011, Iqbal et al. 2013, Iqbal et al. 2014, Wong et al. 2015).

1.9.1 PK gene isoforms, their expression regulation, and subcellular localization

Mammals have four isoforms of pyruvate kinase, namely PKR, PKL, PKM1 and PKM2 (Harada et al. 1978), encoded by two distinct pyruvate kinase genes (*PKLR* and *PKM*). The expression of PK isoforms is tightly regulated to exhibit tissue specificity and to meet the metabolic demands of tissues in which they are preferentially expressed. *PKLR* gene of *Homo sapiens*, positioned in chromosome 1q21, encodes for PKR and PKL isoforms in erythrocytes and liver by transactivating alternate promoters (Noguchi et al. 1987). *PKM* gene, located on chromosome 15q23, encodes alternative splice variants PKM1 and PKM2 with 12 exons, of which the PKM1 retains exon 9 and skips exon 10; whereas, PKM2 retains exon10 (Noguchi et al. 1986). The proteins encoded by the mutually exclusive exons represented in PKM1 and PKM2, thus differ by 23 of the 56-amino acid stretch at their C-terminal end. PKM2 expression dominates in cells with high proliferative capacities, such as embryonic cells, stem cells, and transformed cancer cells. Embryonic cells that show PKM2 expression gradually replace it with the tissue-specific isoforms during their

differentiation. Thus, the expression of PKM1 is demonstrated to be ideal for the cell types (tissues- of muscle, brain, and heart) that are highly differentiated and require a large quantity of energy (ATP) supply **(Fig. 1.10 and Table 1.2)**.

The expression of PKM gene is regulated by hormones (insulin, triiodothyronine-T3), cytokines (interleukin-2), mitogens, nutrient status and hypoxia. PKM gene possesses the putative consensus DNA binding sites for numerous transcription factors, including Sp1, Sp2, HIF-1alpha and Myc. Sp1/Sp2 and HIF1-alpha transcription factors are experimentally validated to regulate PKM2 expression (Iqbal et al. 2014). c-Myc controlled expression of hnRNPs' (heterogeneous nuclear ribonucleoproteins) has been shown to regulate the alternative splicing of PKM transcripts by repressing the presence of exon 9 and supporting the inclusion of exon 10 in PKM primary transcript to yield the PKM2 spliced isoform **(Fig. 1.10)** (David et al. 2010). Nuclear localization of PKM2 has been associated with various non-glycolytic functions and the nuclear presence of PKM2 is regulated by epidermal growth factor (EGF), Interleukin-3 (IL-3), lipopolysaccharide and hypoxia (details of non-glycolytic features are documented separately).

1.9.2 Structure and function of PKM2

PKM2 consists of 531 amino acids and its sequence partitioned into A-, B- and C-domains possesses characteristic functional features. The interface between A- and B-domain together forms the catalytic active site; whereas, C-domain involves allosteric activator- fructose 1, 6 bisphosphates (FBP) - binding site, and nuclear localization signal sequence (NLS) and intersubunit contact domain (ISCD). The protein sequence of PKM2 that stretches across the ISCD domain markedly differs from its alternate splice variant PKM1 by 23 amino acids, offering characteristic kinetic features (i.e. allosteric regulation by FBP) to PKM2, and its ability to associate with unique protein partners including phosphotyrosine proteins. PKM2 exists both in tetrameric and dimeric forms, however, all other PK isoforms (i.e. PKL, PKR, and PKM1) occur as tetramers. The A-domain of PKM2 monomers associate to give rise to a dimer and two dimers interact at the interface of ISCD (C-domain) to form the PKM2 tetramer. Tetrameric form of PKM2 has a higher affinity towards PEP, demonstrating more pyruvate kinase activity. Whereas, dimeric PKM2 shows a lower affinity towards PEP and remains nearly inactive at physiological conditions. PKM2, one of the rate-limiting glycolytic enzymes, is known to be allosterically

regulated, besides FBP, by other metabolic intermediates, like serine, phosphatidyl serine and succinylaminoimidazolecarboxamide ribose-5'-phosphate (SAICAR). Amino acids, such as alanine, phenylalanine, and tryptophan are known to allosterically inhibit the activity of PKM2.

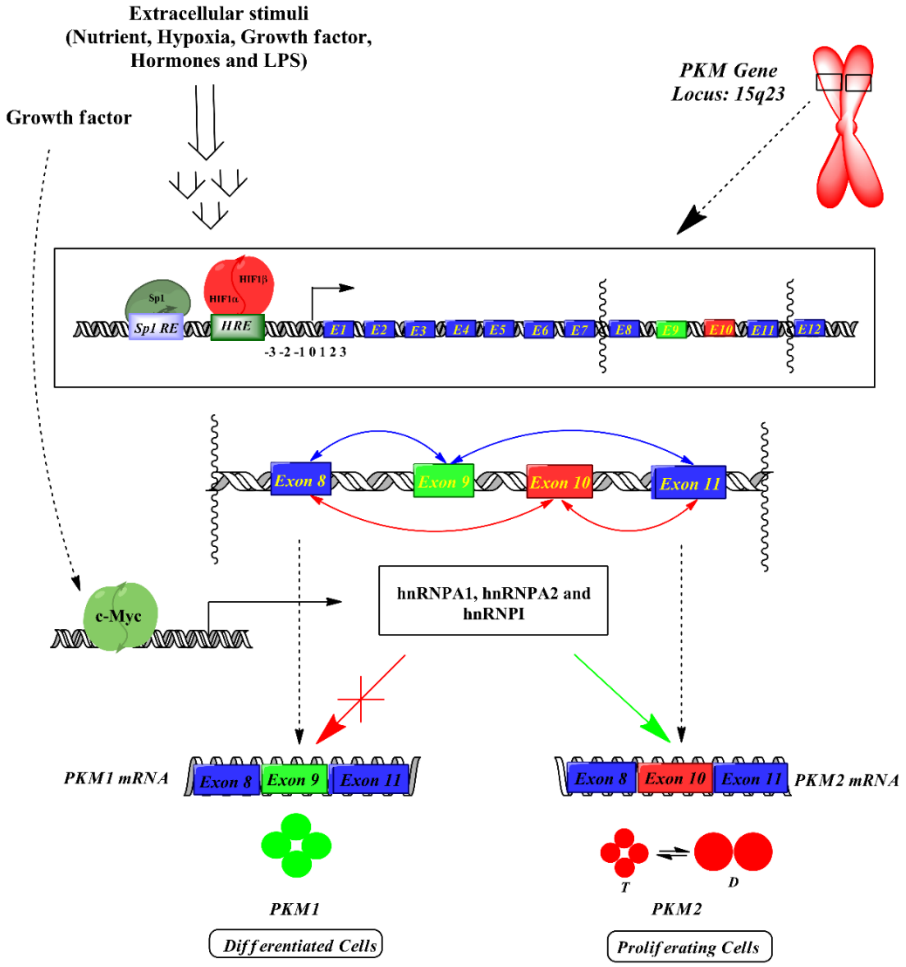

Fig. 1.10. Schematic representation of human PKM gene, its isoforms, and expression regulation. *PKM gene occupies q23 band position in chromosome 15, encoding 2 mutually exclusive alternative splice variants, PKM1 and PKM2. The expression of PKM is tightly regulated by various extracellular stimuli, such as nutrients, hypoxia, growth factors, hormones, cytokines and lipopolysaccharides (LPS) that largely influence glycolytic pathway. PKM promoter region harbors consensus binding sites for numerous transcription factors, including Sp1, Sp2, HIF-1α; and an extra level of c-Myc controlled expression of hnRNPs' (heterogeneous nuclear ribonucleoproteins) regulates the alternative splicing of PKM transcripts. Higher expression of*

hnRNPs represses the inclusion of exon 9, enabling the proliferating cells to preferentially express PKM2; whereas a low expression of hnRNPs includes exon 9 to express PKM1 (Chaneton et al. 2012, Keller et al. 2012, Iqbal et al. 2014).

Table 1.2. Molecular and biochemical properties of human pyruvate kinase enzyme

Molecular Features	Pyruvate kinase muscle isoforms			
	R	***L***	***M1***	***M2***
Name of gene	PKLR	PKLR	PKM	PKM
Chromosome no.	1	1	15	15
Size of gene	19.43 kb	19.43 kb	32.79 kb	32.79 kb
No. Of amino acids	574	543	531	531
Molecular mass of subunit (Da)	61,830	58,494	58,062	57,937
Cellular localization	Cytoplasmic		Cytoplasmic	Cytoplasmic & Nuclear
Tissue specificity	Erythrocytes	Liver	Brain, Heart, Skeletal Muscle etc.	Embryonic cells, Cancer cells, and Proliferating cells
Biochemical properties				
Subunit structure	Monomer and Tetramers			Monomer Dimer and Tetramer
Allosteric	Yes	Yes	No	Yes
Allosteric activator	FBP	FBP	----	FBP, Serine, SAICAR

1.9.3 Role of PKM2 in cancer

1.9.3.1 PKM2 in cancer metabolism

In recent years, PKM2 biology has generated enormous interest, especially with regards to its role in cancer. Numerous studies have revealed that the embryonic PKM2 reappears during tumor development, in order to help cancer cells achieve metabolic transformation required for cell division and other important cancer traits, like invasion and migration. Intriguingly, PKM2 has been shown to be vital in producing a unique metabolic phenotype of 'aerobic glycolysis' or 'Warburg effect' in cancer cells. Despite an elevated PKM2 expression, cancer cells choose to accumulate enzymatically inactive dimeric form of PKM2 by promoting subunit dissociation. Low activity dimeric PKM2 retards the final step of glycolysis, thus resulting in the pile-up of glycolytic intermediates, which are a precursor of pentose phosphate pathway (PPP) for biomass production, in addition to a balanced supply of ATP via glycolysis. The dimer: tetramer ratio of PKM2 in cancer cells is influenced by numerous factors, like drop in concentration of allosteric activator FBP, competitive binding of tyrosine phosphorylated proteins at the FBP-binding pocket (Christofk et al. 2008), dominant negative mutation at ISCD region (Anitha et al. 2004), interaction with oncoproteins (e.g. HPV16 E7 Oncoprotein) and remarkably by post-translational modifications (PTMs) (Gupta and Bamezai 2010, Iqbal et al. 2014). Amongst the PTMs of PKM2, phosphorylation of Tyr105 residue is carried out by oncogenic tyrosine kinases (e.g. FGFR1, BCR-ABL, JAK2). In addition, acetylation of lysine-305, oxidation of cysteine-358 have been shown to facilitate the formation of dimeric PKM2, eventually contributing to aerobic glycolysis in the tumor (Gupta et al. 2014, Iqbal et al. 2014). In a study carried out by Iqbal et al, insulin was shown to regulate cancer metabolism by induction of high expression of PKM2, regulated by PI3K-mTOR-HIF1-α pathway, along with simultaneous inactivation of the same through ROS up-regulation, depicting a dual regulatory control within a cell to favor aerobic glycolysis and anabolism **(Fig. 1.11)** (Iqbal et al. 2013). Further, it was shown that cancer cell treated with DNA damaging agent could stimulate PKM2 Tyr105 phosphorylation and redirect the glycolytic flux towards pentose phosphate pathway (PPP) for anabolism (Kumar and Bamezai 2015). Recently, PARP-14 has been shown to contribute to aerobic glycolysis by negatively regulating JNK-1 (pro-apoptotic factor) and preventing Thr365 phosphorylation of PKM2 and its activation.

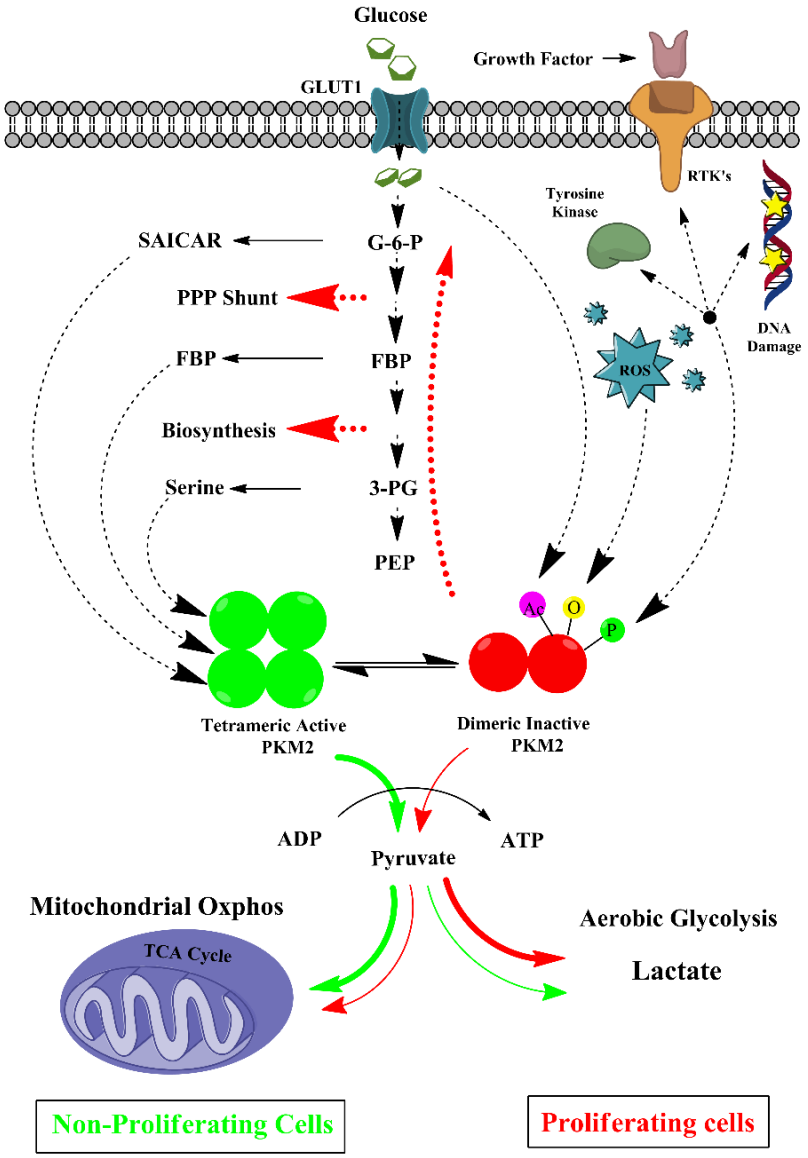

Fig. 1.11. Schematic illustration of the features that coordinate the dimeric and tetrameric state of PKM2 isoform and its resultant impact on metabolic phenotypes. Oncogenes, ROS, nutrient status and post-translational modifications of PKM2 facilitate enzymatically inactive dimeric state (Red), which in turn reprogram the glycolytic pathway to exhibit aerobic glycolysis, essential for the biosynthesis of macromolecules to support cell growth and rapid proliferation. Conversely, FBP, SAICAR, and serine promote an active tetrameric state of PKM2 (Green), which couples glycolysis with mitochondrial oxidative phosphorylation (OXPHOS) to yield ample amount of

energy to meet the demands of differentiated cells. Red arrows in the illustration indicate the flux of the glycolysis and fate the glycolytic intermediates, as a result of the dimeric state of PKM2. Green arrows signify the path of glycolytic intermediates and flux governed by the tetrameric PKM2. Abbreviations: PPP - pentose phosphate pathway; SAICAR - succinylaminoimidazolecarboxamide ribose-5'-phosphate; G-6-P-Glucose-6-phosphate; FBP - fructose-1, 6-bisphosphate, 3-PG - 3-phosphoglyceric acid; PEP - phosphoenol pyruvate; RTKs - receptor tyrosine kinase; TCA - tricarboxylic cycle; ROS - reactive oxygen species.

1.9.3.2 Non-metabolic attributes of PKM2 in cancer

Besides regulating cancer metabolism, PKM2 plays an important role in tumor progression via non-metabolic attributes e.g. gene regulation. A study carried out by Lee et al, was first of its kind to demonstrate PKM2 as a transcription co-activator that interacted with Oct-4 (transcription factor) to enhance transactivation of its target genes that retain pluripotency in embryonic stem cells (Lee et al. 2008). Several other studies also showed that PKM2 could act as a transcriptional co-activator of, HIF1α, the signal transducer and activator of transcription (Stat-3), β-catenin and aryl hydrocarbon receptor (AhR). This transcriptional co-activation results in expression of target genes involved in regulation of cell proliferation, survival and metabolic reprogramming **(Fig. 1.12)**.

On the other hand, emerging studies propose that physical binding of PKM2 with a group of transcription factors could regress their transactivation in a context-dependent manner. As a proof of concept, Atsushi Hamabe *et al.* revealed that cancer cells undergoing epithelial–mesenchymal transition (EMT) direct PKM2 inside the nucleus where it binds to TGFβ induced factor homeobox 2 (TGIF2) (Hamabe et al. 2014). PKM2 bound to TGIF2 results in repression of E-cadherin (CDH1) expression, thus, allowing epithelial to mesenchymal transition. A Recent study by Li Xia *et al.* unraveled yet another co-repressor feature, where PKM2 interacted with P53 and repressed it to transactivate cell cycle inhibitors (*p21* and *p27*) upon exposure of cancer cells to DNA damaging agents (Xia et al. 2016). This study provides a plausible explanation for the resistance shown by cancer cells against DNA damaging drugs.

Another important non-metabolic attribute of PKM2 associated with tumor progression is by virtue of its protein kinase activity. Inactive dimeric PKM2 acts as a protein kinase, whereas the tetramer behaves as an enzyme, pyruvate kinase. Gao *et al.* found that the dimeric PKM2 with PEP as phosphate donor phosphorylates Stat3 at Tyr705 residue to transactivate factors that promote cell proliferation (Gao et al. 2012). Another study by Yang *et al.* showed that EGF stimulation mobilized dimeric PKM2 into the nucleus to interact and phosphorylate Thr11 of H3 to control the expression of c-Myc and cyclin D1 in cancer cells (Yang et al. 2012). Further, studies by Lv *et al.* describe that acetylation of PKM2 at lysine 433 residue, mediated by p300 acetyltransferase in response to diverse mitogenic and oncogenic signals, enable PKM2 to localize inside the nucleus and carry out Stat3 and H3 phosphorylation and transactivation, leading to expression of proteins that promote cell proliferation **(Fig. 1.12)** (Lv et al. 2013).

Apart from its role in cell cycle initiation, PKM2 supports cell cycle progression by governing the precise chromosomal segregation by phosphorylating Tyr207 residue of spindle checkpoint protein Bub3. Recently, binding of SAICAR with PKM2 has been shown to enhance its protein kinase activity, where several novel putative protein substrates were reported to be phosphorylated by SAICAR–PKM2 complex. Earlier studies by Mazurek *et al.* have reported that the individuals with gastrointestinal and colorectal tumors secreted dimeric PKM2 in blood plasma and in stool, resulting in the use of dimeric PKM2 as a diagnostic and prognostic marker. However, the mechanism by which cancer cells secrete dimeric PKM2 in circulation and its precise function in cancer progression has remained obscure (Mazurek 2011). A Recent study in this direction has shown the involvement of secreted dimeric PKM2 in tumor angiogenesis by stimulating angiogenic endothelial cell proliferation, migration, and cell- ECM adhesion. In addition, the non-secreted intracellular dimeric PKM2 of cancer cells promotes angiogenesis by transactivating HIF1α to enable the expression of vascular endothelial growth factor (VEGF), a proangiogenic factor.

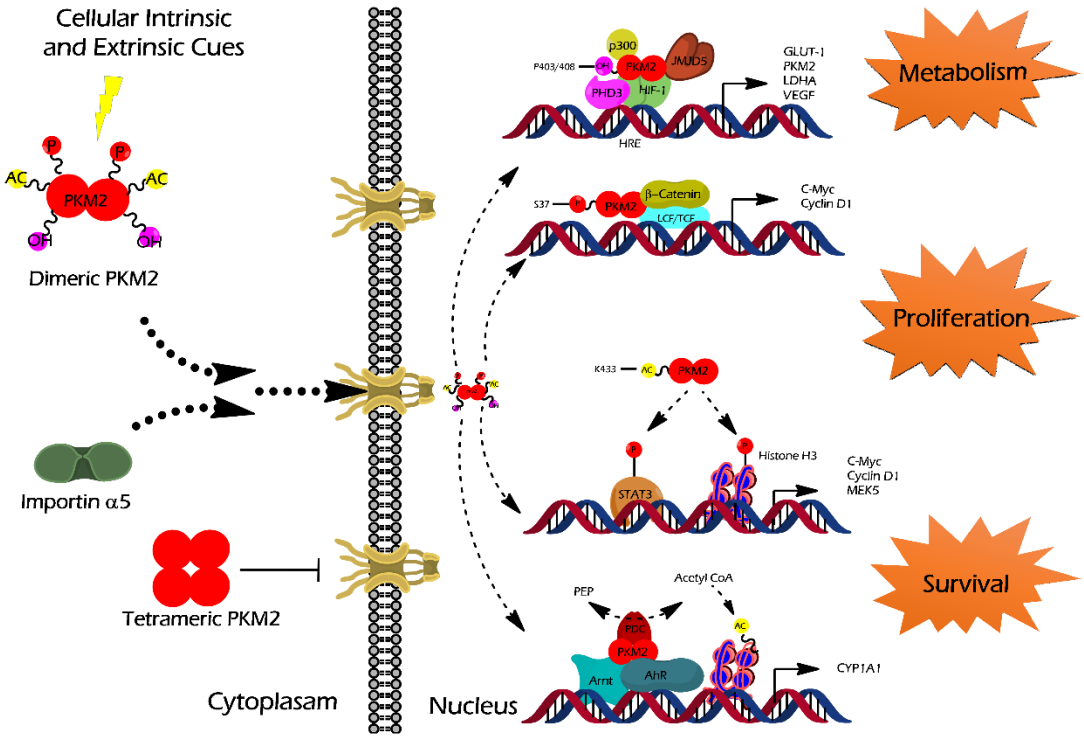

Fig. 1.12. Schematic representation of the non-glycolytic nuclear function of PKM2. α- importin mobilizes post-translationally modified PKM2 dimer inside the nucleus in response to the distinct extrinsic stimuli. In brief, nuclear PKM2 exhibits the characteristic features of a transcriptional co-activator and a protein kinase to enhance the transactivation of HIF1α, β-catenin, STAT3 and AhR, transcription factors. The transactivation of mentioned transcription factors together code for the factors that control, cell proliferation, metabolism, and survival. Abbreviations: OH – hydroxylation; Ac – acetylation. P – phosphorylation; JMJD5 - Jumonji C domain-containing dioxygenase; HIF1- hypoxic inducible factor 1; PHD3 – HIF prolyl-hydroxylase 3; HRE – hypoxic response elements; LCF/TCF – lymphoid enhancing factor/T-cell factor; LDHA – lactate dehydrogenase A; GLUT1 – glucose transporter 1; PDK1 – pyruvate dehydrogenase kinase; STAT 3 – signal transducer and activator of transcription 3; MEK5 - Mitogen-Activated Protein Kinase Kinase 5; CYP1A1 - cytochrome P450 family 1 subfamily A member 1; Ahr – aryl hydrocarbon receptor; Arnt – aryl hydrocarbon receptor nuclear translocator.

1.10 PKM2 as a therapeutic target in cancer and the strategies to improve its efficacy.

Considering the variety of benefits that PKM2 confers to the cancer cells, it has turned out to be a promising therapeutic target. Several reports have suggested strategies that target PKM2 to retard tumor progression. Natural compounds like resveratrol, gemcitabine, and shikonin have been shown to inhibit PKM2 (Chen et al. 2011, Iqbal and Bamezai 2012, Pandita et al. 2014). Small interfering RNA (siRNA) against PKM2 has been shown to significantly abrogate the tumor growth and induce caspase-dependent apoptosis in cancer cells, both *in vitro* and *in vivo*. It is also reported that silencing of PKM2 may have a synergistic effect with anticancer drugs (Kumar and Bamezai 2015). Synthetic small molecule inhibitors ((N-(3-carboxy-4- hydroxy) phenyl 1-2, 5,-dimethylpyrole) and Arava), identified through high throughput screen, have been shown to selectively target PKM2 activity. In addition, cell permeable structural analogs of FBP, TEPP-46 (ML265; thieno-[3,2-b]pyrrole[3,2-d]pyridazinone) and DASA-58 (ML203; substituted N,N′-diarylsulfonamide), that drive PKM2 tetramer formation in cancer cells, have been shown to inhibit human lung carcinoma progression in xenograft mouse models (Gupta et al. 2014, Iqbal et al. 2014) .

On the contrary, recent studies have highlighted the limitation that exist in the strategy of targeting PKM2 in cancer. Where the knockdown of PKM2 *in vitro* and *in vivo* has been reported to affect proliferation and viability of cancer cells of different tissue origin heterogeneously (Christofk et al. 2008, Goldberg and Sharp 2012, Cortés-Cros et al. 2013, Israelsen et al. 2013), and has raised doubts about the efficacy of targeting PKM2 in tumors at a global scale. To find out what determines such a heterogeneous response, more studies are required to examine the key features that confer protection against PKM2 knockdown induced growth inhibition and cell death in cancer cells. A deep insight, in this context, may answer some of these contradictions and rationalize a promising therapeutic strategy to enhance the efficacy of PKM2 targeting in cancer cells, a subject partly researched on in the present work.

CHAPTER-2
Aims and objectives

Chapter-2

2.1 Rationale of the Study

Cancer cells acquire a unique metabolic signature of aerobic glycolysis (Warburg effect) and undergo metabolic fine-tuning to feast on glucose and excrete a major chunk as lactate (Warburg 1956). Preferential expression of glycolytic enzymes like HK2 (Isoform 2 of Hexokinase), PKM2 (Isoform M2 of Pyruvate kinase) and LDHA (Lactate dehydrogenase A subunit), by cancer cells has been proposed to result in the Warburg effect. Amongst all, PKM2 has emerged as a key factor that regulates aerobic glycolysis in cancer cells (Christofk et al. 2008, Mazurek 2011). The preferential expression of PKM2 and its enzymatically inactive dimeric state serves a pivotal role in cancer growth by governing aerobic glycolysis (Mazurek et al. 2005, Gupta et al. 2010, Mazurek 2011, Iqbal et al. 2013, Iqbal et al. 2014, Wong et al. 2015).

Growing body of evidence highlights that the rewiring of cancer metabolism provides a multitude of advantages including, precursors for macromolecular synthesis, rapid ATP generation, and rapid proliferation (Vander Heiden et al. 2009, Cairns et al. 2011). Moreover, due to their high proliferation rate and poor vasculature, malignant tumors frequently outpace the diffusion limits of blood supply, and often face the challenge of hypoglycemia. This situation raises an important question of how nutrient insufficiency affects the metabolism of these cells. Also, what remains unanswered is whether these cells rely on glycolysis, like their richly vascularized counterparts and how do the critical glycolytic enzymes respond to nutrient deprivation?

In the recent past, the axis of LKB1-AMPK has been shown to provide tolerance to nutrient deprivation in cancer cell (Kato et al. 2002, Jeon et al. 2012, Liang and Mills 2013), however, how AMPK contributes to metabolic phenotype of cancer cells; and the mechanistic link through which AMPK exhibits tolerance to hypoglycemic situation remains largely elusive. Thus, as part of this thesis work, an attempt was made to unravel the effect of AMPK signaling pathway on adaptive metabolic phenotype and its outcome which made cancer cells survive the fluctuations of available nutrient conditions.

Further, understanding the mechanisms through which HPV facilitates metabolic remodeling to nurture tumor progression in nutrient replete condition and how it survives nutrient deprived condition provides a model to understand metabolic reprogramming in other non-viral human cancers. Since, nearly 20% of HPV-driven cervical adenocarcinoma and 30% of lung adenocarcinoma have been shown to lack LKB1 expression or harbor a loss of functional mutation (Hezel and Bardeesy 2008, Wingo et al. 2009, Marcus and Zhou 2010) that failed to activate AMPK, an attempt was made to understand the impact of HPV-18 encoded oncoprotein on metabolic remodeling in proliferating tumor cells. In addition, it was proposed to understand how HPV-driven cervical carcinomas tolerated nutritional stress in absence of LKB1expression. It was expected that to rationalize therapeutic strategies based on unique glycolytic metabolism of cancer cells in association with the cellular status of the LKB1-AMPK pathway, could prove meaningful.

With this background, following Aims and Objectives were proposed for the Study:

2.2 Aims and Objectives

1. Investigate the role of AMPK signaling in regulation of rate limiting glycolytic enzyme(s) that are critical to tumor metabolism (Warburg Effect).

2. Examine the impact of AMPK signaling and HPV 18 encoded E6 Oncoprotein in regulation of PKM gene and their resultant influences on an overall glycolytic flux, pro-cancerous metabolic features and growth of tumors in *in-vitro* assays.

3. Characterize the cellular localization pattern, and the interactome of PKM gene splice product- PKM1, along with its functional relevance, compared to PKM2.

CHAPTER-3
Materials & Methods

Chapter-3

Materials and Methods

3.1 Mammalian Cell Culture

MCF-7 (Human Breast Adenocarcinoma), MDA-MB-231 (Human Breast Adenocarcinoma), PC-3 (Human Prostate Adenocarcinoma), H1299 (Non-Small Cell Lung Carcinoma), A549 (Lung Carcinoma), A431 (epidermoid carcinoma), HeLa (Human Cervical Adenocarcinoma), HEK293T (Human Embryonic Kidney Cell line) and L6 (Rat Skeletal Muscle) were procured (ATCC, USA) or (NCBS, INDIA) and were cultured in DMEM (Sigma, USA), supplemented with 1% penicillin/streptomycin (Sigma, USA), 10 % (Vol./Vol.) heat inactivated Fetal Bovine Serum (Gibco - Life technologies) and maintained in the incubator at 37°C supplied with 5% CO_2 (Thermo Scientific Heraeus® - UK) in a humidified atmospheric condition. Cells were grown up to a monolayer and passaged routinely on every 3rd or 4th day based upon their confluence. Detailed procedure of cell culture medium preparation, cryopreservation and cell counting using hemocytometer; and cell passaging methods are provided in appendix-I. Glucose deprivation was accomplished by culturing the cells in glucose free DMEM media (Sigma) supplemented with antibiotics and 10 % dialyzed FBS (Gibco - Life technologies), supplemented in addition with required glucose concentration.

3.2 RNA Extraction, cDNA preparation and RT-PCR (qRT and Semi-quantitative PCR)

Total RNA isolated from cells with TRI Reagent (Sigma-Aldrich) was reverse transcribed into cDNA, using Superscript® III Reverse Transcriptase kit (Life Technologies). qRT-PCR analysis was carried out in BIORAD CFX96 Touch^{TM} Real-time PCR Detection system, using SYBR Green PCR master mixture (Applied Biosystems). The relative gene expression was calculated using the comparative C_T method ($2^{-\Delta\Delta CT}$). Results were analyzed and presented as fold change after normalizing with the control group, where actin served as an endogenous control. Primers used for

the RT-PCR analysis are mentioned in **Table 3.1**. For semi-quantitative RT-PCR, images of PCR products resolved in 2-3% agarose gel were obtained by SYNGENE gel documentation system and densitometric analysis performed using ImageJ software (http://imagej.nih.gov/ij/) to calculate the changes in the ratio of gene expression, which were plotted after normalizing with the expression of ACTINB (ACTB).

3.3 Semi-quantitative RT-PCR assay to examine PKM1/PKM2 mRNA proportion

RNA was isolated from 2 X 10^6 cells using TRI Reagent (Sigma-Aldrich). 2µg from total RNA was subjected to DNAse I (Applied Biosystems) treatment to remove contaminating DNA and was reverse transcribed into cDNA, using Superscript® III Reverse Transcriptase kit (Life Technologies). Alternatively, spliced transcripts, PKM1 (exon 9 included) and PKM2 (exon 10 included) were PCR amplified together, using primers specific to Exon 8 and Exon 11 (Exon-8 5′-GAAACAGCCAAAGGGGACT-3′ and Exon-11 5′-CATTCATGGCAAAGTTCACC-3′) as described earlier (Clower et al. 2010). The amplified products were equally divided into 2 aliquots (approx. 20 µl), one of which was subjected to restriction digestion with Ale I restriction enzyme and the other one served as an uncut control. Ale I specifically cuts at exon 10 of PKM2 and leaves PKM1 undigested. Details of restriction mapping with AleI restriction enzyme to examine the proportion of PKM1 and PKM2 expression in human cancer cells are provided in appendix-I. Images of semi-quantitative RT-PCR products resolved in 3 % agarose gel were obtained by SYNGENE gel documentation system. Densitometry analysis was performed using ImageJ software (http://imagej.nih.gov/ij/) to calculate the percentage of PKM isoform expressions in human cancer cells.

3.4 Cloning and Site Directed Mutagenesis

The Coding Sequences of AMPKα2, c-Myc, PKM1 and PKM2 isoforms were PCR amplified from cDNA prepared using H1299 cells, using the primers mentioned in **Table. 3.2**. The PCR amplified fragments were sequenced to cross-check the background mutations and were cloned in pcDNA™3.1/myc-His $^{(-)}$ A vector **(Table. 3.3)**. Expression vector pcDNA™3.1/myc-His ($^-$) A,

Lentiviral transfer vector (pLKO.1), and packaging vectors (psPAX and pMD2.G), were a kind gift from Prof. Shyamal K Goswami and Dr. Goutam K Tanti (SLS, JNU, New Delhi). Full-length constructs of 'pcDNA-LKB1-HA tag' was a generous gift from Dr. Shaida Andrabi (University of Kashmir, Srinagar, J&K). Lentiviral transducing vector, pLKO.1 encoding shPKM1 and shPKM2 was a generous gift from Dr. Marta Cortes Cros (Novartis, Basel). LentiViral shRNA vectors targeting the expression of AMPKα1 and α2 ((pLKO.1 shAMPKα1 -TRCN0000000861) and (pLKO.1shAMPKα2 - TRCN0000002171 were procured from Sigma-Aldrich. Lentiviral shRNA vector targeting the expression of c-Myc (pLKO.1 shc-Myc) was constructed in-house, using synthetic oligonucleotides mentioned in Table 2. Site Directed
Mutagenesis (SDM) was performed using Quick Change Site directed mutagenesis Kit (Agilent Technologies), according to the manufacturer's protocol. In brief, Wild Type (WT) construct of AMPKα2 was truncated and constitutively active AMPKα2 T172D mutant was generated, using the site directed mutagenesis **(Table. 3.3)**.

3.5 Mammalian transfection and Stable gene expression

To establish stable gene expression, constructs (pcDNA – PKM1, PKM2, C-Myc & LKB1) were transfected using Lipofectamine® LTX reagent (Life Technologies), as per the manufacturer's instruction. Briefly, after 48 hours of the post transfection, cells were selected in G418 (1 mg/mL) containing selection medium for 2 weeks to generate stable cell lines.

3.6 Lentivirus production and stable gene knockdown

For stable gene knockdowns, the lentiviral particles were generated as described previously (Cortes-Cros et al. 2013). In brief, HEK 293T cells were transfected with transfer vector (LKO.1) harboring shRNAs and psPAX & pMD2.G packaging vectors, using Lipofectamine® LTX. After 48 hours of post-transfection viral particles were harvested and used to infect the target cells. Infected cells were selected in puromycin (2µg/mL) containing DMEM medium for the course of 7 days for generating cell lines with stable gene knockdown.

Table 3.1. List of primers used in RT-PCR to analyze the gene expression status.

Name	Sequence (5' - 3')	Amplicon Size
HK1 Forward	TACTTCACGGAGCTGAAGGATG	197 bp
HK1 Reverse	AGCCATCAGGAATGGACCTT	
HK2 Forward	CCAACCTTAGGCTTGCCATT	196 bp
HK2 Reverse	CTTGGACATGGGATGGGGTG	
PKM Exon 9 Forward	AGGCAGCCATGTTCCAC	150 bP
PKM Exon 9 Reverse	TGCCAGACTCCGTCAGAACT	
PKM Exon 10 Forward	TGCAATTATTTGAGGAACTCC	102 bP
PKM Exon 10 Reverse	CACTGCAGCACTTGAAGGAG	
LDHA Forward	GACCTACGTGGCTTGGAAGA	176 bp
LDHA Reverse	TCCATACAGGCACACTGGAA	
LDHB Forward	CCAACCCAGTGGACATTCTT	219 bp
LDHB Reverse	AAACACCTGCCACATTCACA	
c-Myc Forward	GCTTTTTTGCCCTGCGTGAC	200 bp
c-Myc Reverse	CGCACAAGAGTTCCGTAGC	
PTBP1 Forward	ACGGACCGTTTATCATGAGC	194 bP
PTBP1 Reverse	CATCAGGAGGTTGGTGACCT	
hnRNPA1 Forward	TTGTGAACTCAGCCAAGCAC	241 bP
hnRNPA1 Reverse	CAGCGTCACGATCAGACTGT	

hnRNPA2/B1 Forward	GGCTACGGAGGTGGTTATGA	241 bP
hnRNPA2/B1 Reverse	CCCATGGCAAATAGGAAGAA	
PGC1 A Forward	TGTCACCACCCAAATCCTTATTT	75 bP
PGC1 A Reverse	TGTGTCGAGAAAAGGACCTTGA	
NRF1 Forward	CCATCTG GTGGCCTGAAG	93 bp
NRF1 Reverse	GTGCCTGGGTCCATGAAA	
NRF2 Forward	ACACGGTCCACAGCTCATC	83 bp
NRF2 Reverse	TGTCAATCAAATCCATGTCCTG	
TFAM Forward	GAACAACTACCCATATTTAAAGCTCA	95 bp
TFAM Reverse	GAATCAGGAAGTTCCCTCCA	
COI Forward	TTCTGACTCTTACCTCCCTCTC	110 bp
COI Reverse	TGGGAGTAGTTCCCTGCTAA	
ND3 Forward	CCACAACTCAACGGCTACATA	143 bp
ND3 Reverse	AGGAGGGCAATTTCTAGATCAAA	
ATP6 Forward	TAGCCCACTTCTTACCACAAGGCA	138 bp
ATP6 Reverse	TGAGTAGGTGGCCTGCAGTAATGT	
Actin Forward	ACTCTTCCAGCCTTCCTTC	171 bp
Actin Reverse	ATCTCCTTCTGCATCCTGTC	

Table 3.2. List of primers and shRNA oligo's used for gene expression, Site-directed mutagenesis and shRNA transducing vectors.

Name of Gene	Primers	Restriction Site
PKM1/2 Forward	ATATGAATTCATGTCGAAGCCCCATAGTGAAG	EcoRI
PKM1/2 Reverse	ATATGGATCCCGGCACAGGAACAACACGCA	BamHI
AMPKa2 Forward	ATATGGATCCATGGCTGAGAAGCAGAAGCA	BamH1
AMPKa2 312 Reverse	ATATAAGCTTATATAAACTGTTCATTACTTCTG ATTCTGT	HindIII
AMPKa2 Reverse	ATATAAGCTTACGGGCTAAAGTAGTAATCA	HindIII
c-Myc Forward	ATATCTCGAGATGCCCCTCAACGTTAGCTTC	Xho I
c-Myc Reverse	ATATAAGCTTCGCACAAGAGTTCCGTAGC	Hind III
LKB1 Forward	ATATCTCGAGATGGAGGTGGTGGACCCGCA	XhoI
LKB1 Reverse	ATATGAATTCCTGCTGCTTGCAGGCCGACA	EcoRI
	shRNA Custom designed Oligo's	
shc-Myc	CCGGCCTGAGACAGATCAGCAACAACTCGAGT TGTTGCTGATCTGTCTCAGGTTTTTG	AgeI
shc-Myc	AATTCAAAAACCTGAGACAGATCAGCAACAA CTCGAGTTGTTGCTGATCTGTCTCAGG	EcoRI
	Site Directed Mutagenesis Primers	
AMPKα2 T172D Forward	TTTCTGAGAGATAGTTGCGGA	NIL
AMPKα2 T172D Reverse	TCCGCAACTATCTCTCAGAAA	NIL

Table 3.3. Constructs generated and used in the study and their restriction sites

Name of Vector	Gene of Interest	Restriction Site I	Restriction Site II	Vector Type
pcDNA™3.1/myc-His (-) A	PKM1	EcoRI	BamHI	Mammalian expression
pcDNA™3.1/myc-His (-) A	PKM2	EcoRI	BamHI	Mammalian expression
pcDNA™3.1/myc-His (-) A	AMPKα2	BamHI	Hind III	Mammalian expression
pcDNA™3.1/myc-His (-) A	AMPKα2 T172D	BamHI	Hind III	Mammalian expression
pcDNA™3.1/myc-His (-) A	LKB1	XhoI	EcoRI	Mammalian expression
pcDNA™3.1/myc-His (-) A	c-Myc	XhoI	Hind III	Mammalian expression
pLKO.1	shPKM1	AgeI	EcoRI	Mammalian Expression, Lentiviral, RNAi
pLKO.1	shPKM2	AgeI	EcoRI	Mammalian Expression, Lentiviral, RNAi
pLKO.1	shc-Myc	AgeI	EcoRI	Mammalian Expression, Lentiviral, RNAi
pLKO.1	shAMPKα1	AgeI	EcoRI	Mammalian Expression, Lentiviral, RNAi,
pLKO.1	shAMPKα2	AgeI	EcoRI	Mammalian Expression, Lentiviral, RNAi,
pGEX-4T-1	PKM1	BamH 1	Xho 1	Bacterial expression
pGEX-4T-1	PKM2	BamH 1	Xho 1	Bacterial expression

3.7 Expression, purification of Recombinant PKM1 or PKM2 (rGST-PKM1 or rGST-PKM2)

For protein expression, competent E.coli BL21 strain was transformed with pGEX4T1 constructs habouring cDNA of M1 or M2 isoform of PKM gene; and grown overnight in 10 ml LB, luria broth, containing 100µg/ml ampicillin at 37ºC in an orbital shaker. Secondary culture was scaled-up by inoculating 10% of overnight culture in a fresh 100 ml LB media for 2-3 hours. Upon achieving a density of OD_{600nm}, 1mM of IPTG was added into the secondary culture and incubated at 20ºC for 10-12 hours in a shaker to induce protein expression. Following the protein expression induction, cells were harvested and sonicated (5 sets of pulse with 25% amplitude, 15 sec ON and 45 Sec OFF cycle) in 5-10 ml of GST pull down buffer (50 mM Tris-HCL pH8, 500 mM NaCl, 10 % glycerol and with 1mM PMSF). The resultant slurry was cleared by centrifugation and the soluble protein fraction was incubated with GST beads (Sigma Aldrich). The GST bead bound protein complex was washed thrice with GST pull down buffer and the protein eluted by adding 10mM reduced glutathione. The purity of recombinant protein was examined by resolving it in a 10% SDS gel and activity measured by LDH coupled assay (described elsewhere in detail).

3.8 Glycolytic Enzyme Assays and Glycerol Gradient Centrifugation.

Hexokinase (HK) activity was measured through an enzyme glucose-6-phosphate dehydrogenase (G6PD) coupled assay, following the reduction of NADP. 5 µg of whole cell protein lysate was added with the mixture of 100 mM Tris-HCl (pH 8), 5 mM $MgCl_2$, 100 mM glucose, 0.8 mM ATP, 1 mM NADP and 2 units of G6PD and reaction was quantified spectrophotometrically at 340nm for 5 min (Marini et al. 2013). Lactate Dehydrogenase (LDH) catalytic activity was measured spectrophotometrically at 340 nm, through the conversion of pyruvate into lactate, following the oxidation of NADH. To the mixture of 200mM Tris-HCl (pH 7.3), 6.6 mM NADH and 30 mM Sodium pyruvate in the final volume of 1mL, 5 µg of protein lysate was added to measure the LDH activity. Pyruvate kinase (PK) activity was measured by the routine procedure adopted in the laboratory and as described previously (Iqbal et al. 2013). Specific activity of enzymes (HK, LDH and PK) per mg of cell lysate was calculated as:

$$\text{Units/mg} = \frac{\text{OD340/min}}{\text{6.22× mg lysate / mL reaction mixture}}$$

Glycerol gradient ultracentrifugation experiment was performed by loading 750 µg of protein lysates on top of 15-33% step gradient and centrifuged at 50,000 rpm for 18 hours at 4°C in SW55Ti rotor (Beckman Coulter); and fractions (75µl approx.) collected and examined for PK activity as previously mentioned (Gupta et al. 2010), followed by Immunoblot analysis.

3.9 In-Gel Lactate Dehydrogenase Assay (Zymography)

Native agarose gel electrophoresis was performed as described (Ross et al. 2010); to characterize the five known LDH isozymes, using the protein lysates of cultured cancer cells. 1.5% agarose gel was cast in 25 mM Tris-HCl and 250 mM glycine (pH 9.5) buffer, and loaded with 50 µg of protein followed by electrophoresis for 120 min at 100v in 5mM Tris-HCl and 40 mM glycine (pH 9.5) running buffer to resolve the proteins. The patterns of LDH isozymes were visualized by incubating the gel for 20 min at 37^0C in a solution containing lactate (29 mM), NAD^+ (0.42 mM), NBT (0.93 mM) and PMS (0.51 mM) dissolved in 10 mM Tris-HCl (pH 8.5).

3.10 Immunoblotting Analysis

Whole cell protein lysates were prepared using modified RIPA buffer containing (50 mM Tris-HCl pH 7.2, 150 mM NaCl, 0.5% Sodium deoxycholate, 0.1% SDS, 1% Triton X 100) and additionally 1 mM PMSF, Protease Inhibitor Cocktail and Phosphatase Inhibitor Cocktail II and III (Sigma). Briefly, the cell pellets were re-suspended in modified RIPA buffer and incubated in ice for 30 min. Further, the resultant mixture was cleared by centrifugation for 30 min at 12000g for 15 min at 4°C; and the supernatant was collected in pre chilled tubes. Protein concentration was quantified by BCA method as per manufacturer's protocol (Thermo scientific). 30 µg of protein was resolved on 10% SDS-PAGE and transferred to the nitrocellulose membrane. The membrane was blocked with 5% BSA (Tris Buffer Saline Tween 20) and probed with respective primary antibodies at 4°C overnight. The blots were further incubated in HRP conjugated secondary antibodies for 1 hour and proteins detected by the addition of Luminata Forte. Primary

antibodies used in the study were: PKM1 (#SAB4200094), PKM2 (#SAB4200095), Myc-tag (#C 3956), LC3B (L7543) and β-Actin (#A1978), which were procured from Sigma-Aldrich. AMPKα (#5831), p-AMPKα (T172) (#2535), ACC (#3676), p-ACC (Ser79) (#11818), p-PKM2 (Y105) (#3827), P70 S6 Kinase (#2708), p-P70 S6 Kinase (T389) (#9234), p-S6 (Ser 235/236) (#4858), p-S6 (Ser 240/244) (#5364), Histone H3 (#5192), PARP (#9542), COX IV (#4850), β-Tubulin (#2128) and Histone-H3 (#4499) were obtained from Cell Signaling Technology. Secondary antibodies, anti-Rabbit HRP (# 7076) and anti-Mouse HRP (# 7074), were from Cell signaling Technology. Secondary antibodies, chicken anti-Rabbit Alexa 488 (# A-11008) was procured from Molecular probes.

3.11 Immunohistochemistry using Tumor Tissues

Tumor tissues from sporadic breast cancer patients (provided by Dr. Gaurav Agarwal from Sanjay Gandhi Postgraduate Institute of Medical Sciences, Lucknow), were collected as detailed earlier (Pal et al. 2010, Pal et al. 2011) with the prior approval from Jawaharlal Nehru University ethical committee. ImmunoHistochemistry (IHC) was performed as described previously (Mohseni et al. 2014). In brief, clinically and histologically defined sporadic breast cancer tissue samples were fixed for 24 hours in phosphate buffer saline with 10% formalin and embedded in paraffin, followed by sectioning (4µm serial section), and staining with anti-pACC (Ser79), anti-PKM1 and anti-PKM2, respectively (with the assistance of Dr. Chitra Sarkar, Department of Pathology, AIIMS, New Delhi).

3.12 Subcellular fractionation and Co-immunoprecipitation

Nuclear and cytoplasmic fractions were obtained by using NE-PER extraction kit (Thermo Scientific #78833) and fractions of mitochondria extracted, using mitochondrial isolation kit (Thermo Scientific #89874), according to the manufacturer's instructions. Co-immunoprecipitation (Co-IP) was performed using the kit procured from Thermo Scientific. In brief, the antibodies were cross-linked with the amine-activated Agarose A beads and incubated with cell lysates at 4°C overnight. Protein complex bound to the beads were washed thrice with

lysis buffer and then eluted by adding elution buffer. The resultant IP products and inputs were subjected to immunoblotting analysis with the antibodies of interest.

3.13 Confocal microscopy

Cells grown on coverslips were fixed by adding 3.7% paraformaldehyde, dissolved in phosphate buffer saline (PBS) for 20 min and cells were permeabilized with blocking buffer (5% chicken serum in 1 X PBS) containing 0.1% Triton X 100 for 1 hour at room temperature. Slides were incubated overnight at 4°C with primary antibodies to mark their subcellular localization. Excessive antibodies were washed and coverslips incubated with secondary antibody (anti-rabbit Alex 488 or anti-rabbit Alex 594) for 1 hour at room temperature. Nuclei were stained with DAPI (Sigma-Aldrich) and the mitochondria with MitoTracker Red (Molecular probes, Life Technologies). Coverslips were mounted on glass slides with Prolong® Antifade reagent (Molecular probes, Life Technologies), and cells examined, followed by imaging, using Nikon Eclipse Ti-S Inverted Microscope. The data was analyzed using NIS- Elements image analysis software (Nikon).

3.14 LC-MS studies

His and Myc-tagged PKM1 was purified from the lysates of H1299 stable cells, using His-pull down and Myc-IP. We first used His-tag for pull-down and then immunoprecipitated PKM1 using myc-tag from the elute we got after His-pull down. The resultant eluent was subjected to in-solution Trypsin digestion. In brief, the eluted proteins were mixed with surfactant RapiGest (Waters) and were reduced with DTT and alkylated, using iodoacetamide. Samples were digested with 2µg of sequencing grade trypsin gold (Promega) at 37°C overnight and subjected to LC/MS-MS analysis (LC-MS/MS Waters SYNAPT G2 with 2D nano ACQUITY System). Mass spectrum obtained from the LC/MS was analyzed using Protein Lynx Global SERVER (PGLS); and the interactome for PKM1 was generated. We acknowledge, Mr. Plabon Borah (AIRF – JNU, New Delhi) for providing assistance in LC/MS analysis.

3.15 Computational prediction of protein subcellular localization

To predict subcellular localization of PKM1 (Uniprot I.D.: P14618-2) and PKM2 (Uniprot I.D.: P14618), the amino acid sequences of PKM isoforms were examined using six online computation tools that employ various algorithms to predict the subcellular localization. In brief, these tools employ algorithms that involve homology-based annotation, amino acid composition, localization signal sequences (sorting signals) and functional motifs to predict the subcellular localization. The following computational tools were used to assess the subcellular localization of PKM isoforms: CELLO v.2.5: http://cello.life.nctu.edu.tw/, HSLpred: http://www.imtech.res.in/raghava/hslpred/, Hum-mPLoc 2.0: http://www.csbio.sjtu.edu.cn/bioinf/hum-multi-2/, SubLoc v1.0: http://www.bioinfo.tsinghua.edu.cn/SubLoc/, YLoc: http://abi.inf.uni-tuebingen.de/Services/YLoc/webloc.cgi, and BaCelLo: http://gpcr.biocomp.unibo.it/bacello/.

3.16 Glucose uptake, Lactate Release and ATP Assays

Glucose consumption and lactate release levels were measured in culture medium that was collected after growing the cells under appropriate conditions, using Glucose (Hexokinase) assay kit (Sigma-Aldrich) and Lactate Colorimetric/Fluorometric assay Kit (BioVision), following the manufacturer's specifications. The concentration of the ATP was measured using the ATP bioluminescence assay kit (BioVision) as per the manufacturer's instruction.

3.17 FACS Analysis

To assess the mitochondrial membrane potential and mass, the stable knockdown cells were trypsinized and stained with 100nM Mito Tracker Red CMXROS dye (Invitrogen # M7512) to examine mitochondrial membrane potential or MitoTracker Green dye (Invitrogen # M 7514) to examine mitochondrial mass and incubated for 30 min at 37ºC. To acquire the fluorescence MitoTracker signals, samples were run on flow cytometry (BD biosciences, USA); and the data acquired were analyzed using inbuilt "Cellquest Pro" software.

3.18 Cell proliferation Assay (CCK8 Assay)

Cell proliferation was measured using cell counting kit-8 reagent (CCK8, Dojindo Molecular Technologies, Inc.). In brief, to each well of a 96-well plate, the stable cells were seeded at a density of 10,000 cells/well. Following 12 hours of seeding, the adherent cells were washed with phosphate buffer saline and replaced with fresh 100µl growth medium. Cell proliferation was measured at every 24-hour interval, starting from 0 to 72 hours, by adding 10µl of CCK8 reagent to the appropriate groups and incubated at 37ºC for 1 hour. Absorbance was quantified at a wavelength of 450 nm using a microplate reader (Molecular Devices). Cells were seeded in triplicates for each group in these experiments and in addition, the experiment was repeated twice.

3.19 Statistical Analysis

Data was represented as mean ± SEM. Level of significance was tested with paired Student *t* test or ANOVA (Two-way ANOVA and Two-way ANOVA), using Prism software (GraphPad). P<.05 was considered to be statistically significant. Tested significance was displayed in the figures as ***** P<0.05; ****** P<0.01; ******* P<0.001.

CHAPTER~4
Results

Chapter-4

Results

4.1 AMPK activation by glucose depletion or AICAR treatment affects glycolytic pathway enzyme, Pyruvate kinase M, expression and its isoform switch.

AMP-activated protein kinase plays a pivotal role in conserving the cellular energetic homeostasis by remodeling the metabolic phenotype to resist nutritional stress. In recent years, extensive studies have appreciated the importance of LKB1-AMPK pathway in tumorogenesis, where the axis of LKB1-AMPK is shown to provide tolerance to nutrient deprivation in cancer cells (Kato et al. 2002, Jeon et al. 2012, Liang and Mills 2013). However, how AMPK contributes to metabolic phenotype of cancer cells, and the mechanistic link through which AMPK exhibits tolerance to hypoglycemic situation that arises upon tumor progression, remains largely elusive.

In order to comprehend the effect of AMP-activated protein kinase on crucial glycolytic enzymes that govern aerobic glycolysis, lung (H1299) and breast (MCF-7) adenocarcinoma cells were cultured under declining concentrations of glucose (25, 10, 5, 1, .1 and 0 mM) and the cell lysates run in the gels and transferred to the membrane. Immunoblots of the membranes, when analyzed for the expression status of PKM1, PKM2, AMPK, p-AMPK (T172) and p-ACC (Ser 79), revealed the activation of AMPK signaling kinase with simultaneous PKM expression switch toward PKM1 **(Fig. 4.1A and 4.2A).** The p-ACC (Ser79) profile served as a marker to show the degree of AMPK activation. To validate if AMPK played a role in PKM isoform switch, we treated cells with a concentration gradient of AICAR (5-Aminoimidazole-4-carboxamide ribonucleotide), an agonist of AMPK; and replicated the pattern of PKM isoform switch **(Fig. 4.1B and 4.2B)** as observed under glucose insufficient experimental conditions. Further, to confirm these observations, cells were pretreated with or without Compound C (C.C.), an inhibitor of AMPK kinase and subjected to AMPK activation using glucose insufficient condition or AICAR treatment. Immunoblots depicted that the pretreatment with C.C. specifically impaired the function of AMPK, assessed by using p-ACC (ser79) and switched splice variant from PKM2 to PKM1 **(Fig. 4.1C and 4.2C)**, supporting the conclusion of an involvement of AMPK in PKM2 to PKM1 switch. In order to

ensure that the antibodies used for the two isoforms were not cross-reacting, the recombinant GST tagged PKM1 and PKM2 proteins were used to validate their specificity **(Fig. 4.1D)**.

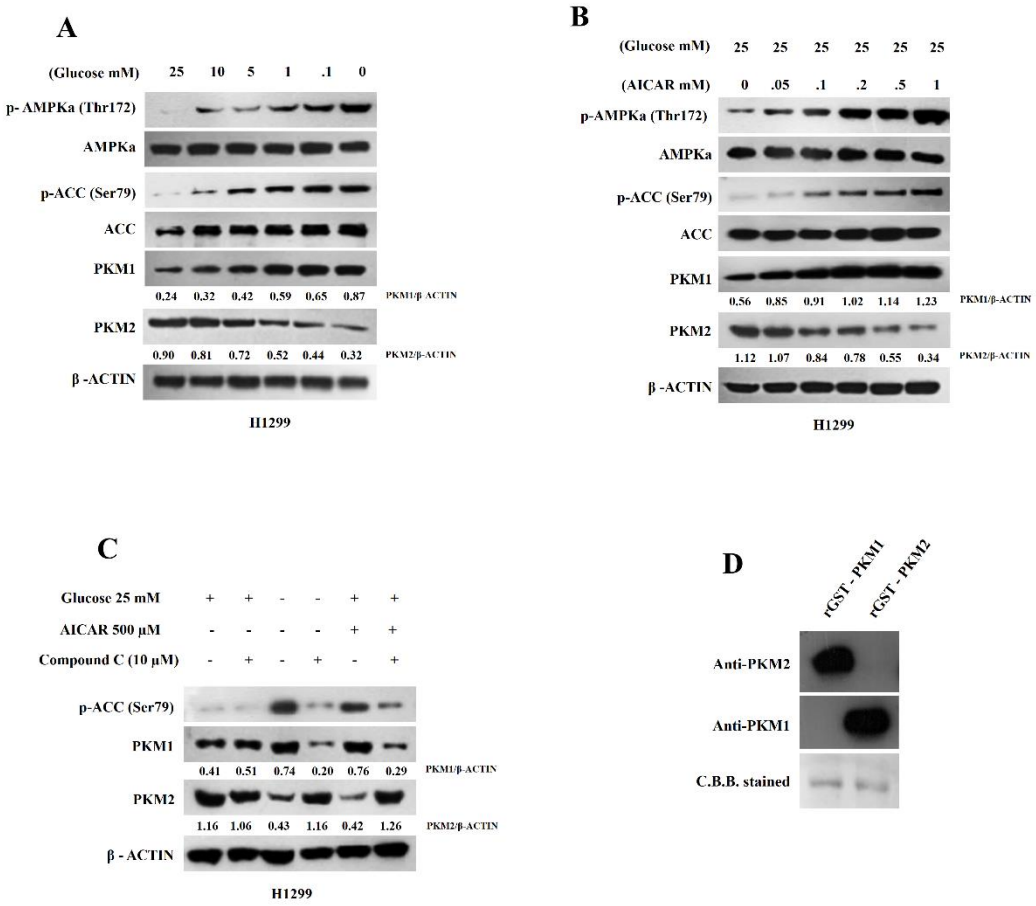

Fig.4.1. PKM1 expression under hypoglycemic conditions is regulated by AMPK pathway. ***(A-C) Immunoblots of:*** ***(A)*** *p-AMPKα(T172), AMPKα, p-ACC (S79), ACC, PKM1 and PKM2 from the protein lysates of H1299 cells, grown in glucose-free medium, supplemented with relative lowering concentration of glucose (25, 10, 5, 1, .1, 0 mM) for a period of 8 hours to show AMPK activation and PKM expression status.* ***(B)*** *the protein lysates of H1299 cells cultured in enriched glucose (25mM) medium and treated with a gradient of AICAR (0, .5, .1, .2, .5, 1 mM) for 8 hours, using the indicated antibodies, to show AMPK activation and PKM isoform expression status.* ***(C)*** *p-ACC (S79), PKM1 and PKM2 to show AMPK activation and PKM expression status in protein lysates of H1299 cells, pretreated with or without 10 µM Compound C (inhibitor of AMPK) for 30 minutes and cultured in the presence and absence of glucose or 500µM of AICAR as indicated, for the period of 8 hours. The relative expression levels (signals) of PKM1 and PKM2 from the above*

immunoblots were quantified using ImageJ and normalized to β-Actin. ***(D)*** *Immunoblotting with anti-PKM1 and anti-PKM2 to show the specificity for purified recombinant PKM1 (rGST-PKM1) and PKM2 (rGST-PKM1), C.B.B. Coomassie Brilliant Blue stained.*

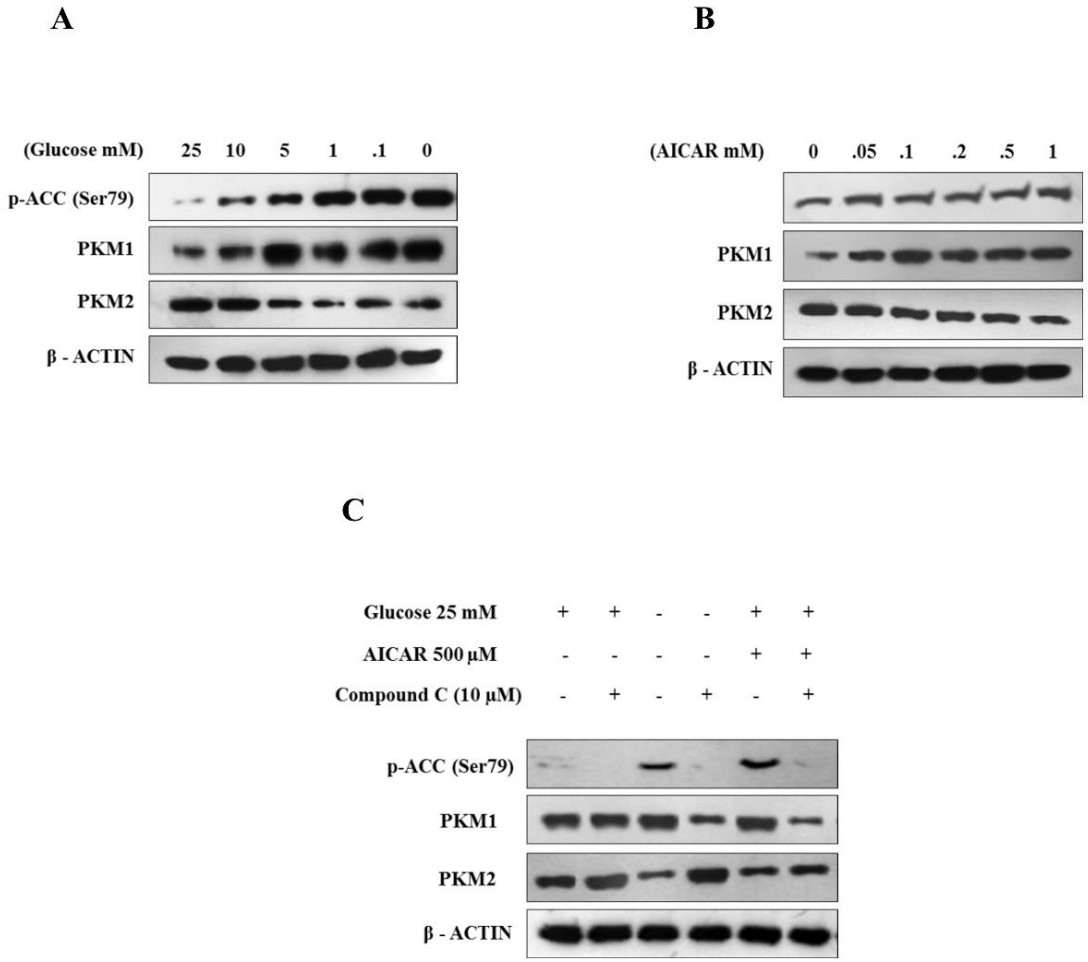

Fig. 4.2 AMPK regulates the pyruvate kinase M2 to M1 isoform switch in MCF-7 cells. ***(A)*** *Immunoblot of p-ACC (S79), PKM1 and PKM2 from the protein lysates of cells, grown in glucose-free medium, supplemented with relative lowering concentration of glucose (25, 10, 5, 1, .1, 0 mM) for a period of 8 hours;* ***(B)*** *Immunoblot for p-ACC (S79), PKM1 and PKM2 from the protein lysates of cells, treated with a gradient of AICAR (0, .5, .1, .2, .5, 1 mM) for 8 hours;* ***(C)*** *Immunoblot of p-AMPKα, AMPKα (T172), p-ACC (S79), ACC, PKM1 and PKM2 from the protein lysates of H1299 cells, pretreated with or without 10 µM Compound C (inhibitor of AMPK) for 30 minutes, and cultured in the presence and absence of glucose or 500µM of AICAR as indicated, for the period of 8 hours.*

4.2 AMPK requires its protein kinase feature (Thr172 phosphorylation) to regulate the pyruvate kinase M2 to M1 isoform switch in cancer cells.

Further, to explore if the protein kinase activity of AMPK (i.e., Threonine 172 phosphorylation, pT172, mediated by LKB1) was critical to activate PKM isoform switch, H1299 and A549 cells cultured with enriched glucose (25mM) were transiently transfected with T172D AMPKα2 constitutively active (CA) mutant (AMPKα2 T172D-Myc) **(Fig. 4.3A)**, resulting in PKM2 to PKM1 switch with increased Ser79 ACC phosphorylation. Whereas, cells transfected with vector or wild-type AMPKα2 (AMPKα2-Myc) failed to show such a switch **(Fig. 4.3B)**, suggesting the involvement of the activation of AMPK and the LKB1-AMPK axis in the regulation of PKM isoform switch.

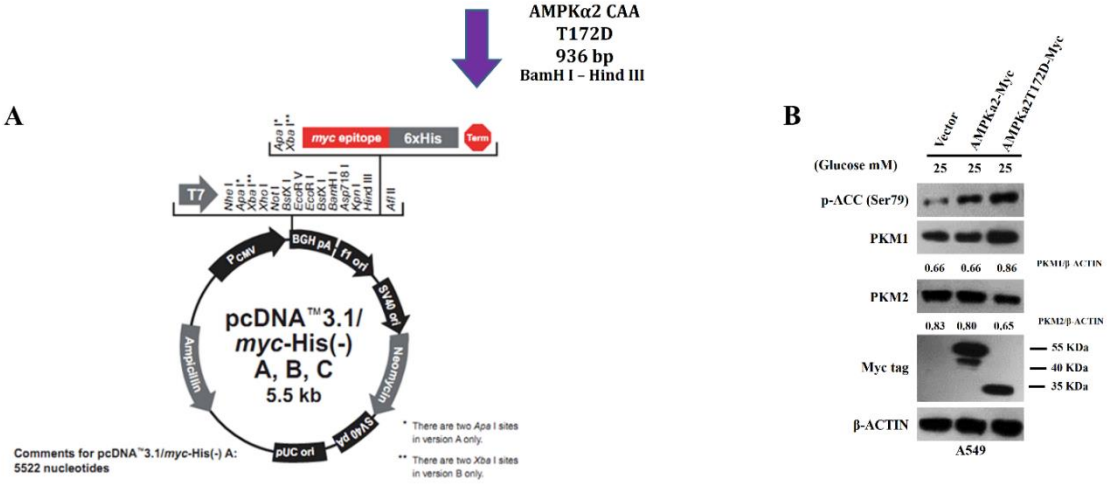

Fig. 4.3. AMPK requires LKB1 kinase to regulate the pyruvate kinase M2 to M1 isoform switch in cancer cells. ***(A)*** *schematic diagram depicts the construct of pCDNA3.1-AMPKα2T172D-Myc that encodes Myc-tagged AMPKα2 constitute active protein.****(B)*** *Immunoblots of the protein lysates of H1299 and A549 cells transfected with empty vector (pcDNA3.1), Myc-tagged wild-type AMPKα2 (AMPKα2-Myc) or AMPKα2 constitutively active T172D mutant (AMPKα2T172D-Myc) and cultured under enriched (25mM) glucose conditions and probed with Myc-tag and pACC (ser79) antibodies to show the expression and functional validation of AMPKα2 Wild-type and Mutant; also, depicting the results of probing with PKM1 and PKM2 antibodies to show their expression status. The relative expression levels (signals) of PKM1 and PKM2 were quantified using ImageJ and normalized to β-Actin.*

4.3 AMPK activation by glucose depletion affects pyruvate kinase activity, but not of hexokinase and lactate dehydrogenase.

Besides the expression regulation of PKM isoforms, the effect of AMPK was also examined for rest of the known glycolytic enzymes that govern aerobic glycolysis. We cultured, H1299 and MCF-7 cells in glucose free medium and supplemented with selected standardized concentrations (25, 5 & 1mM) of glucose to mimic, nutrient replete (25 mM), human physiological (5mM) and near glucose deplete condition (1mM), to stimulate AMPK in cell culture condition. Cell lysates assayed for the activity of critical enzymes (HK, PK and LDH) associated with aerobic glycolysis showed a significant increase in the PK activity with decreasing glucose concentrations; whereas the activity of HK and LDH remained unaltered **(Fig. 4.4A).** Immunoblots showed a consistent decrease in PKM2 protein expression with unaltered PKM2-Tyr105 phosphorylation and a shift in expression from PKM2 to PKM1 **(Fig. 4.4B),** suggesting that the enhanced PK activity apparently resulted due to an increased expression of alternatively spliced PKM1. The results of semiquantitative RT-PCR in H1299 and MCF-7 cells also depicted the switch towards PKM1, without altering significantly the expression of isoforms of hexokinase (HK1 and HK2) and lactate dehydrogenase (LDHA and LDHB) at RNA level **(Fig. 4.4C).** The appearance of PKM1 isoform at mRNA and protein level in the experimental lung (H1299) and breast cancer (MCF-7) cell lines concomitantly with PKM2 contradicted the exclusiveness of the latter in cancer cells as reported earlier (Mazurek et al. 2005, Christofk et al. 2008). In order to find out if the two alternatively spliced forms of PKM co-expressed in cancers, we observed that the expression of PKM2 increased with the advancing stages of sporadic breast tumors when compared with the adjoining normal tissues. To our surprise, PKM1 co-expressed along with PKM2 in these tissues and showed a similar trend of increasing expression with advancing stages of the tumors **(Fig. 4.5A)** The prevalence of co-expression was confirmed further in cultured cancer cells of different tissue origins, where we examined 6 different cell lines (MCF-7, MDA-MB-231, PC-3, H1299, A549 and HeLa), derived from four different tissue (Breast, Lung, Prostate and Cervical) origins and compared with two other non-cancerous (L6-rat skeletal muscle and HEK293-Human Embryonic Kidney) cell lines **(Fig. 4.5B).** The phenomenon of co-expression was also confirmed at RNA level in cultured human cancer cells, using semi-quantitative RT-PCR followed by exon-specific restriction digestion of PKM2, a modified technique adopted from David et al. 2010 (David et al.

2010), to examine the proportion of the expression of the two isoforms **(Fig. 4.5C-D)**. Further, to understand the relevance of the co expressing isoform of PKM1, we proposed to study its interactome, sub-cellular localization, role in aerobic glycolysis and cell viability, using mostly lung cancer cell lines, unless specified otherwise.

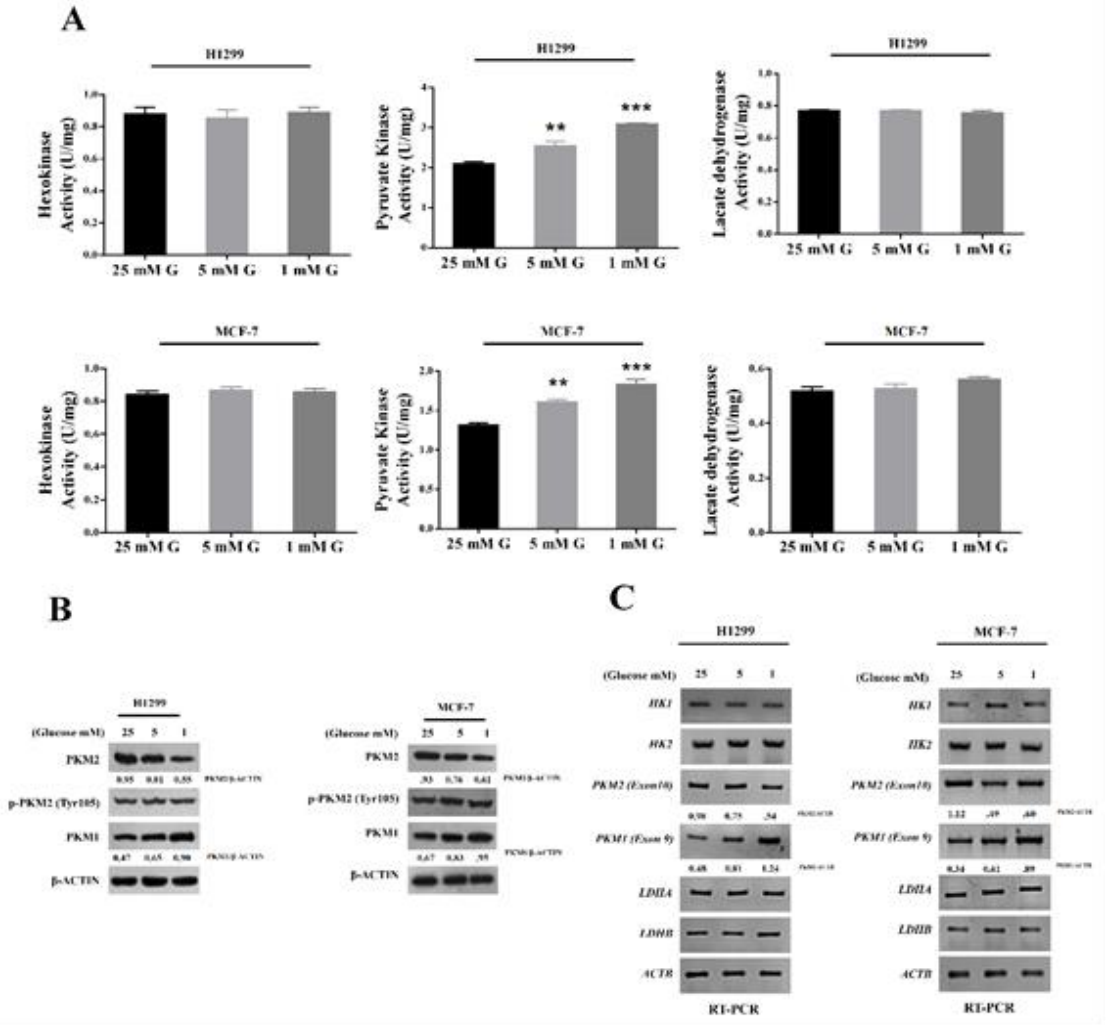

Fig. 4.4. Effect of glucose depletion on glycolytic pathway enzymes and the pyruvate kinase isoform switch. ***(A)*** *Relative enzyme activity of glycolytic enzymes: Hexokinase, HK; Pyruvate Kinase, PK; and Lactate Dehydrogenase, LDH; in the protein lysates of H1299 and MCF-7 cells, cultured in glucose-free medium, supplemented with (25mM, 5mM, 1mM) glucose for a period of 8 hours.* ***(B)*** *Immunoblot of PKM2, p-PKM2 (Try105) and PKM1 from protein lysates of cells as in 'A' with relative expression levels (signals) quantified using ImageJ and normalized to β-Actin.* ***(C)*** *RT-PCR analysis to show the relative expression of genes involved in glucose metabolism (HK1, HK2, PKM1, PKM2, LDH A, LDHB) from H1299 (Left) and MCF-7 (Right) cells, cultured*

*in glucose-free medium, supplemented with (25 mM, 5mM, 1mM) glucose for a period of 8 hours. *P < 0.05, **P < 0.01, ***P < 0.001.*

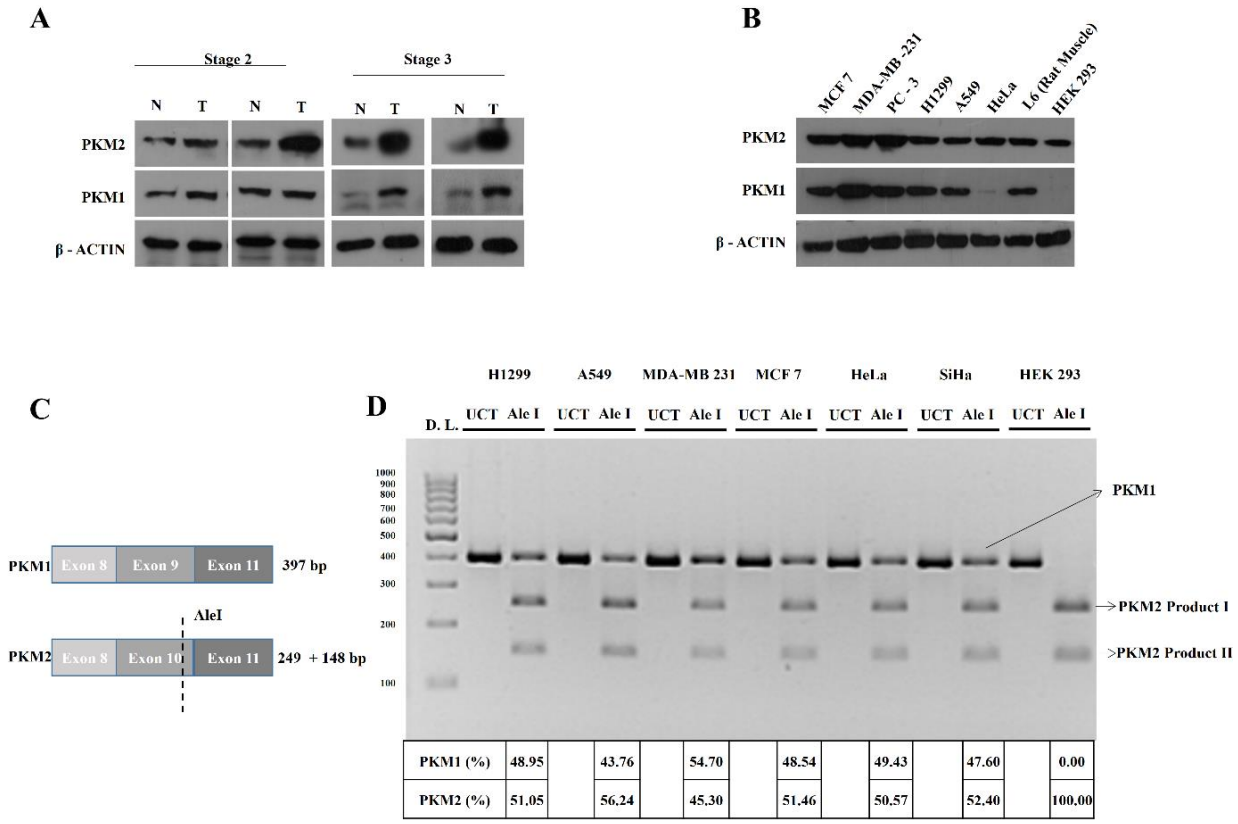

Fig. 4.5. Co-expression of PKM1 and PKM2 in tumor cells and cancer cell lines. ***(A)*** *Immunoblotting with anti-PKM1 and anti-PKM2 to demonstrate co-expression of PKM1 and PKM2 isoforms of pyruvate kinase in stage II and stage III sporadic breast tumors in comparison to their normal tissue pair (N – Normal tissue, T – Tumor tissue).* ***(B)*** *Expression status of PKM1 and PKM2 in six human cancer cell lines of four different tissue origins and two non-cancerous cell lines, used as a control.* ***(C)*** *Schematic representation to depict the approach employed to assay PKM1/PKM2 mRNA ratio in human cancer cells.* ***(D)*** *Semi-quantitative RT-PCR followed by PKM2 exon-specific restriction digestion with AleI restriction enzyme to examine the proportion of PKM1 and PKM2 expression in human cancer cells, using AleI restriction enzyme. UCT–Uncut, Ale I – Restriction digested and D.L – DNA Ladder. Uncut PKM1 and PKM2, 397 bp, Ale I undigested PKM1, 397 bp, Ale I digested PKM2 product I, 249 bp, and Ale I digested PKM2 product II, 148 bp.*

4.4 AMPK mediated PKM2 to PKM1 switch in glucose deprived condition influences the oligomeric state of pyruvate kinase but not of lactate dehydrogenase.

The observation of co-existence of both PKM1 and PKM2 in cell lines and tumor samples necessitated correlating the observed changes to the oligomeric (dimer: tetramer, using glycerol gradient density ultracentrifugation) status of the two isoforms, which showed a significant shift in response to the hypoglycemic culture conditions **(Fig. 4.6).** H1299 cells cultured in 25mM of glucose exhibited predominantly enzymatically inactive dimeric form of PKM and showed a shift towards tetramer peak under lower glucose concentrations (5mM and 1mM). The oligomeric status, however, of LDH when investigated in H1299 and replicated in MCF-7 cells in presence of similar glucose concentrations, using in-gel-activity-assay (Zymography), remained unaltered **(Fig. 4.7A-B)**.

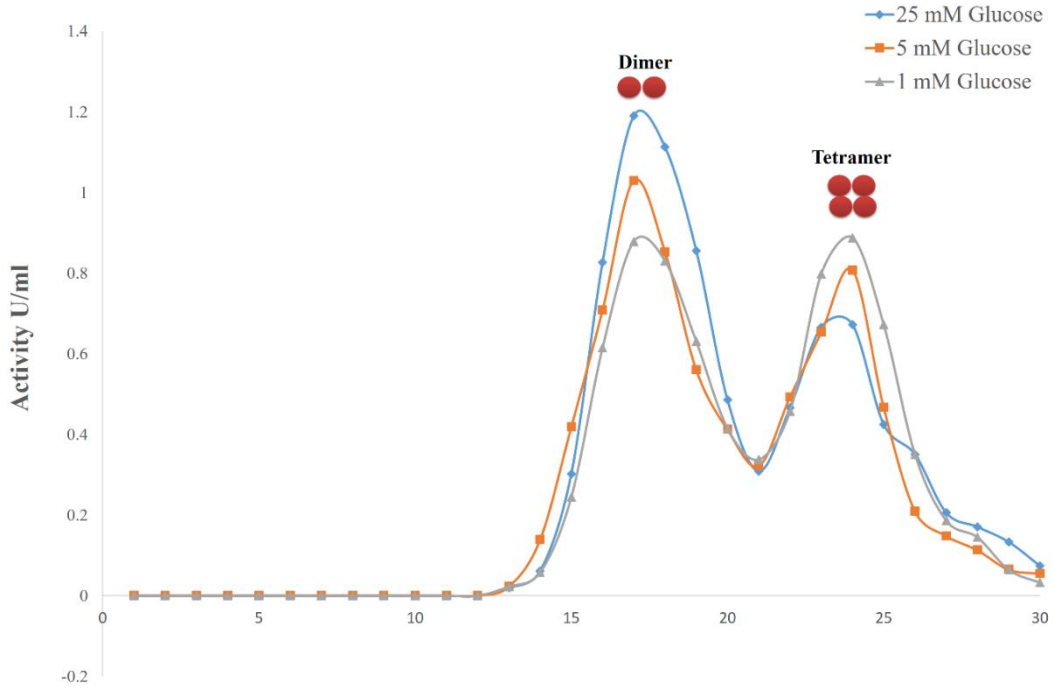

Fig. 4.6. Glucose inadequacy shifts the tetramer : dimer ratio of PKM. *(A) Dimeric and Tetrameric peaks of PK, resolved by spectrometric PK enzyme assay of the fractions collected from glycerol density gradient ultracentrifugation, loaded with protein lysates of H1299 cells cultured in glucose-free medium, supplemented with (25mM, 5mM, 1mM) glucose for a period of 8 hours.*

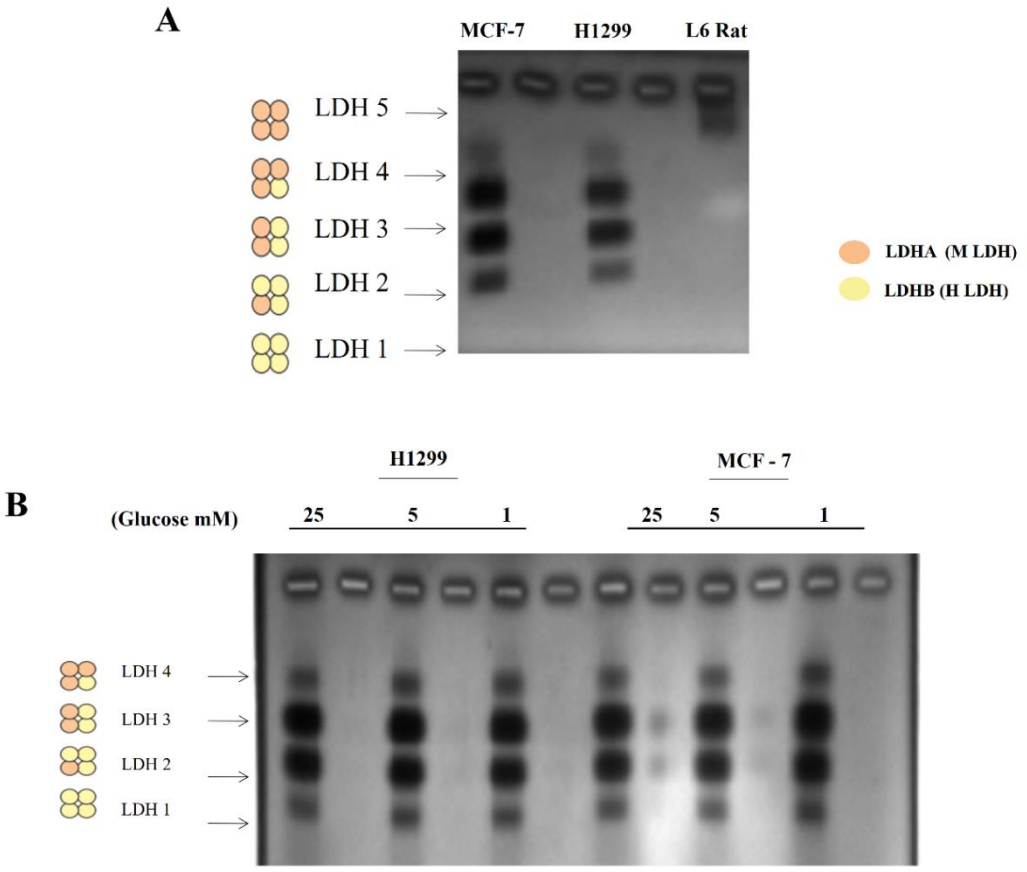

Fig. 4.7. Effect of Glucose deprivation on LDH isozymes and their oligomeric status. ***(A)*** *The oligomeric patterns of LDH in MCF-7, H1299 and L6 Rat muscle cells, assessed through 'in-gel activity assay' (Zymography);* ***(B)*** *LDH Zymography, displaying the oligomeric status in protein lysates of H1299 and MCF-7 cells, cultured in glucose free DMEM medium and supplemented with 25 mM, 5mM, 1mM glucose for a period of 8 hours.*

4.5 Prediction and validation of AMPK phosphorylation sites of M1 and M2 isoforms of pyruvate kinase.

To examine if the activated AMPK interacted and phosphorylated PKM isoforms to influence its glycolytic activity, computationally two sites (Threonine 45 and 93), both in M1 and M2 isoforms of PK; and one additional site (Serine 403) exclusive to PKM1, as consensus phosphorylation sites of AMPK with moderate stringency, were predicted **(Fig. 4.8A).** For subsequent validation, we

generated H1299 stable cells, overexpressing either Myc-His-tagged- PKM1 (PKM1-Myc-His) or PKM2 (PKM2-Myc-His) **(Fig. 4.8B)**. These isoforms when independently immunoprecipitated (IP) from whole cell lysates of H1299 stable cells cultured under depleted glucose (1mM) condition and subjected to LC-MS/MS analysis, revealed neither a physical interaction between PKM isoforms and AMPK, nor phosphorylation on the predicted sites in either of the PKM isoforms, in accordance with the PKM1 and PKM2 interactome and the coverage map **(Fig. 4.8C)**.

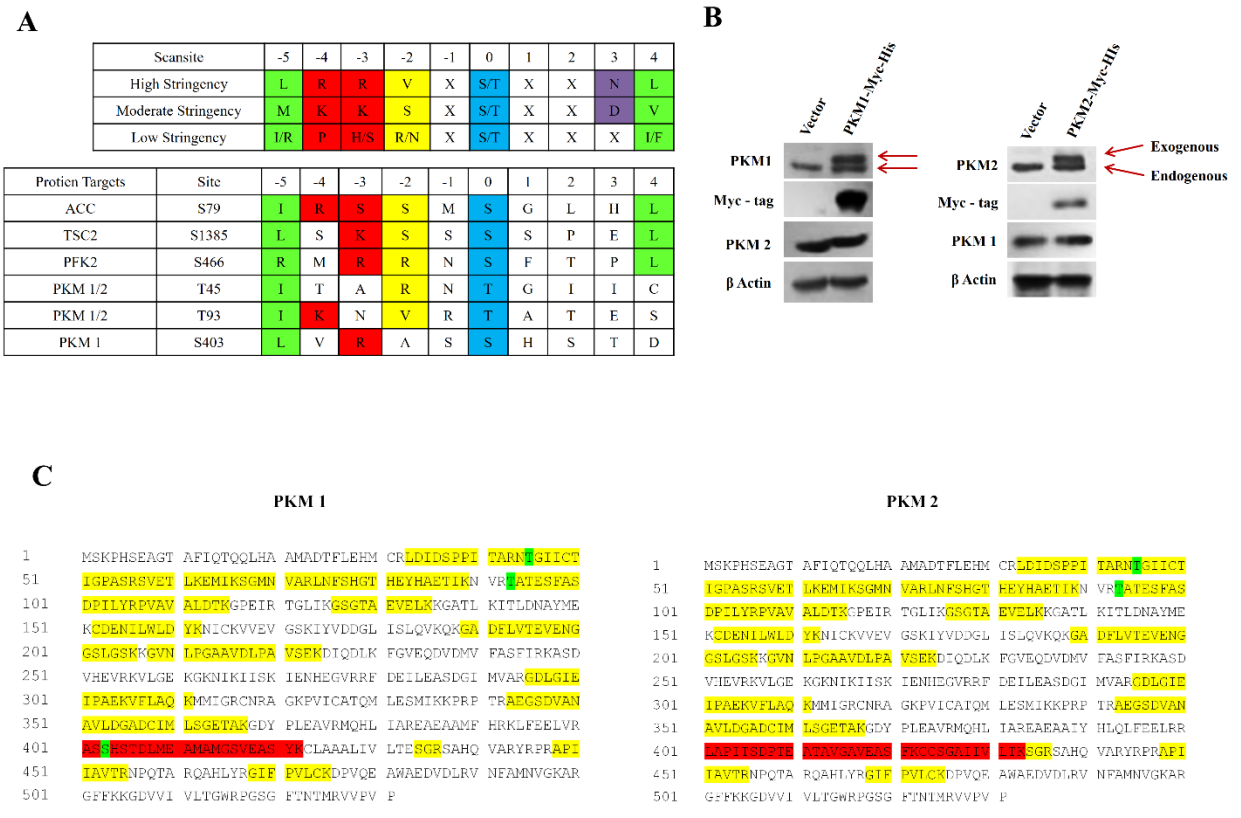

Fig. 4.8. Identification and characterization of AMPK consensus phosphorylation sites and interactome of M1 and M2 isoforms of pyruvate kinase. *(A) The AMPK consensus phosphorylation motif shown in top panel were acquired from Gwinn et al (2008). where the level of stringency represents the optimal match with the motif. The potential AMPK consensus phosphorylation site in both PKM1 and PKM2 (Threonine 45 and 93) and PKM1 alone (Serine 403) were predicted using Scansite3. ACC1, TSC-2, and PFK2 are reference targets, previously recognized phosphorylation sites of AMPK. (B) Immunoblots of the protein lysates of H1299 stable cell lines, expressing empty vector, Myc-His-tagged PKM1 (Left) or Myc-His-tagged PKM2*

(Right) with Myc-tag, PKM1, and PKM2 antibodies to show over-expression of PKM1 or PKM2. (C) LC/MS, coverage map of M1 and M2 isoforms of pyruvate kinase, amino acid sequence highlighted in yellow color shows the sequence covered by M/S analysis; Green color represents amino acid predicted to be phosphorylated as in A., red color shows the M1 and M2 specific sequences obtained from independent M/S analysis of PKM1 and PKM2.

4.6 Identification of protein interacting partners of human PKM1 using LC/MS-MS.

The complex of PKM1 and its interacting partners were co-purified by Myc-tag immunoprecipitation from whole cell lysates of H1299 cells stably expressing Myc-tagged-PKM1 (PKM1-Myc-His) **(Fig. 4.8B)** and subjected to Liquid Chromatography-Mass spectrometry (LC-MS) based analysis. From the results of two independent LC-MS studies, nearly 30 interacting proteins of PKM1 were found **(Table 4.1),** which involved the proteins from cytoplasm, mitochondria, and nucleus, as an integral part of diverse cellular machinery of, glycolytic pathway, mitochondrial electron transport chain, protein translation, protein folding, DNA replication and cytoskeletal networks **(Fig. 4.9)**.

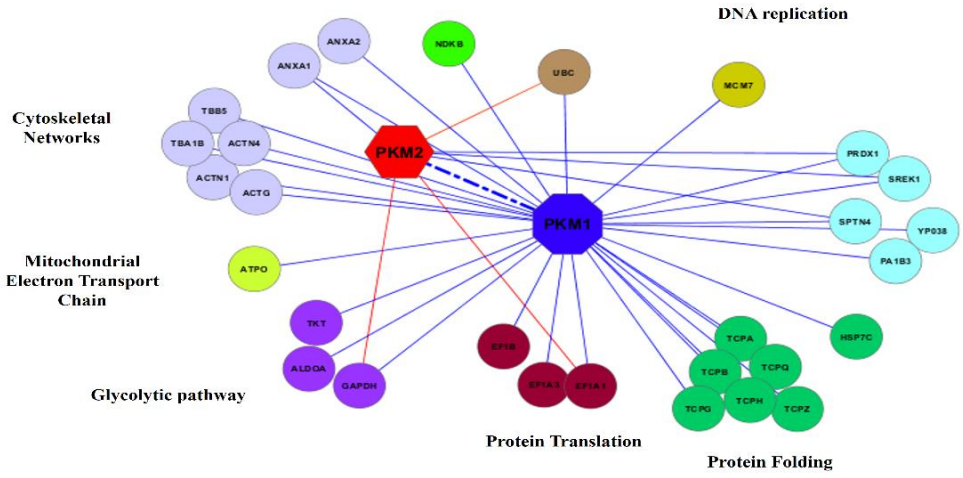

Fig. 4.9. Identification of protein interacting partners of human PKM1 using LC/MS-MS. ***(A)*** *Cytoscape map of PKM1 interactome, involving a total of 30 interacting partners of PKM1, co-immunoprecipitated with myc tagged PKM1 from H1299 lysate and identified using LC/MS-MS*

from two biological replicates. The identified interacting partners were further separated with distinct color codes and marked as an integral part of cellular machinery like; glycolytic pathway, mitochondrial electron transport chain, protein translational, protein folding, DNA replication and cytoskeletal networks.

Table. 4.1. List of proteins identified as PKM1 interacting partners using LC/MS-MS.

Accession I.D.	Entry	Description	Mass (Da)	Peptides	Coverage (%)	PLGS Score
P63261	ACTG	Actin cytoplasmic 2	41765	13	31.4667	892.889
P12814	ACTN1	Alpha actinin 1	102992	32	28.5874	623.7095
O43707	ACTN4	Alpha actinin 4	104788	58	48.5181	1891.53
P04083	ANXA1	Annexin A1	38689	14	28.9017	336.3753
P07355	ANXA2	Annexin A2	38651	12	28.9086	850.7295
P48047	ATPO	ATP synthase subunit O mitochondrial	23262	7	33.8028	315.8188
P33993	MCM7	DNA replication licensing factor MCM7	81256	24	32.267	712.8558
P68104	EF1A1	Elongation factor 1 alpha 1	50109	33	47.8355	4913.585
P24534	EF1B	Elongation factor 1 beta	24748	3	10.6667	411.1423
P04075	ALDOA	Fructose bisphosphate aldolase A	39395	14	48.3517	1219.534
P04406	G3P	Glyceraldehyde 3 phosphate dehydrogenase	36030	26	60.597	1782.219
P11142	HSP7C	Heat shock cognate 71 kDa protein	70827	16	22.1362	524.3831
P22392-2	NDKB	Isoform 3 of Nucleoside diphosphate kinase B	30117	15	36.7041	1039.605
Q9H254-4	SPTN4	Isoform 4 of Spectrin beta chain	243272	20	12.0241	281.8018

P14618-2	KPYM	Isoform M1 of Pyruvate kinase isozymes M1 M2	58025	24	40.678	584.7386
Q06830	PRDX1	Peroxiredoxin 1	22096	10	38.191	1235.415
Q15102	PA1B3	Platelet activating factor acetylhydrolase IB subunit gamma	25718	10	37.2294	333.5217
P0CG48	UBC	Polyubiquitin C	85533	32	31.5374	1067.547
Q5VTE0	EF1A3	Putative elongation factor 1 alpha like 3	50153	26	38.961	3000.535
A6NJU9	NPIL5	Putative NPIP like protein LOC613037	125886	20	20.826	242.025
P14618	KPYM	Pyruvate kinase isozymes M1 M2	57900	29	43.5028	896.5508
Q8WXA9	SREK1	Splicing regulatory glutamine lysine rich protein 1	59345	32	24.2126	298.4866
P17987	TCPA	T complex protein 1 subunit alpha	60410	12	22.6619	496.8228
P78371	TCPB	T complex protein 1 subunit beta	57452	16	42.243	524.3919
Q99832	TCPH	T complex protein 1 subunit eta G	59328	17	21.7311	673.8492
P49368	TCPG	T complex protein 1 subunit gamma	60495	19	32.6605	740.262
P50990	TCPQ	T complex protein 1 subunit theta GN	59582	21	34.854	483.6839
P40227	TCPZ	T complex protein 1 subunit zeta	57987	19	34.6516	658.8874
P29401	TKT	Transketolase	67834	16	29.695	325.851
P68363	TBA1B	Tubulin alpha 1B chain	50119	35	44.1242	5546.314
P07437	TBB5	Tubulin beta chain	49638	39	43.6937	2897.446

4.7. PKM1 and PKM2 localize differentially to subcellular organelles.

To support the observation of PKM1 interaction with proteins of different subcellular organelles, the amino acid sequence of PKM1 was analyzed, using six online computational tools to predict the subcellular localization of PKM1 and compare the same with PKM2. The predictions revealed that both PKM1 and PKM2 localized predominantly in the cytoplasm, followed by their presence in mitochondria and at appreciative levels in the nucleus **(Table. 4.2)**. This was further confirmed by immunoblotting studies with subcellular fractions and confocal microscopy. Results revealed a differential localization pattern of PKM isoforms in H1299 and A549 cells, where PKM1 localized within the cytosol, mitochondria, and nucleus; whereas, PKM2 localized predominantly in the cytoplasm and with appreciative levels in the nucleus, showing an apparent absence in the mitochondria **(Figs. 4.10A–F)**. Interestingly, the interactome data of PKM1 revealed a possible interaction between co-expressed PKM1 and PKM2 isoforms; where LC-MS data of PKM1 isoform exhibited the peptide sequence corresponding to that of PKM2 isoform. To validate the interaction between PKM1 and PKM2, confocal microscopy and co-immunoprecipitation (Co-IP) studies were carried out. The distribution and strong interaction within cytoplasm between the endogenous PKM1 (immunostained with anti-PKM1 and Alexa594-Red) and exogenously expressed Myc-tagged PKM2 (PKM2-Myc) (immunostained with anti-Myc and Alexa 488-Green) was visualized using confocal microscopy **(Fig. 4.11A)**. The IP of Myc-tag from the lysate of H1299 cells stably expressing PKM1-Myc showed the co-precipitation of endogenous PKM2, re-confirming the interaction between the two. This was further validated in the reciprocal experiment between exogenously expressing PKM2-Myc and endogenous PKM1 **(Fig. 4.11B)**. The likelihood of the hetero-oligomers, expected to be formed through PKM1-PKM2 interaction, was examined by separating PKM oligomers (dimer and tetramer) from H1299 cell lysates in a glycerol step gradient subjected to ultracentrifugation (Gupta et al. 2010, Iqbal et al. 2013). The precise location of PKM dimer or tetramer was detected by examining pyruvate kinase activity (**Fig. 4.11C)**, followed by Westerns of the same glycerol fraction with PKM1 and PKM2 specific antibodies, which established the formation of heterotetramers of PKM1 and PKM2 without forming heterodimers. **(Fig. 4.11D).**

Table 4.2. *In silico* subcellular localization prediction of PKM isoforms (PKM1 and PKM2).

Software	Localization		Basis of Prediction
	PKM1	PKM2	
CELLO v.2.5	Cytoplasm RELIABILITY: Cytoplasmic 2.831 Mitochondrial 0.958 Nuclear 0.043 Peroxisomal 0.116 Cytoskeletal 0.020 Plasma Membrane 0.009 ER 0.007	Cytoplasm RELIABILITY: Cytoplasmic 2.940 Mitochondrial 0.958 Nuclear 0.055 Peroxisomal 0.111 Cytoskeletal 0.029 Plasma Membrane 0.014 ER 0.007	Amino acid composition and its physicochemical properties (Yu et al. 2006).
HSLpred	Mitochondrial Protein.	Cytoplasmic Protein.	Support vector machine-based hybrid modules that involve amino acid composition, dipeptide compositions and evolutionary information of protein (Garg et al. 2005)
Hum-mPLoc 2.0.	Cytoplasm and Mitochondrion	Cytoplasm and Mitochondrion	Gene ontology, functional domains and sequential evolutionary information (Chou and Shen 2006)

SubLoc v1.0	Mitochondrial Expected accuracy = 74 %	Mitochondrial Expected accuracy = 56 %	Uses vector support machine Amino acid composition (Hua and Sun 2001)
YLoc	**Cytoplasm** Probability: Cytoplasm 80.2%, Nucleus 16.9%, Mitochondrion 3.0%, Secreted pathway 0.0%	**Cytoplasm** Probability: Cytoplasm 88.2%, Nucleus 7.9 %, Mitochondrion 3.8 %, Secreted pathway 0.0 %	Sequence-based predictions (amino acid composition, sorting signals) (Briesemeister et al. 2010)
BaCelLo	Cytoplasm LOCALIZATION STEPS: Intracellular - Nucleus or Cytoplasm - Cytoplasm	Cytoplasm LOCALIZATION STEPS: Intracellular - Nucleus or Cytoplasm - Cytoplasm	Support vector machine-based amino acid compositions of both the N- and C-terminal (Pierleoni et al. 2006).

Table. 4.2. *In silico* subcellular localization prediction of PKM isoforms. The methods to predict subcellular Localization of PKM1 and PKM2 were acquired from Zambo et al. (Zambo et al. 2016); where the amino acid sequence of PKM isoforms PKM1 (P14618-2) and PKM2 (P14618) was examined using six online computational tools that employed different algorithms to predict the subcellular localization of PKM isoforms.

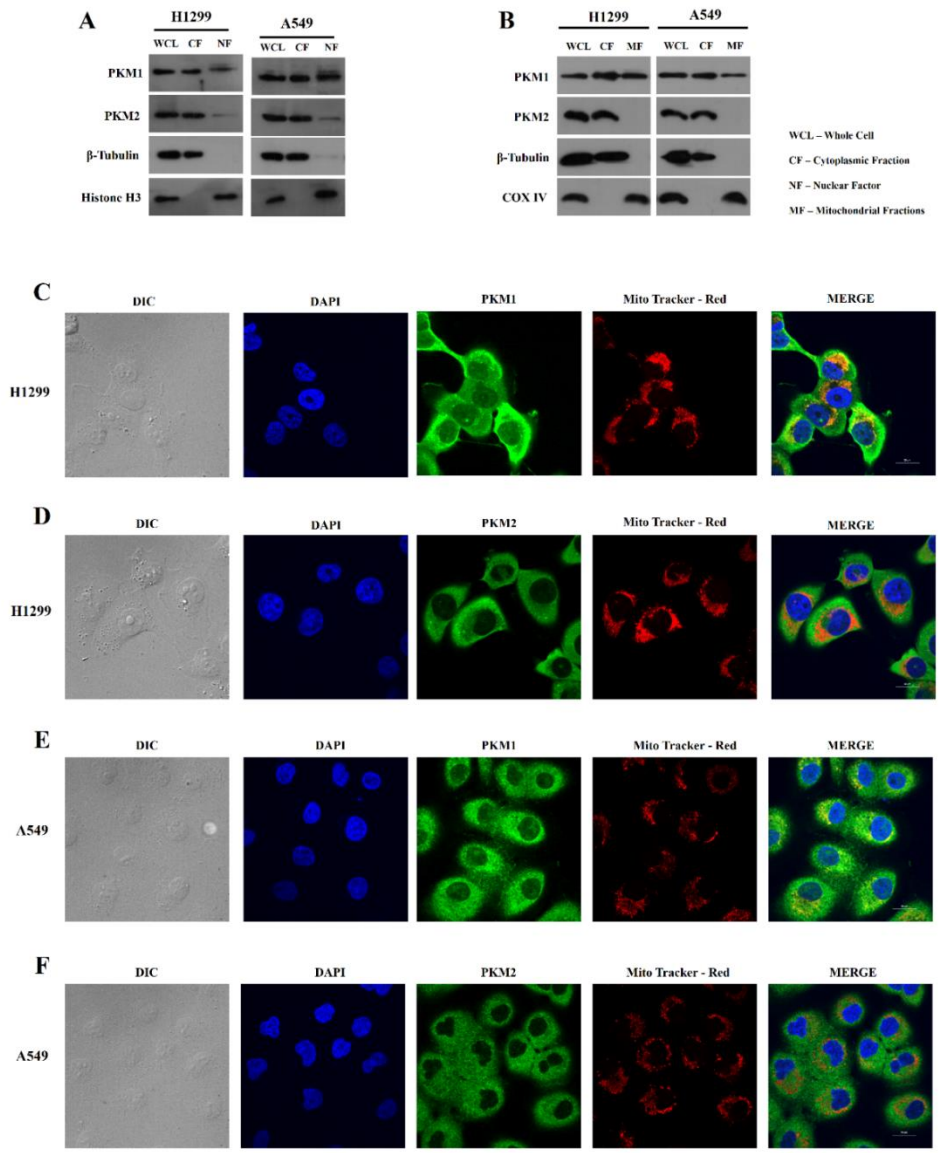

Fig. 4.10. Sub-cellular localization of PKM isoforms and their validation. ***(A)*** *Immunoblots showing PKM1 and PKM2 in the lysate of H1299 (left panel) and A549 (right panel) cells collected by fractionating the cytoplasm and the nucleus (W.C.L. – Whole cell Lysate, C.F. - Cytoplasmic Fraction and N.F. Nuclear Fraction). PARP and β-Tubulin served as loading controls for nucleus, and cytoplasm, respectively.* ***(B)*** *Immunoblots of PKM1 and PKM2 from a lysate of H1299 (left panel) and A549 (right panel) cells collected by fractionating the cytoplasm and the mitochondria (W.C.L. – Whole cell Lysate, C.F. - Cytoplasmic Fraction, M.F. Mitochondrial Fraction). COX IV and β-Tubulin served as loading controls for mitochondria, and cytoplasm respectively.* ***(C-F)*** *Confocal microscopy images demonstrating the subcellular localization of PKM1 or PKM2 in*

H1299 and A549 cells, immunostained with antibodies of PKM2 (Green) or PKM1 (Green); mitochondria were stained with Mito-tracker Red (Red) and the nucleus was stained with DAPI (Blue). Merged figures are shown with a scale bar of 20µm.

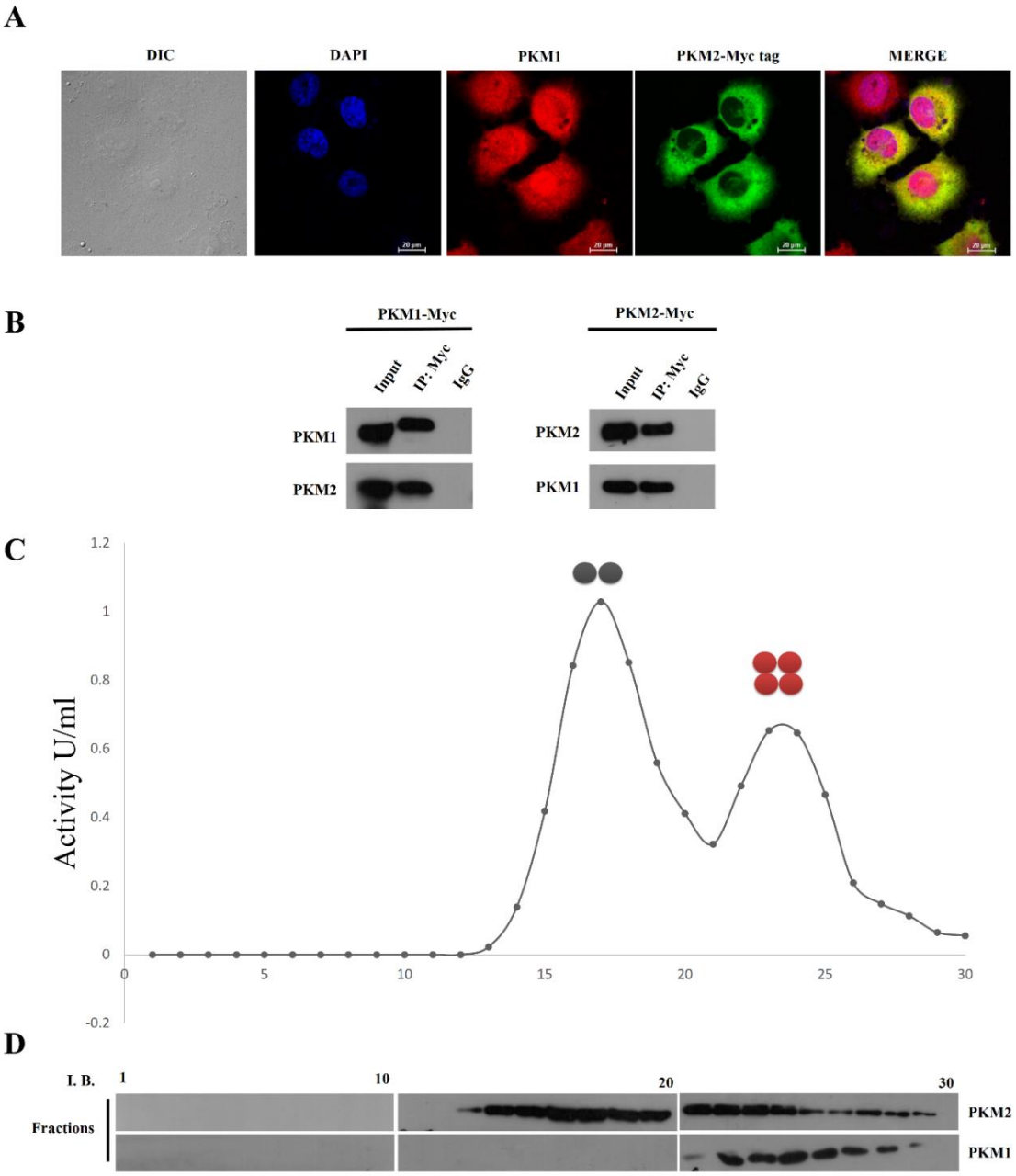

Fig. 4.11. ***PKM1 and PKM2 interaction and hetero-oligomeric formation contribute to the net pyruvate kinase activity. A)*** *Confocal microscopy images, displaying the co-localization of endogenous PKM1 (Immunostained with anti-PKM1 and secondary-anti-Alexa589; Red) and*

exogenously expressed Myc-tagged PKM2 (Immunostained with anti-Myc-tag and secondary-anti-Alexa488: Green) in H1299 cells; Nucleus was stained with DAPI (Blue); figures are shown with a scale bar of 20µm. ***(B)*** *Immunoprecipitation (IP) performed with anti-Myc-tag in lysates of H1299 cells, stably expressing Myc-tagged PKM1 (PKM1-Myc) (left panel), or Myc-tagged PKM2 (PKM2-Myc) (right panel), followed by immunoblotting with PKM1 or PKM2 antibodies, to show the interaction between PKM-isoforms (IgG - used as Isotype control).* ***(C)*** *Dimeric and tetrameric peaks of PKM2, resolved by examining pyruvate kinase activity from the fractions collected after glycerol density gradient ultracentrifugation, loaded with protein lysates from H1299 cells.* ***(D)*** *Immunoblotting with anti-PKM1 and anti-PKM2 of the glycerol density gradient fractions as mentioned in panel C to measure the distribution of PKM1 and PKM2 in the separated peaks in panel* ***(C)***.

4.8 Alternative splicing in favor of PKM1 is regulated by AMPK by downregulating the expression of hnRNPs.

Given the observation of LKB1-AMPK pathway driven preferential expression of PKM1 isoform, the link between the LKB1-AMPK pathway and the PKM1-expression switch was investigated. Since c-Myc, a downstream effector of MTOR (Mammalian Target of Rapamycin) controls transcription activation of hnRNPs (Heterogeneous nuclear ribonucleoproteins) and results in PKM1 repression and preferential expression of PKM2 (Clower et al. 2010, David et al. 2010, Sun et al. 2011), it was pertinent first to investigate if the activated LKB1-AMPK pathway antagonized MTOR-c-Myc-hnRNP axis to regulate alternative splice switch towards PKM1 isoform under insufficient glucose condition. We observed that glucose deprived (1mM) cells resulted in the switch in expression towards PKM1, repressing MTOR signaling pathway and the expression of its downstream effector, c-Myc, an observation which was similar to the what was detected in cells cultured under enriched glucose (25mM) condition in presence of the MTOR inhibitor, Rapamycin **(Fig. 4.12A).** Likewise, the expression status of: c-Myc, hnRNPs [hnRNPA1, hnRNPA2 and PTB] and PKM isoforms at RNA level in H1299 cells, pretreated with or without AMPK inhibitor (C.C) and/or stimulated for AMPK activation, revealed that activation of AMPK downregulated the expression of c-Myc and hnRNPs in association with PKM2 to PKM1 isoform switch. This switch in expression was prevented by the pretreatment of AMPK inhibitor (C.C), confirming the effect

of AMPK on c-Myc-hnRNP axis by down-regulating c-Myc and hnRNPs and the PKM isoform switch **(Fig. 4.12B-D).**

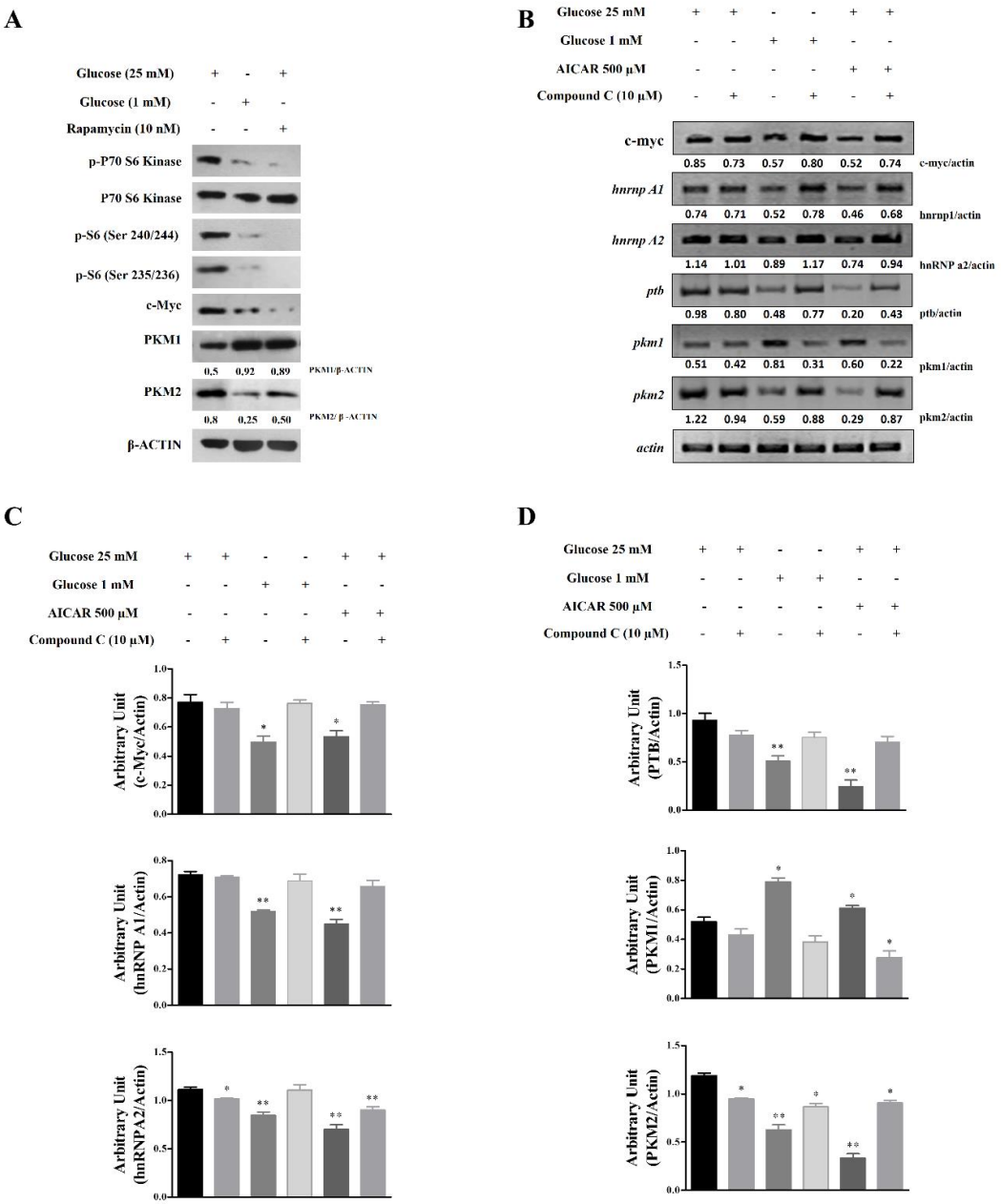

Fig. 4.12. AMPK regulates the alternative splicing of PKM isoforms. *(A) Immunoblots of the protein lysates of H1299 cells, grown under enriched (25mM) or insufficient (1mM) glucose medium or enriched (25mM) glucose medium with 10 nM Rapamycin for 8 hours, using the indicated antibodies to show an antagonistic relation between AMPK and MTOR signaling*

*pathways. The relative expression levels (signals) of PKM1 and PKM2 were quantified using ImageJ and normalized to β-Actin. (B) RT-PCR of c-Myc, hnRNPA1, hnRNPA2, PTBP1, PKM1 and PKM2 using H1299 cells grown under enriched (25mM) or insufficient (1mM) glucose medium or enriched (25mM) glucose medium with 10 nM Rapamycin for 8 hours; RT-PCR bands were subjected to densitometric analysis using Image J software and the ratio was plotted using the loading control ACTINB (ACTB), (C-D) Bars represent the relative RNA expression levels of hnRNPA1, hnRNPA2, PTBP1, PKM1 and PKM2 in H1299 cells as of (B) * P < 0.5, **P < 0.01, ***P < 0.001.*

4.9 AMPK driven PKM1 expression supports metabolic shift towards glycolysis from oxidative phosphorylation to support ATP synthesis.

Since AMPK is known to be involved in maintaining energy homeostasis (Shackelford and Shaw 2009), it was hypothesized that the AMPK driven PKM switch would influence aerobic glycolysis and the cellular energy of cancer cells in culture. In this context, to investigate the specific glycolytic implications of AMPK induced PKM2 to PKM1 switch, stable knockdowns of PKM1 and PKM2 were generated in H1299 cells **(Fig. 4.13A)**. Subsequently, aerobic glycolysis and energy status was measured in these cells, grown under enriched (25mM) and insufficient (1mM) glucose conditions, revealing that knockdown of PKM1 significantly reduced the glucose uptake, lactate release, and ATP production **(Fig. 4.13B-D)**, under glucose insufficient condition, compared to their respective vector (pLKO.1) and shPKM2 transduced cells. Expectedly, knockdown of PKM2 reduced the glucose uptake and lactate release, however, ATP production remained unaltered in cells cultured with enriched (25mM) glucose **(Fig. 4.13B-D)**. Whereas, under glucose depletion, PKM2 knockdown did not affect metabolism, probably because of the replacement of PKM1 isoform upon AMPK induction.

Further, AMPK-PKM1 dependent augmented ATP production in glucose depleted cancer cells **(Fig. 4.13D)** prompted us to examine the glycolytic and OXPHOS contribution to the ATP production in nutritionally deprived cancer cells. The glycolytic ATP levels in stable H1299 cells transduced with vector, shPKM1 or shPKM2, and cultured under enriched (25mM) and insufficient (1mM G) glucose conditions, followed by treatment with Oligomycin (a specific inhibitor of mitochondrial ATP synthase). It was clear in Oligomycin treated experiments with a

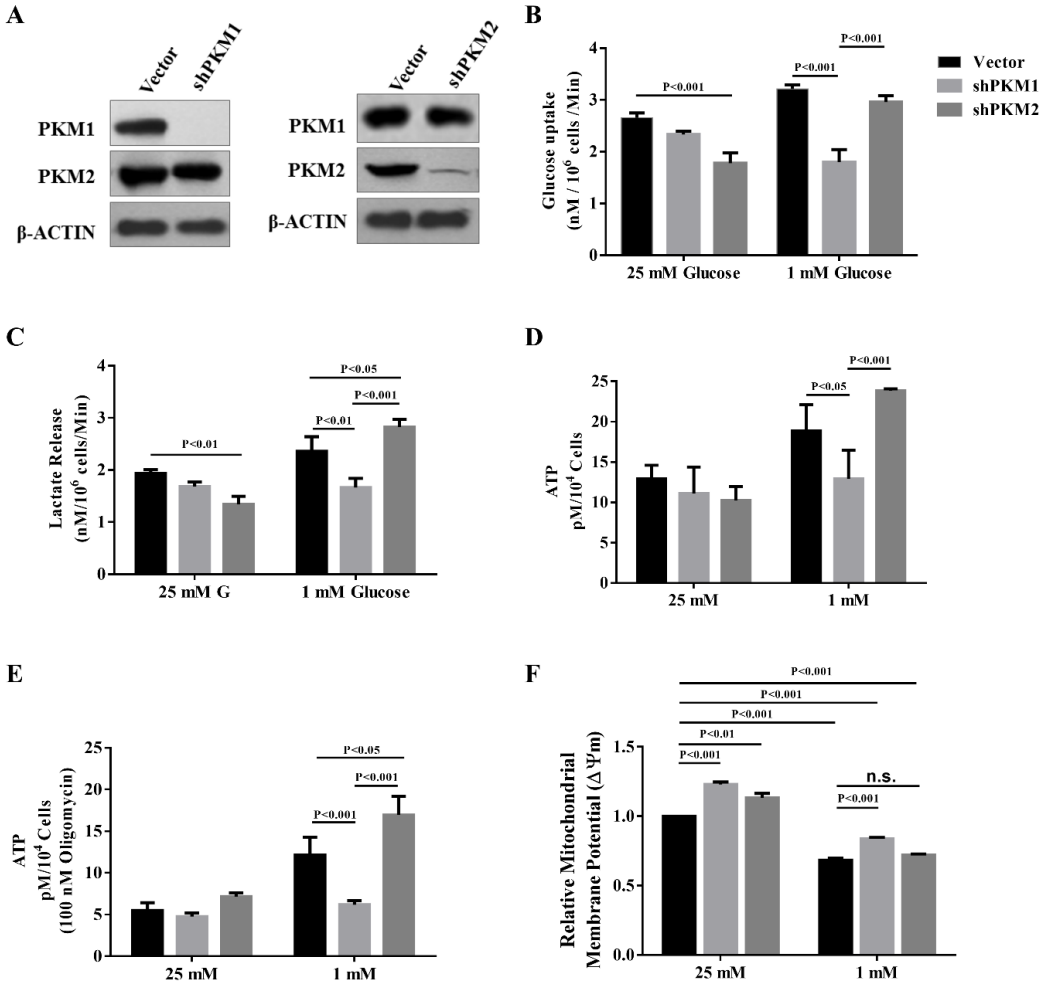

Fig. 4.13. Loss of PKM1 negatively affects the aerobic glycolysis and ATP production in glucose depleted cancer cells. *(A) Immunoblots to validate stable knockdown of PKM1 (Left) and PKM2 expression (right) in H1299 cell lines transduced with lentiviruses containing empty vector (pLKO.1) or shPKM1 or shPKM2; (B, C and D) Glucose uptake (B); Lactate release (C) and Intracellular ATP (D) levels in H1299 cells stably expressing with vector, PKM1 or PKM2 targeting shRNAs, cultured in enriched (25mM) or insufficient (1mM) glucose medium for 24 hours. (E) ATP levels in Vector, shPKM1, and shPKM2 transduced H1299 stable cells is shown under enriched (25mM) or insufficient (1mM) glucose culture condition, with or without 100nm Oligomycin treatment for 24 hours. (F) Bar diagram depicts the relative mitochondrial membrane potential in H1299 cells stably transduced with control vector (pLKO.1), shPKM1 or shPKM2 and cultured under enriched (25mM) or insufficient (1mM) glucose culture condition. For all the experiments above (n=3; mean ± SEM),*P < 0.05, **P < 0.01, ***P < 0.001.*

knock-down expression of PKM2 under insufficient glucose conditions that PKM1 contributed to a substantial increase in ATP production through glycolysis **(Fig. 4.13E)**. The large drop in ATP upon PKM1 knockdown, compared to vector and shPKM2, substantiated this further **(Fig. 4.13E)**.

Given that the cancer cells depend on aerobic glycolysis for energy generation under nutrient-starved condition through the AMPK-PKM1 axis, the mitochondrial-membrane potential ($\Delta\Psi m$) was examined under nutrient-deprived condition to perceive the status of oxidative phosphorylation. Results revealed that H1299 stable cells that are transduced with shPKM1 or shPKM2 and cultured under enriched (25mM) glucose condition exhibited an increase in mitochondrial - membrane potential ($\Delta\Psi m$), compared to the cells transduced with vector alone **(Fig. 4.13F)**. However, under insufficient (1mMG) glucose condition, the cells that exclusively expressed PKM2 and were knocked-down for PKM1, exhibited a further increase in potential, when compared with cells transduced with vector or shPKM1. Moreover, when compared with H1299 cells cultured under replete glucose condition, there was a concomitant decrease in net mitochondrial - membrane potential ($\Delta\Psi m$) in cells cultured under 1mM glucose **(Fig. 4.13F)**. Together, the data suggested that under glucose insufficient conditions, AMPK driven PKM2 to PKM1 switch in cancer cells promote aerobic glycolysis to enhance the ATP production.

4.10. AMPK driven PKM1 expression is essential for cancer cell survival under glucose depletion.

The preferential requirement of PKM isoforms (M1 or M2) under enriched (25mM) and insufficient (1mM) glucose conditions in H1299 cells, transduced with vector (LKO.1), shPKM1 and shPKM2 was assessed. As is known, the knockdown of PKM2 retarded the cell proliferation rate (vector vs. shPKM2: $P< 0.01$; 48 hrs and 72 hrs), but PKM1 knockdown did not affect the proliferation of cells in presence of 25 mM glucose **(Fig. 4.14A).** However, glucose-depleted cells showed a remarkable sensitivity to PKM1 silencing (vector vs. shPKM1: $P< 0.001$; 72 hrs and shPKM1 vs. shPKM2: $P<0.01$; 72 hrs). The viability of cells differed markedly in prolonged glucose depletion (1mM), resulting in cell death, which did not differ between PKM2 knockdown cells and the vector **(Fig. 4.14B).** Further, immunoblotting with apoptosis markers in the lysates of stable H1299 cells transduced with vector, shPKM1 and shPKM2 and cultured under limited glucose (1mM), revealed the PARP cleavage only in PKM1 knockdown cells **(Fig. 4.14C)**. To

further corroborate our *in vitro* observations, we performed immunohistochemistry (IHC) on sporadic breast tumor tissue (4 µm serial) sections to examine the spatial distribution of PKM1 and PKM2. PKM1 was found to be confined to a subset of cells which also showed the presence of pACC (Ser79) (a marker we used to locate hypoglycemic tumor microenvironment). PKM2 distribution, however, was spatially different from pACC (Ser79) positive regions, though with an appreciative co-expression of both PKM1 and PKM2 **(Fig. 4.15 A).** Together, these results demonstrated that the expression of PKM2 is critical for cancer cells to proliferate, as is known in literature, under nutritionally enriched conditions; whereas, an AMPK dependent PKM switch towards PKM1 is necessary for cancer cells to survive in glucose insufficient conditions **(Fig. 4.15B).**

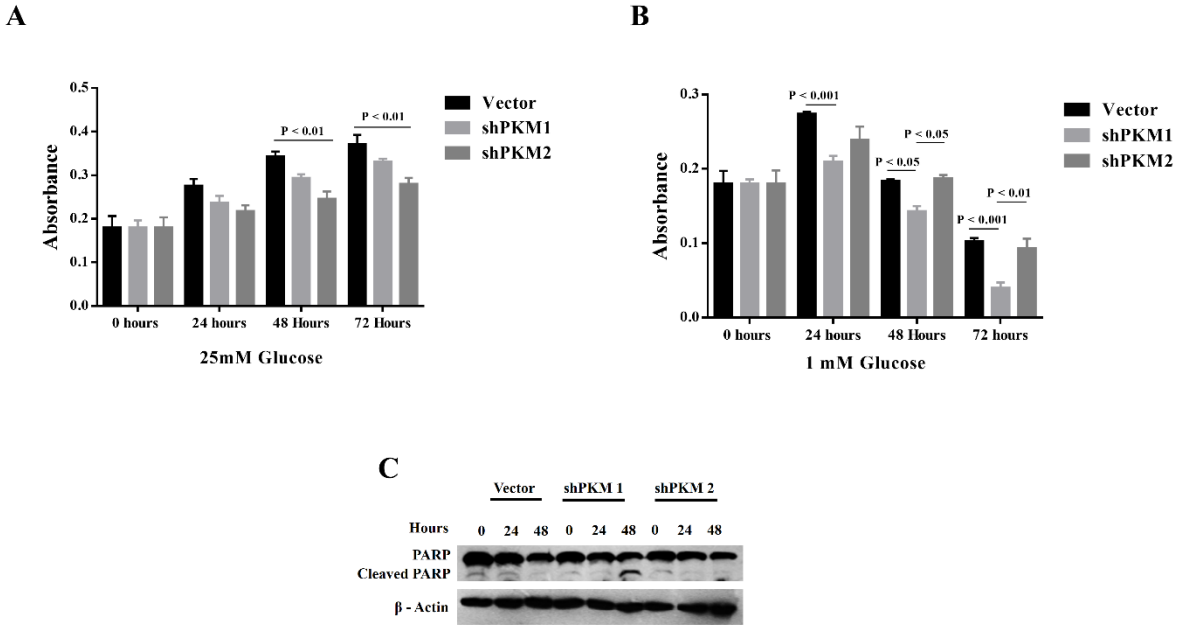

Fig 4.14. Loss of PKM1 expression inhibits survival and enhances apoptosis of glucose deprived cancer cells. ***(A and B)*** *Bars represent the proliferation rate of stable H1299 cells transduced with lentiviruses expressing empty vector (pLKO.1), shPKM1 or shPKM2, and cultured under glucose enriched (25mM) or insufficient (1mM) conditions for a period of 72 hours; where cell proliferation rate was assayed every 24 hours. For all the experiments mentioned (n=4; mean ± SEM), statistical analyses were performed using two-way ANOVA with Tukey's multiple comparison test (GraphPad Prism),*P < 0.05, **P < 0.01, ***P < 0.001.* ***(C)*** *Immunoblot for cleaved PARP to assess apoptosis in lysates of H1299 cells stably transduced with vector*

(pLKO.1), shPKM1 or shPKM2 and grown in glucose free medium supplemented with 1mM of glucose for the indicated time periods.

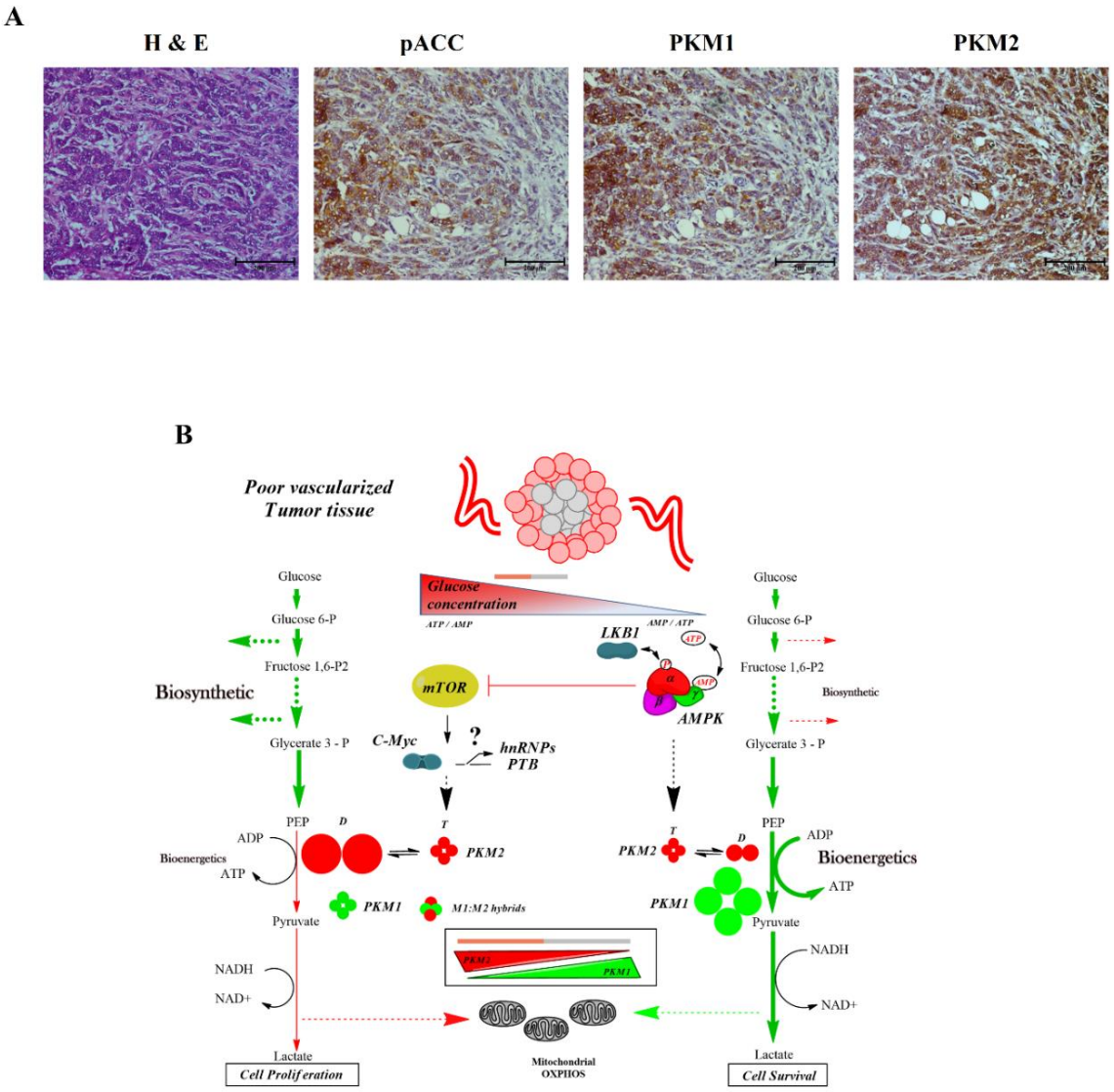

Fig. 4.15 Immunohistochemistry analysis to reveal differential distribution of PKM1 and PKM2 in tumor tissues. ***(A)*** *Hematoxylin and eosin (H & E), anti-pACC, anti-PKM1 and anti-PKM2 staining of representative serial sections from sporadic breast tumor tissues (representative of images of 8-Stage III ductal invasive carcinoma) is shown. Scale bars shown are of 200µm.* ***(B)*** *Schematic illustration of the dynamic regulation of expression of PKM1 and PKM2 by antagonistic signaling pathways of LKB1-AMPK and MTOR-hnRNPs in response to the nutritional status of*

tumor microenvironment which provides proliferative (PKM2) and survival (PKM1) advantage. The latter is proposed to be under nutrition deprivation (poor vascularized regions of a tumor) state; where ATP is generated through aerobic glycolysis predominantly. OXPHOS apparently operates in the cells regardless of glucose and PKM status.

4.11 Ectopic expression of LKB1 is essential in tumor cells that lack LKB1 to trigger AMPK mediated PKM1 expression under glucose deprivation.

Given that the axis of LKB1-AMPK-PKM1 was observed to be essential to tolerate nutritional deprivation, it has been suggested that a significant number of lung, breast and cervical carcinoma cases lack LKB1 expression and exhibit glucose addiction. To study the significance of functional LKB1, upstream to AMPK, to regulate PKM isoform switch; the cell lines, A549 (Ji et al. 2007) and MDA-MB-231 (Shen et al. 2002) lacking LKB1 were transfected with vector or Myc-tagged-LKB1 (LKB1-Myc) constructs and subjected to AMPK activation by glucose depletion (1mM). Both cell lines harboring LKB1-Myc showed a switch towards PKM1, which was not observed in vector-transfected controls **(Fig. 4.16).**

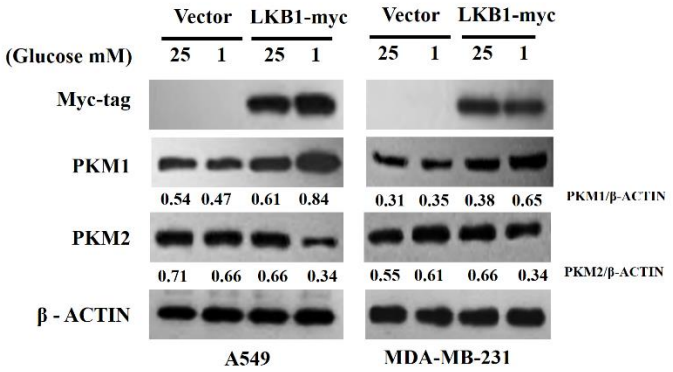

Fig. 4.16 AMPK requires LKB1 kinase to regulate the pyruvate kinase M2 to M1 isoform switch in cancer cells that lack LKB1. *Immunoblots from the protein lysates of A549 and MDA-MB 231 cells stably transfected with empty vector (pcDNA3.1) or Myc-tagged LKB1 (LKB1-Myc), cultured in glucose enriched (25mM) and deplete (1mM) medium for a period of 8 hours, probed with Myc-tag, PKM1 and PKM2 antibodies, to show overexpression of LKB1-Myc and PKM expression status.*

4.12 Ectopic expression of LKB1 is required for AMPK activation along with the pre-treatment of MG132 (proteasome inhibitors) to prevent PKM1 degradation in HPV18 positive HeLa (cervical cancer) cells under glucose deprivation.

Since HeLa cells are known to lack LKB1 expression, the observation of relatively less PKM1 expression **(Fig. 4.5B)** despite the presence of a sufficient level of RNA expression which was comparable to PKM2, was surprising. It suggested exploring reasons for the same and finding out if the integration of HPV18 in the genome of HeLa cells played any role. Therefore it was pertinent to investigate if the ectopic expression of LKB1 for AMPK activation could facilitate AMPK mediated PKM1 expression. Results revealed that the ectopic expression of LKB1 in HeLa cells in presence and absence of glucose or 500µM of AICAR indeed triggered the expression of PKM1 in AMPK dependent manner. However, PKM1 thus produced underwent proteasomal degradation, which required MG132, a proteasome inhibitor to prevent the degradation **(Fig. 4.17A).** A comparison with HPV^{-ve} A431 skin cancer cell line with endogenous LKB1 expression, used as a control, exhibited AMPK mediated PKM1 switch under the mentioned conditions **(Fig. 4.17B).**

Further, the half-life of PKM1 and PKM2 proteins in the cycloheximide chase experiment was examined. HeLa cells treated with 100 µg of cycloheximide (CHX) to block nascent polypeptide synthesis and harvested at different time points (2, 4, 8, 12 and 24 hours) were subjected to immunoblotting analysis to compare the rate of protein decay in comparison to the initial levels (0 hours). Results revealed that PKM1 in HeLa cells had a relatively weak protein stability ($t_{1/2}$ = 2 hours), when compared with PKM2 ($t_{1/2}$ = 10 hours) **(Fig. 4.18A-C).** To explore the pathway which targeted PKM1 and PKM2 for proteolysis, HeLa cells were treated with cycloheximide in combination with MG132 (proteasome inhibitor) and chloroquine (lysosome inhibitor). Results revealed that the half-life of PKM2 was extended by the co-treatment of chloroquine with CHX; whereas, MG132 co-treatment, failed to prevent PKM2 degradation **(Fig. 4.19A and B).** In case of PKM1, the combination of MG132 with CHX stabilized PKM1 accumulation with time, however, co-treatment of chloroquine failed to prevent degradation **(Fig. 4.19A and B)**. Altogether, the results suggested that HeLa cells choose to degrade PKM1 through proteasome and PKM2 using lysosome.

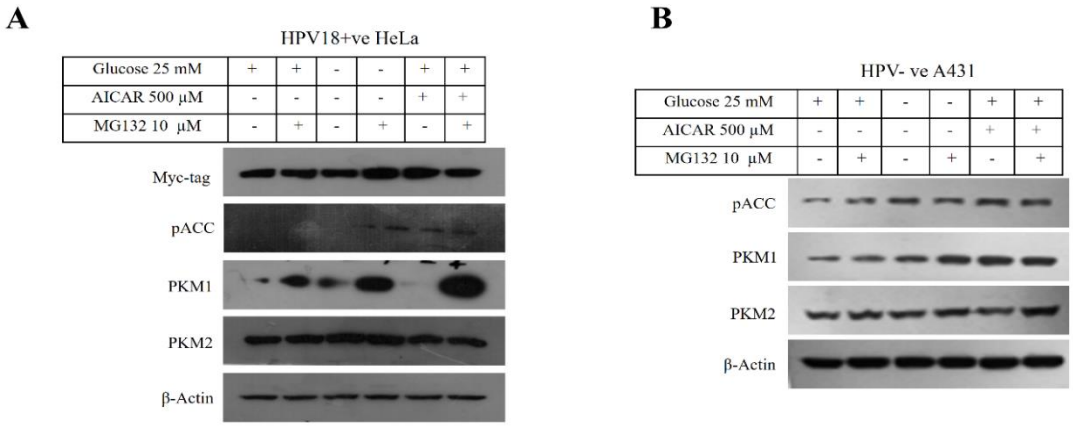

Fig. 4.17. HeLa cells require LKB1 re-constitution and MG132 treatment to stimulate AMPK mediated PKM1 expression. ***(A)*** *Immunoblot of Myc-tag, p-ACC (S79), PKM1, PKM2 and Actin from the protein lysates of HeLa cells transfected with empty vector (pcDNA3.1) or re-constituted with Myc-tagged LKB1 (LKB1-Myc) and cultured in presence and absence of glucose or 500µM of AICAR as indicated, for a period of 8 hours.* ***(B)*** *Immunoblot of p-ACC (S79), PKM1, PKM2 and Actin from the protein lysates of A431 cancer cells cultured in presence and absence of glucose or 500µM of AICAR as indicated for a period of 8 hours.*

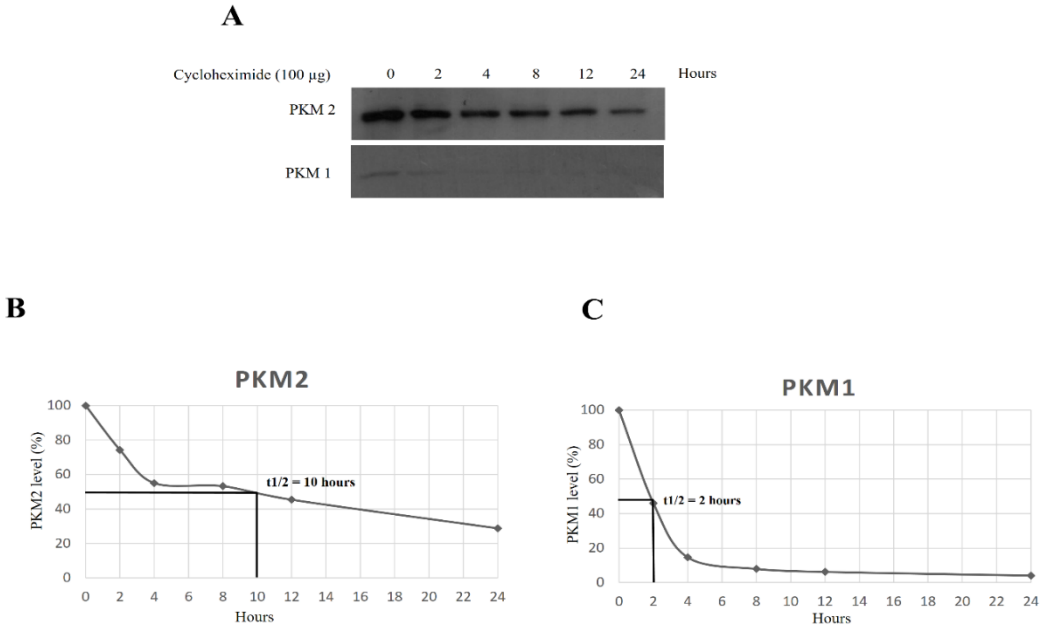

Fig 4.18. Cycloheximide chase experiment to analyze the stability of PKM1 and PKM2. *(A) Immunoblots of PKM1 and PKM2 from the protein lysate of HeLa cells treated with 100 µg of*

cycloheximide and harvested at the indicated time intervals. (B-C) The level of remaining, un-degraded PKM2 (B) and PKM1 (C) at different time points, were plotted as percentage, following the quantification of bands in the immunoblots from A and normalized against the initial levels t=0; 100% (0 hour of CHX treatment).

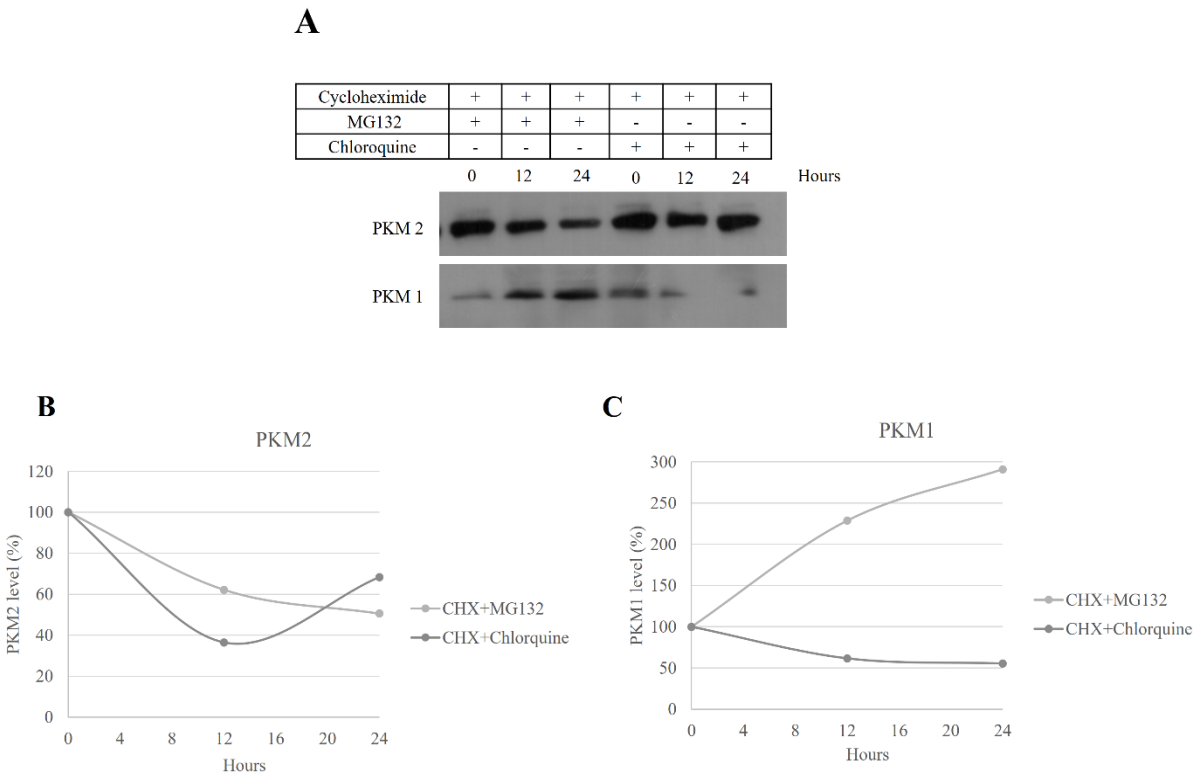

Fig. 4.19. Proteasome inhibitor prevents PKM1 degradation and lysosome inhibitor prevents PKM2 degradation in HeLa cells. (A) *Immunoblots of PKM1 and PKM2 from the protein lysate of HeLa cells treated with combination of 100 µg of cycloheximide + 10 µg MG132 or 100 µg of cycloheximide + chloroquine for the indicated time periods. (B-C) The level of remaining, un-degraded PKM2 (B) and PKM1 (C) at different time points, plotted in graphs as percentage, following the quantification of bands in the immunoblots from A and normalized against the initial levels t=0; 100%.*

4.13 HPV encoded E6 and E7 viral oncoproteins regulate expression switch of PKM isoforms and glycolytic pathway enzymes to favor aerobic glycolysis.

To comprehend the role of HPV encoded oncoproteins (E6 and E7) in the expression of PKM isoforms and the core glycolytic enzymes that govern aerobic glycolysis, HPV18+ve HeLa cells were transfected with siRNA to target the expression of E6 and E7 oncoproteins. The silencing of E6 and E7 oncoproteins was validated by semi-quantitative RT-PCR **(Fig. 4.20A)**. Subsequent to this, the expression level of key glycolytic enzymes that govern aerobic glycolysis, like HK1, HK2, LDHA, LDHB and PKM1/2, were examined and found with a significant decrease in their expression **(Fig. 4.20A and B).** Further, to evaluate the absolute expression levels of PKM1 and PKM2 in HeLa cells transduced with si18E6/E7, a semi quantitative RT-PCR was performed, using PKM primers flanking Exon 8 and Exon 11 followed by the restriction digestion with Ale I enzyme. Results revealed a significant shift in the isoforms of PKM from PKM2 to PKM1 **(Fig. 4.20C and D)**.

4.14 HPV18 encoded E6 and E7 oncoproteins regulate c-Myc and the splicesome factors to regulate PKM isoform switch.

Since transcriptional factor, c-Myc mediated transactivation of hnRNPs (Heterogeneous nuclear ribonucleoproteins) controls the preferential expression of PKM2 and PKM1 repression (Clower et al. 2010, David et al. 2010, Sun et al. 2011); it was appropriate to examine the expression status of c-Myc and hnRNPs to correlate with observed PKM2 to PKM1 switch in HeLa cells transfected with 18E6 and E7siRNA. As anticipated, silencing of E6 and E7 oncoproteins significantly down regulated the expression of c-Myc, hnRNPA1, hnRNPA2 and PTBP1; correlating with PKM2 to PKM1 switch **(Fig. 4.21A and B).**

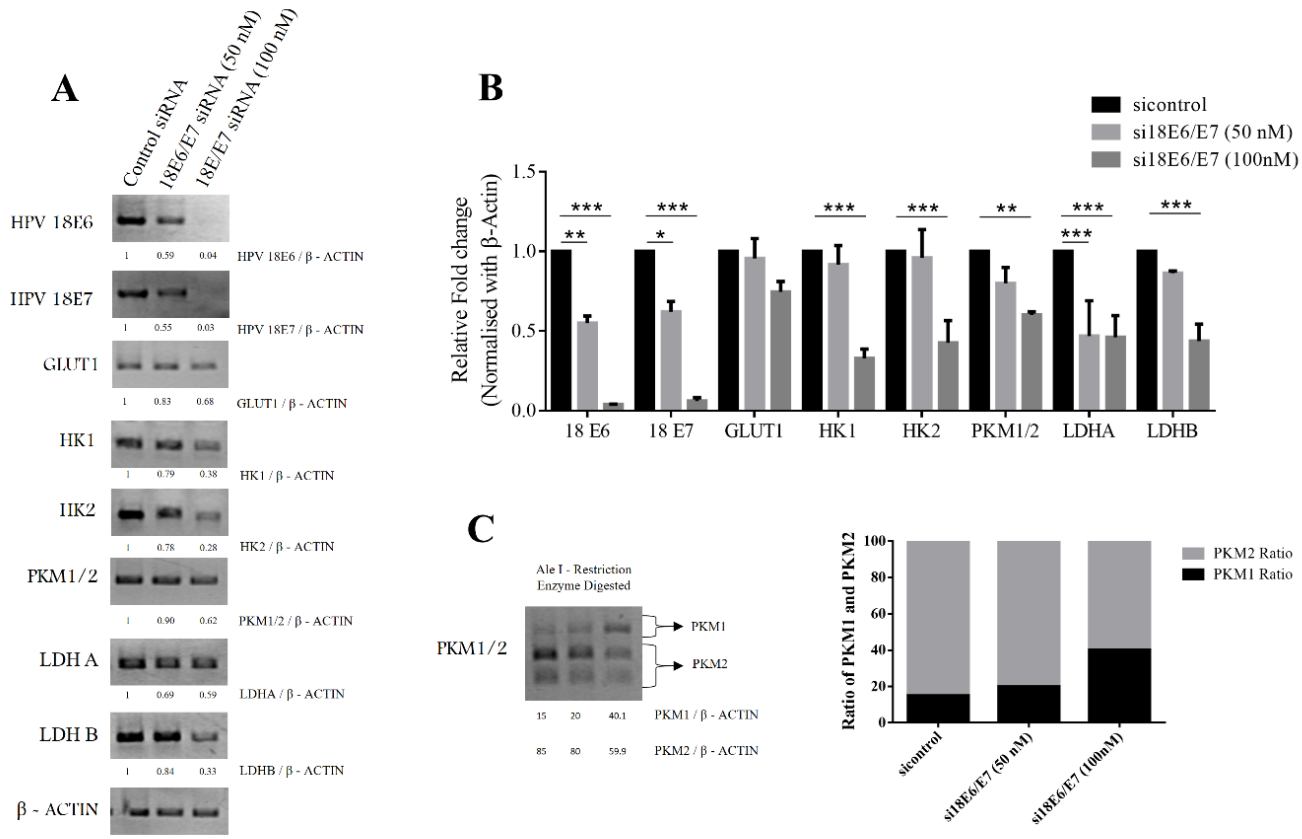

Fig. 4.20. Effect of HPV18 encoded oncoprotein E6 and E7 silencing on glycolytic pathway enzymes in HeLa cells. *(A) RT-PCR of HPV18E6, HPV18E7, GLUT1, HK1, HK2, PKM1/2, LDHA and LDHB, using HeLa cells transfected with 50nM or 100nM of siRNA, to silence the expression of E6 and E7 oncoprotein. RT-PCR bands were subjected to densitometric analysis using Image J software and the ratio was plotted using the loading control ACTINB (ACTB). (B) Bars represent the relative RNA expression levels of HPV18E6, HPV18E7, GLUT1, HK1, HK2, PKM1/2, LDHA and LDHB in HeLa cells as of (A) * P < 0.5, **P < 0.01, ***P < 0.001. (C) Semi-quantitative RT-PCR followed by PKM2 exon-specific restriction digestion with AleI restriction enzyme to examine the proportion of PKM1 and PKM2 expression in HeLa cells transfected with 50nM or 100nM of siRNA, after silencing the expression of E6 and E7 oncoprotein. (D) Bar diagrams showing a relative percentage of PKM1 and PKM2 as of (C).*

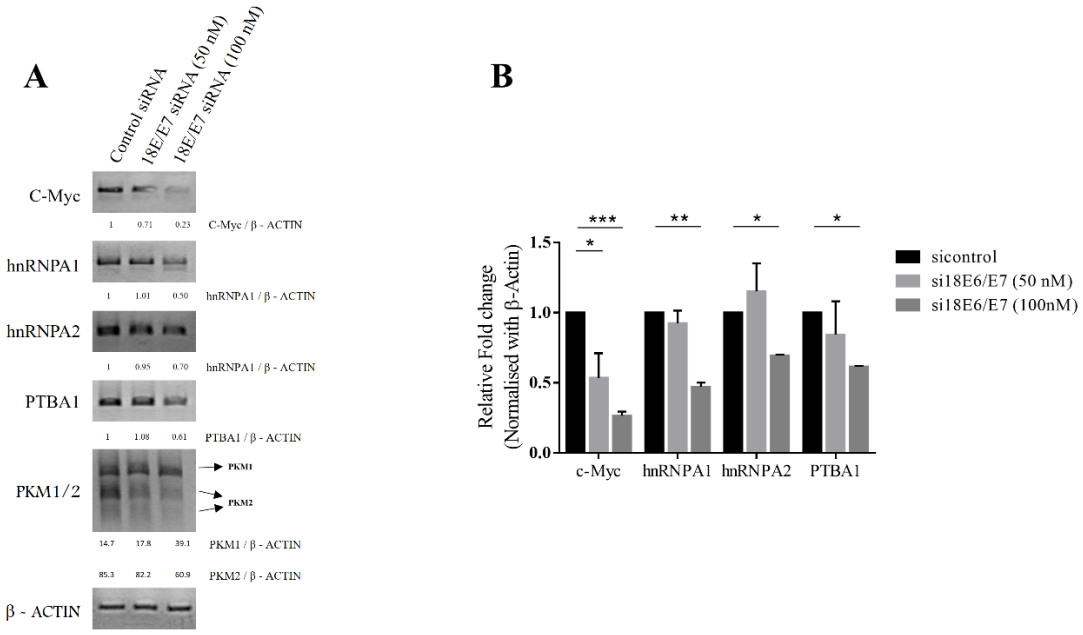

Fig. 4.21. C-Myc and its downstream splicesome factors (hnRNPS') govern the E6 and E7 oncoprotein stimulated PKM switch. *(A) RT-PCR of c-Myc, hnRNPA1, hnRNPA2, PTBP1, and PKM1/2 using HeLa cells transfected with 50nM or 100nM of siRNA to silence the expression of E6 and E7 oncoprotein; RT-PCR bands were subjected to densitometric analysis using Image J software and the ratio was plotted using the loading control ACTINB (ACTB). (B) Bars represent the relative RNA expression levels of hnRNPA1, hnRNPA2, PTBP1, PKM1 and PKM2 in HeLa cells as of (A) * P < 0.5, **P < 0.01, ***P < 0.001.*

4.15 PKM1 or PKM2 knockdown differentially affect net pyruvate kinase activity, ATP level and cell proliferation of lung cancer cell lines.

M2 isoform of pyruvate kinase (PKM2) has emerged as a potential candidate to target different types of tumors. However, recent studies have highlighted the limitation that exists in the strategy of targeting PKM2 in cancer. The knockdown of PKM2 in *in vitro* and *in vivo* has been reported to affect proliferation and viability of cancer cells of different tissue origin heterogeneously (Christofk et al. 2008, Goldberg and Sharp 2012, Cortés-Cros et al. 2013, Israelsen et al. 2013). In

order to find out what determines such a heterogeneous response and to examine the key features that confer protection against PKM2 knockdown induced growth inhibition and cell death in cancer cells, the lentivirus harboring shRNA targeting PKM1 or PKM2 mRNA in human lung cancer cell lines (A549 and H1299) was introduced to generate stable knockdowns for PKM isoforms. PKM1 or PKM2 knockdown was validated with Western blotting **(Fig. 4.22A).** When measured for PK activity, H1299 cells that were subjected to PKM2 knockdown, exhibited 90% reduction in the net PK activity; whereas, PKM1 knockdown reduced the activity by 26% in comparison to vector (pLKO.1) transfected cells **(Figs. 4.22B-C left panels)**. In A549 cells silenced for PKM2, the activity was reduced by 67%; and PKM1 silencing reduced the activity by 58% **(Figs. 4.22B-C right panels)**, suggesting a differential contribution of PKM2 and PKM1 isoforms to the net PK activity in the two (H1299 and A549) cell lines. Intriguingly, stable knockdown of PK isoforms in A549 cells significantly reduced the cellular ATP level; whereas, in H1299 cells the knockdown left the level of ATP unaltered **(Fig. 4.22D)**. However, H1299 cells that were transiently transduced with shPKM1 or shPKM2 showed a reduction in the total cellular ATP level (Data not shown), which probably suggests that H1299 stable cells for PKM1 and PKM2 knockdown passaged for successive generations attained energy homeostasis. When measured for cell proliferation rate, H1299 cells stably transduced with shPKM2 demonstrated a significant reduction in their proliferation (vector vs. shPKM2, 24 hrs; $P< 0.001$, 48 hrs; $P< 0.001$ and 72 hrs; $P< 0.001$); whereas, the proliferation rate of cells transduced with shPKM1 remained unaffected **(Fig. 4.23A)**. Likewise, stable PKM2 knockdown in A549 cells showed a remarkable reduction in their proliferation rate (vector vs. shPKM2, 48 hrs; $P< 0.001$ and 72 hrs; $P< 0.01$). However, in contrast to H1299, stable PKM1 knockdown in A549 cells also exhibited proliferation reduction (vector vs. shPKM1, 48 hrs; $P< 0.001$ and 72 hrs; $P< 0.001$) **(Fig. 4.23B)**. The effect of PKM silencing on H1299 and A549 cell proliferation was further validated using colony forming assay, where PKM2 silencing significantly affected H1299 propagation and colony formation (vector vs. shPKM2; $P< 0.05$) **(Fig. 4.23C)**; whereas, knockdown of either PKM1 or PKM2 largely reduced A549 cell colony forming ability (vector vs. shPKM1; $P< 0.05$ and vector vs. shPKM2; $P< 0.05$) **(Fig. 4.19D)**.

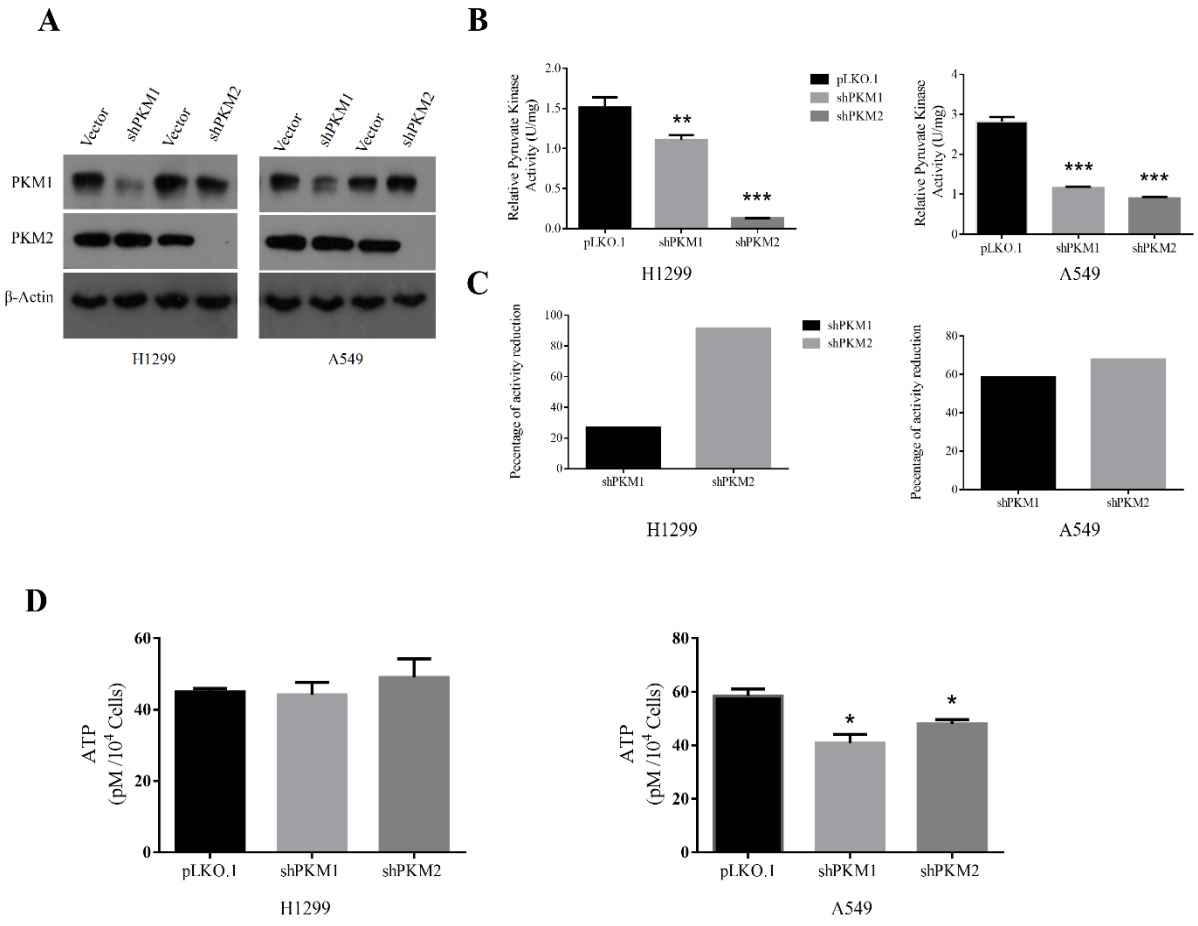

Fig. 4.22. Knockdown of PKM1 or PKM2 differentially affects the metabolism of human lung cancer cells, H1299 and A549. ***(A)*** *Immunoblots to validate stable knockdown of PKM1 and PKM2 expression in H1299 (left panel) and A549 (right panel) cells, transduced with vector control (pLKO.1), shPKM1 or shPKM2.* ***(B)*** *Relative pyruvate kinase enzyme activity from protein lysates of H1299 (left panel) and A549 (right Panel) cells stably transduced with control vector (pLKO.1), shPKM1 or shPKM2.* ***(C)*** *Bar diagrams showing a relative reduction in the percentage of pyruvate kinase activity after silencing of PKM1 and PKM2 in H1299 (left panel) and A549 (right panel) cells.* ***(D)*** *Intracellular ATP levels in H1299 (left panel) and A549 (right panel) cells stably transduced with vector (pLKO.1), shPKM1 or shPKM2. *P < 0.05, **P < 0.01, ***P < 0.001.*

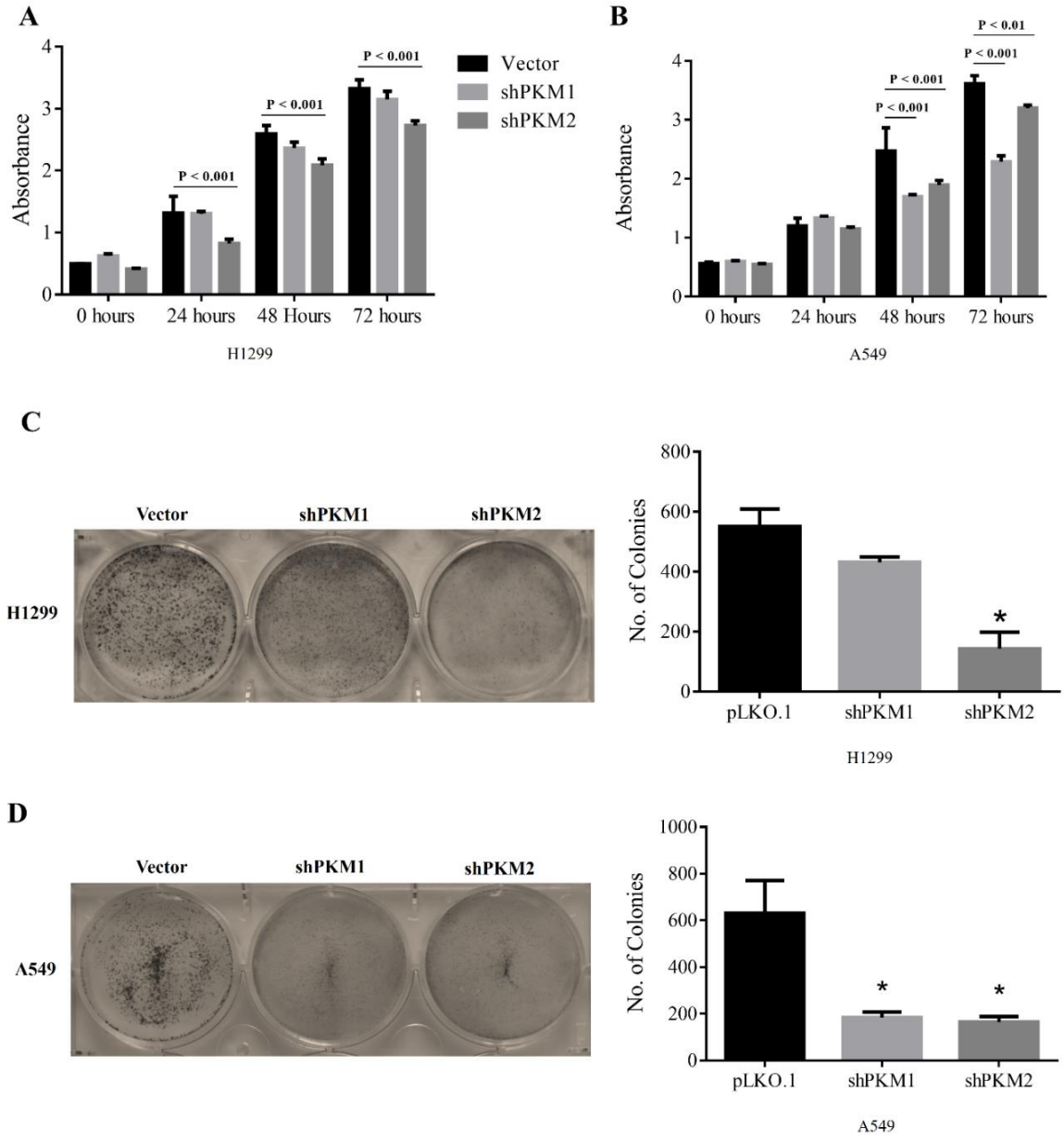

Fig. 4.23. PKM1 or PKM2 silencing differentially affects the proliferation of H1299 and A549 cells. ***(A-B)*** *CCK8 assay to examine the proliferation rate of* ***(A)*** *H1299 cells and* ***(B)*** *A549 cells, stably transduced with vector (pLKO.1), shPKM1 or shPKM2 and cultured for a period of 72 hour; cell proliferation rate was assayed at every 24 hour interval.* ***(C-D)*** *Bars represent the number of colonies obtained from the anchorage-dependent clonogenic assay of H1299 (left) and A549 (right) stable cells transduced with lentivirus containing empty vector (pLKO.1), shPKM1 or shPKM2. *P < 0.05.*

4.16. PKM knockdown activates AMPK signaling to promote mitochondrial biogenesis and autophagy, evading apoptosis.

The stable knockdown of PKM1 or PKM2 in H1299 cells activated AMPK signaling pathway in response to the perturbed energy (ATP) homeostasis. The activation of AMPK was measured by a marked increase in the Threonine 172 (Thr172) phosphorylation of AMPK and Serine 79 (Ser79) phosphorylation of Acetyl-CoA carboxylase (ACC; a downstream substrate of AMPK) **(Fig. 4.24A left panel)**. Also, we observed that the prolonged abrogation of PKM isoforms (i.e. stable knockdowns that were passaged through successive generations) resulted in the up-regulation of the expression of AMPK alpha subunits. Conversely, stable PKM isoform knockdowns in A549 cells failed to activate AMPK, owing to the lack of the upstream protein kinase LKB1 (Ji et al. 2007, Shackelford et al. 2013, Faubert et al. 2014) **(Fig. 4.24A right panel)**.

Further, the active AMPK in stable H1299 cells stimulated mitochondrial biogenesis, where activation of AMPK in H1299 cell was associated with concomitant increase in mitochondrial-membrane potential ($\Delta\Psi m$) **(Fig. 4.24B)** and-mass **(Fig. 4.24C)**, with an overall increase in the expression of master regulatory transcription factors of mitochondrial biogenesis (PGC 1α, NRF1, NRF2 and TFAM) and mitochondrial-encoded subunits of electron transport chain (ETC) complexes (COX 1, ND3 and ATP6) **(Fig. 4.24D)**. A549 cells that were silenced for the expression of PKM1 or PKM2 failed to show such changes in the mitochondrial membrane potential ($\Delta\Psi m$), mitochondrial content, and expression of genes associated with mitochondrial biogenesis **(Fig. 4.24B-D)**. Remarkably, H1299 cells that were silenced for PKM isoforms showed autophagy, examined using autophagic marker LC3B-II, without showing any sign of apoptosis **(Fig. 4.24E)**; while, A549 cells that failed to activate AMPK pathway in response to PKM isoform silencing underwent apoptosis, but not autophagy. **(Fig. 4.24E)**.

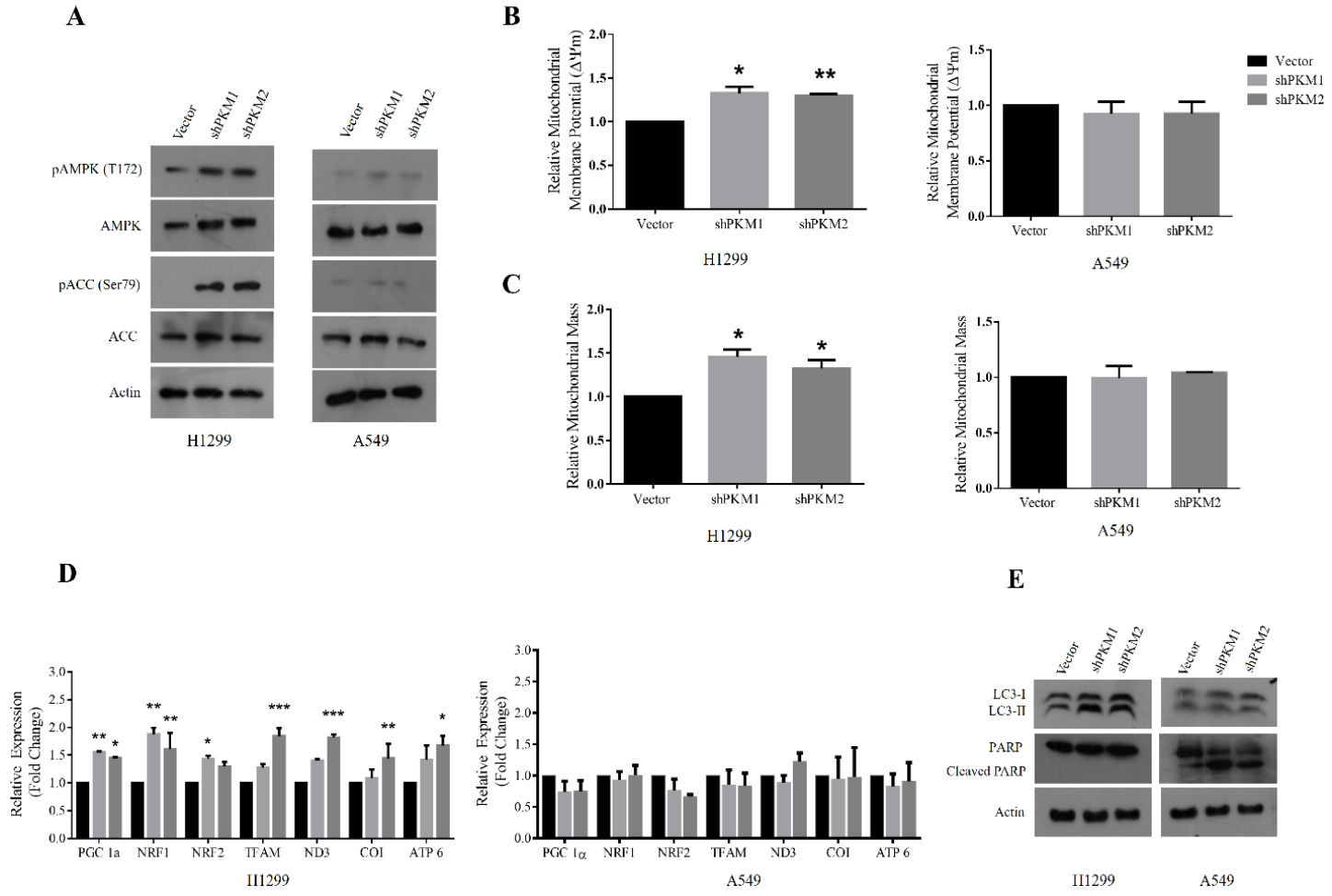

Fig. 4.24. AMPK signaling reprograms energy metabolism pathway to sustain energy homeostasis and to prevent apoptotic cell death. ***(A)*** *Immunoblots from the protein lysate of H1299 (left panel) and A549 (right panel) cells stably transduced with lentivirus containing control vector (pLKO.1), shPKM1 or shPKM2, to show AMPK signaling activation.* ***(B-C)*** *Bar diagram depicts the relative mitochondrial membrane potential* ***(B)*** *and mitochondrial mass* ***(C)*** *in H1299 (left panel) and A549 (right panel) cells stably transduced with control vector (pLKO.1), shPKM1 or shPKM2, *P < 0.05, **P < 0.01.* ***(D)*** *qRT-PCR analysis to show the relative change in expression of the genes involved in mitochondrial biogenesis (PGC 1α, NRF1, NRF2 and TFAM) and mitochondrial-encoded subunits of electron transport chain complexes (COX 1, ND3*

*and ATP6) from H1299 (left) and A549 (right) cells with stable PKM1 and PKM2 knockdown. The bars represent the fold-change after normalizing with the control of each group (vector transfected), *P < 0.05, **P < 0.01, ***P < 0.001.* ***(E)*** *Immunoblots from the protein lysate of H1299 (left panel) and A549 (right panel) cells transduced with lentivirus containing empty vector (pLKO.1), shPKM1 or shPKM2, to assess autophagy and apoptosis, using LC3B-II and Cleaved PARP as markers.*

4.17. Knockdown of AMPK catalytic alpha subunit along with PKM1 or PKM2 induces apoptosis in H1299 cells.

Given that PKM1 or PKM2 silencing in H1299 cells stimulated a metabolic shift to mitochondrial oxidative phosphorylation in an AMPK pathway-dependent manner to preserve energy homeostasis, we speculated that this reprogramming of energy metabolism might have warranted resistance against PKM1 and PKM2 silencing induced cell death in H1299 cells. To test our hypothesis, the expression of AMPK alpha2 catalytic subunit was silenced in H1299 stable cells for PKM1 and PKM2 knockdown and validated with Western blotting (**Fig. 4.25A).**

Furthermore, we observed that the combination of AMPKα2 catalytic subunit and PKM1 or PKM2 knockdown in H1299 cells did not affect the mitochondrial membrane potential (ΔΨm) **(Fig. 4.25B)**, mitochondrial mass **(Fig. 4.25C)**, and expression of genes associated with mitochondrial biogenesis (PGC 1α, NRF1, NRF2 and TFAM) and mitochondrial-encoded subunits of electron transport chain (ETC) complexes (COX 1, ND3 and ATP6) **(Fig. 4.25D)**. When evaluated for cell proliferation rate, H1299 cells that were transduced with the combination of shAMPKα2+shPKM1 or shAMPKα2+shPKM2 demonstrated a significant reduction in their proliferation (vector vs. shAMPKα2+shPKM1, 24 hrs; $P< 0.01$, 48 hrs; $P< 0.001$ and 72 hrs; $P< 0.001$) (vector vs. shAMPKα2+shPKM2, 24 hrs; $P< 0.001$, 48 hrs; $P< 0.001$,72 hrs; $P< 0.001$) **(Fig. 4.25E)**, and also exhibited apoptotic cell death, however, with no sign of autophagy **(Fig. 4.25F)**.

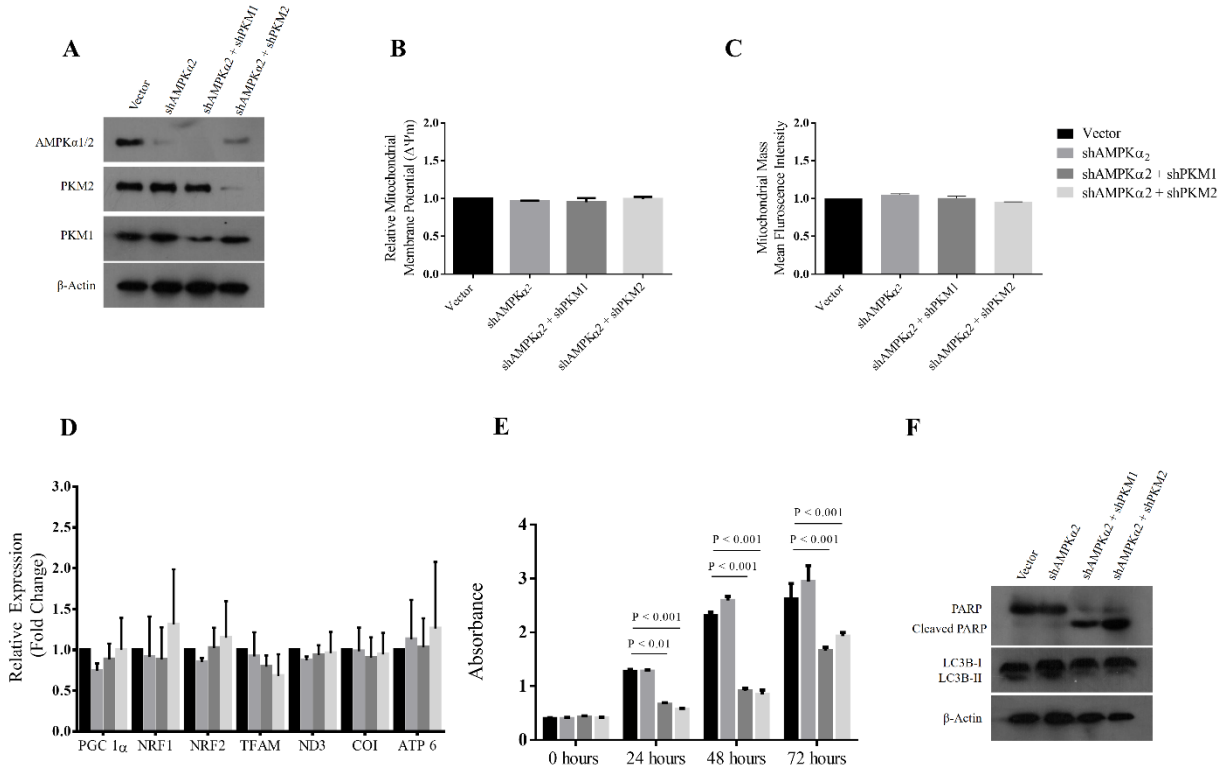

Fig. 4.25. AMPKα2 and PKM1 or PKM2 dual knockdowns induce cell death in H1299 cells by preventing reprogramming of energy metabolism. ***(A)*** *Immunoblots from the protein lysate of H1299 cells stably transduced with control vector (pLKO.1), shAMPKα2, shAMPKα2- and -shPKM1 or -shPKM2 to validate the knockdown of AMPKα2, PKM1, and PKM2. (B-C) Bar diagram depicts the relative mitochondrial membrane potential* ***(B)*** *and mitochondrial mass* ***(C)*** *in H1299 cells stably transduced with control vector (pLKO.1), shAMPKα2, shAMPKα2- and -shPKM1 or -shPKM2.* ***(D)*** *qRT-PCR analysis to show the relative expression change of genes involved in the mitochondrial biogenesis (PGC 1α, NRF1, NRF2 and TFAM) and mitochondrial-encoded subunits of electron transport chain complexes (COX 1, ND3 and ATP6) from H1299 cells for stable AMPKα2 or AMPKα2 and PKM1 or PKM2 knockdown. The bars represent the fold-change after normalizing with the control of each group (vector transfected).* ***(E)*** *CCK8 assay to examine the proliferation rate of H1299 cells stably transduced with control vector (pLKO.1), shAMPKα2, shAMPKα2, and shPKM1 or shPKM2 and cultured for the period of 72 hours; cell proliferation rate was assayed at every 24 hour interval.* ***(F)*** *Immunoblots from the protein lysate of H1299 as mentioned in* ***(A)*** *to measure autophagy and apoptosis, using LC3B-II and Cleaved PARP as markers.*

CHAPTER~5
Discussion

Chapter-5

Discussion

The key challenge in tumor metabolism and growth is to comprehend how rapidly the dividing cancer cells in solid tumors overcome the checkpoints that maintain tissue homeostasis, especially under nutritional stress. To unravel the signaling pathway and its downstream adaptive metabolic phenotype(s) that benefit cancer cells to survive the fluctuations in available nutrients, remains of interest. The study conducted in this thesis attempted to address some of mentioned scientific puzzles by elucidating a novel signaling axis of LKB1-AMPK-PKM1, providing metabolic benefits that nurse cancer cells to overcome the unfavorable condition of nutritional stress. In the light of the results obtained, this work proposes a potential therapeutic strategy of employing silencing of both the PKM isoforms in tumors, that shelter heterogeneous clones of cancer cells with diverse metabolic signatures, after evaluating the cellular status of AMPK.

5.1 LKB1-AMPK axis regulates the switch of Pyruvate Kinase M isoforms to tolerate nutritional stress

The results obtained demonstrated an integral role of LKB1-AMPK signaling pathway in regulating the expression switch from M2 to M1 isoform of the glycolytic enzyme, pyruvate kinase, in response to glucose depletion in cancer cells (**Fig. 4.1 and 4.2**), which did not alter the expression of isoforms of hexokinase (HK1 and HK2) and lactate dehydrogenase (LDHA and LDHB) **(Fig. 4.4 and 4.7)**. The role played by AMPK in PKM isoform switch towards PKM1 under hypoglycemic conditions corroborated with the results obtained after the use of AMPK activator (AICAR) and the inhibitor compound C (C.C) **(Fig. 4.1 and Fig. 4.2)**. The cell lines lacking LKB1 when used in the experiments expressing the constitutively active mutant of AMPK (T172D) demonstrated further the critical importance of LKB1 upstream to AMPK in regulating PKM1 switch **(Fig. 4.3 and 4.16)**. Results showed that the activation of AMPK resulted in the inhibition of MTOR signaling and downregulated c-Myc, hnRNPA1, hnRNPA2 and PTB expression, concomitant with the switching of expression from PKM2 to PKM1 **(Fig. 4.12)**.

Till date in literature, a preferential expression of PKM2 over other tissue isoforms has been considered as one of the metabolic hallmark feature of cancer (Cairns et al. 2011); where PKM2 expression serves the pivotal role in cancer growth (Christofk et al. 2008) by governing aerobic glycolysis (Yang et al. 2012) and performs a non-metabolic role of; co-transcription activation (Luo et al. 2011, Yang et al. 2011), protein kinase function (Gao et al. 2012, Yang et al. 2012) and chromosomal segregation (Jiang et al. 2014). The expression of PKM2 in tumors has been considered to be a strategic step, retaining an intrinsic feature of interchangeable oligomeric states of catalytically active tetramer and an inactive dimer in response to numerous factors (Iqbal et al. 2014). The dynamic oscillation between PKM2 dimer : tetramer replenishes the biosynthetic and bioenergetic needs of cancer cells by redirecting flux of glycolysis towards anabolism or catabolism ; as well as presumably surviving under varying oxygen and nutrient conditions in tumor microenvironment. The co-expression of M1 and M2 isoforms of pyruvate kinase detected in a representative set of sporadic breast cancer tissues and several cancer cell lines **(Fig. 4.5)** elucidated their role by finding how nutrient status of insufficient glucose under culture conditions resulted in a preferential switch of expression towards PKM1 isoform. In addition to their co-existence, a novel interaction between M1 and M2 isoforms of pyruvate kinase, generating heterotetrameric cross-oligomers but not heterodimers was revealed **(Fig. 4.11)**; which in all likelihood contributed to the net pyruvate kinase enzyme activity in cancer cells cultured under enriched glucose condition. The switch towards non-allosteric, catalytically more active PKM1 expression in glucose depleted cancer cells increased the net PKM activity by facilitating the subunit association of PK towards its catalytically more active oligomeric (tetrameric) form **(Fig. 4.6)**. In comparison to the established non-metabolic functions of PKM2 by regulating PKM2 nuclear localization under the influence of growth factors and hormones (Hoshino et al. 2007, Yang et al. 2011), the localization of PKM1 in the cytoplasm, nucleus and mitochondria, as observed in LC-MS/MS interactome data, was interesting **(Fig. 4.9 and Table 4.1);** which was further supported by confocal and immunoblotting analysis of subcellular localization **(Fig. 4.10)**. Altogether, these results widen the scope of the role of both the isoforms of PK, assigning new roles to PKM1. The possible interactions between PKM1 and ATP synthase of mitochondria and MCM-7 of nucleus, as indicated in LC-MS/MS interactome, provided an apparent support to the

proposed role of PKM1, requiring additional functional studies to validate the interaction and to examine the non-metabolic functions of PKM1 in future.

The preferential expression of PKM1 in glucose depleted cancer cells and its increased activity with enhanced aerobic glycolysis, a conclusion drawn from the observation of increased glucose uptake, lactate release rate, and decrease in mitochondrial membrane potential ($\Delta\Psi m$) to maintain energy (ATP) homeostasis **(Fig. 4.13)**, apparently provided endurance for cell survival. Silencing of PKM1 expression by knockdown impaired aerobic glycolysis and apparently energy homeostasis **(Fig. 4.13)**, reducing the survival of glucose depleted cancer cells and inducing the state of apoptosis **(Fig. 4.14)**. However, similar metabolic features were observed with the knockdown of PKM2, showing impaired proliferation rate of cancer cells, under enriched nutrient condition, an observation consistent with the present knowledge in literature (Christofk et al. 2008). The switch from PKM2 to PKM1 expression probably shifted the flux of glycolysis from biosynthesis to bioenergetics phase, essential for cell survival under hypoglycemic conditions. Notably, despite the association of AMPK pathway with mitochondrial biogenesis (Reznick and Shulman 2006), the LKB-AMPK-PKM1 axis in glucose depleted cancer cells uncoupled the mitochondrial oxidative phosphorylation and showed an enhanced aerobic glycolysis for ATP generation; evidenced from the observation of an unaltered ATP levels with Oligomycin treatment, and reduced mitochondrial membrane potential ($\Delta\Psi m$) in glucose depleted cancer cells **(Fig. 4.13)**. It appeared enigmatic, but contemporary studies support the observation of accelerated aerobic glycolysis associated with nutrient depleted cancer cells (Amoroso et al. 2012, Wu et al. 2013). Wu et al, have shown how AMPK inhibited the mitochondrial pyruvate entry in nutrient depleted cancer cells, which is in support of the observation made here. One more plausible justification could be in terms of how real-life tumors encounter the 'recurrent' hypoglycemia with hypoxia, which obliges the cancer cells to prefer aerobic glycolysis over mitochondrial oxidative phosphorylation.

PKM2 has been validated as a potential candidate of glycolysis for therapeutic interventions to target cancer metabolism (Gupta et al. 2014). However, in the background of the observations of co-existence of the two isoforms of PKM **(Fig. 4.5)**, and the preferential expression of one of the isoforms, PKM1, under nutrient deficient conditions **(Fig. 4.1 and 4.2)**, a model of gradient

creation of the two PKM isoforms in malignant tumors is proposed. Where cells nourished with nutrients in the periphery of tumor and in proximity to the blood vessels express PKM2 predominantly in a dimeric state with concomitant low expression of PKM1 tetramer for attaining proliferation advantage. Whereas, the cells in the core of tumors (hypoglycemic/hypoxic centers), starved of nutrients, are programmed to express the PKM1 isoform in an AMPK dependent manner to provide the cancer cells a survival advantage. Thus, the two processes, one driven by PKM2 dimer/tetramer state of attending to the biosynthetic/bioenergetic needs and the other driven by PKM1 tetramer for bioenergetic requirement alone, contribute to the metabolic heterogeneity of real-life tumor cells **(Fig. 4.15)**, demanding the tailor made therapeutics to target both PKM2 in the periphery and PKM1 in the core of solid tumors.

5.2 HPV18^{+ve} HeLa cells constitutively direct PKM1 for proteasomal degradation and transactivate c-Myc to regulate PKM2 expression switch and glycolytic pathway enzymes to favor aerobic glycolysis

Given that the axis of LKB1-AMPK-PKM1 provides tolerance to cancer cells under hypoglycemic condition; mounting evidence in literature suggests that HeLa cells lacking the expression of LKB1 due to promoter hyper-methylation (Tiainen et al. 1999) undergo apoptosis. This happened when cells were cultured under nutrient deprived condition or were treated with agents that increased the cellular AMP/ATP ratio, causing energy perturbation (Nafz et al. 2007, Inge et al. 2009, Shackelford et al. 2013, Whang et al. 2016 Shaw et al. 2004, Jeon et al. 2012) (Shaw et al. 2004, Jeon et al. 2012) . In the present study HeLa cells re-constituted with LKB1ectopic expression and cultured under glucose starved condition or in presence of ACIAR failed to show PKM1 isoform expression switch **(Fig. 4.17)**. However, pre-treatment with MG132 (Proteasome inhibitor) stabilized PKM1 expression **(Fig. 4.17)**. Further, results of cycloheximide chase experiments along with proteolysis inhibitor co-treatment demonstrated that PKM1 in HPV18^{+ve} HeLa cells was constitutively dictated to undergo proteasomal degradation **(Fig. 4.18 and 4.19)**. Intriguingly, siRNA mediated silencing of HPV18 encoded E6 and E7 oncoproteins in HeLa cells significantly decreased the expression of major glycolytic pathway enzymes (that contribute to aerobic glycolysis), in particular showing a shift in the isoforms of PKM from PKM2 to PKM1 **(Fig. 4.20)**. Further experiments emphasized the involvement of c-Myc controlled transcriptional regulation

of hnRNPs' in HPV18 E6 and E7 mediated PKM1 to PKM2 expression switch (Fig 4.21). This was confirmed in the present study by silencing E6 and E7 oncoproteins in HeLa cells, where a significant down-regulation of expression of c-Myc, hnRNPA1, hnRNPA2 and PTB1 was observed; the features which correlated well with PKM2 to PKM1 switch.

5.3 Tumor cells lacking LKB1-AMPK axis are more prone to PKM knockdown induced growth inhibition and apoptosis

The phenotype of altered metabolism in cancer cells has gained enormous attention in recent years. Attempts have been made to develop drugs that could target important metabolic enzymes, like PKM2, which arguably is the critical regulator of aerobic glycolysis in cancer cells. The therapeutic intervention that involves the strategy of silencing the expression of PKM2 has several limitations, although the knockdown of PKM2 affects aerobic glycolysis in cancer cells (Christofk et al. 2008), yet its ability in regressing the proliferation and in inducing cell death of cancer cells from distinct tissue origin has been debated (Goldberg and Sharp 2012, Cortes-Cros et al. 2013, Israelsen et al. 2013, Qin et al. 2014, Chu et al. 2015, Sun et al. 2015).

The experiments in this study in a representative set of sporadic breast cancer tissues and human cancer cell lines of different tissue origin, co-expressing M1 and M2 isoforms of pyruvate kinase **(Fig. 4.4)**, provided an insight in suggesting alternative approaches for therapeutic intervention in cancer cells. Realizing that the cancer cells mostly express both the isoforms of PKM which interact to generate hetero-tetrameric cross-oligomers **(Fig. 4.11)**, besides homo-tetramers of PKM1, PKM2, and homo-dimers of PKM2; contributing to the overall pyruvate kinase activity in cancer cells. Thus, it was obvious from the results that cancer cells involved both PKM1 and PKM2 to drive the glycolysis to yield ATP **(Fig. 4.22)**, emphasizing that PKM1 in cancer cells is not just a bystander. Hence, a standalone therapeutic strategy that silences the expression of PKM2 might not warrant success in regressing the tumor propagation. The abrogation of PKM2 expression in such a situation may be compensated by the expression of PKM1 or the signaling pathway that reprograms energy metabolism to preserve energy homeostasis. This is supported by a recent study conducted by Israelsen et al., where PKM2 knockout reprogrammed tumors to express PKM1, which instead of regressing stimulated tumor propagation (Israelsen et al. 2013). A recent study

by Qin et al. also observed that AKT survival signaling that was activated followed by PKM2 knockdown conferred protection against growth inhibition and apoptosis (Qin et al. 2014).

Interestingly, the result obtained in this work demonstrated that the knockdown of PKM1 and PKM2 affected the glycolytic metabolism and proliferation of A549 and H1299 cells (lung adenocarcinoma cells) differentially **(Figs. 4.22 and 4.23)**. The heterogeneous response between PKM silenced H1299 and A549 cells were because of the presence of LKB1 (a serine/threonine protein kinase upstream to AMPK) and an active AMPK signaling network downstream to LKB1 in H1299 and its absence in A549 cells (Ji et al. 2007, Shackelford et al. 2013, Faubert et al. 2014) **(Fig. 4.24)**. H1299 cells that were silenced for PKM isoforms activated AMPK survival signaling to reprogram energy metabolism by stimulating mitochondrial biogenesis and by triggering autophagy to preserve energy homeostasis and evading apoptosis. Whereas, A459 cells that lack LKB1, failed to activate AMPK in order to maintain the adaptive energy metabolic phenotype governed by AMPK, resulting in enhanced growth inhibition and apoptosis **(Fig. 4.24)**.

Lack of LKB1 or harboring a loss of functional mutation is known in nearly 20-30% percent of lung adenocarcinomas (Marcus and Zhou 2010). In addition, a substantial number of cases with cervical, endometrial and prostate cancers also carry LKB1 mutations (Hezel and Bardeesy 2008). Loss of LKB1 expression has been linked largely to a deregulated cellular metabolism, which generally relies on aerobic glycolysis and supports the aggressive replicative phenotype of the tumors by delivering precursors for biosynthesis (Carretero et al. 2007, Dupuy et al. 2013, Faubert et al. 2014). Taken together, the results in the present work suggest that the cancer cells with aberrant LKB1-AMPK axis could be contained by targeting glycolytic metabolism and energy homeostasis through PKM1 and PKM2 silencing **(Fig. 4.24)**. The conclusions drawn here are consistent with recent studies, which collectively demonstrated that triggering bioenergetic stress by pharmacological or genetic means in LKB1-AMPK pathway deficient tumors could enhance anti-tumorigenic effect (Inge et al. 2009, Hardie and Alessi 2013, Shackelford et al. 2013, Whang et al. 2016).

Further, this study also demonstrated that the cancer cells with active LKB1 could be targeted by employing a strategy of introducing a combination of knockdowns for AMPK catalytic alpha subunit and PKM1 or PKM2 **(Fig 4.25).** To this end, targeting AMPK could be appealing over

LKB1, since LKB1 confers most of its biological role of cellular energy metabolic reprogramming through the bioenergetic sensor AMPK via phosphorylation of threonine 172 residue of AMPK (Shackelford and Shaw 2009, Hardie et al. 2012). Although, numerous strategies that choose to target aerobic glycolysis are underway, the present study emphasizes upon development of a resistance against those strategies through AMPK dependent energy metabolic rewiring. Taken together, the findings provide a rationale for PKM knockdown in LKB1-deficient lung cancer cells, and in addition, propose that the combined silencing of AMPK and PKM isoforms through genetic or pharmacological means may provide a promising therapeutic strategy that could compromise further growth of the tumor cells with a functional background of LKB1-AMPK axis.

References

Reference

Amoroso, F., S. Falzoni, E. Adinolfi, D. Ferrari and F. Di Virgilio (2012). "The P2X7 receptor is a key modulator of aerobic glycolysis." Cell Death Dis **3**: e370.

Anitha, M., G. Kaur, N. Z. Baquer and R. Bamezai (2004). "Dominant negative effect of novel mutations in pyruvate kinase-M2." DNA Cell Biol **23**(7): 442-449.

Arbyn, M., X. Castellsague, S. de Sanjose, L. Bruni, M. Saraiya, F. Bray and J. Ferlay (2011). "Worldwide burden of cervical cancer in 2008." Ann Oncol **22**(12): 2675-2686.

Banko, M. R., J. J. Allen, B. E. Schaffer, E. W. Wilker, P. Tsou, J. L. White, J. Villen, B. Wang, S. R. Kim, K. Sakamoto, S. P. Gygi, L. C. Cantley, M. B. Yaffe, K. M. Shokat and A. Brunet (2011). "Chemical genetic screen for AMPKalpha2 substrates uncovers a network of proteins involved in mitosis." Mol Cell **44**(6): 878-892.

Bardeesy, N., M. Sinha, A. F. Hezel, S. Signoretti, N. A. Hathaway, N. E. Sharpless, M. Loda, D. R. Carrasco and R. A. DePinho (2002). "Loss of the Lkb1 tumour suppressor provokes intestinal polyposis but resistance to transformation." Nature **419**(6903): 162-167.

Behrends, C., M. E. Sowa, S. P. Gygi and J. W. Harper (2010). "Network organization of the human autophagy system." Nature **466**(7302): 68-76.

Ben-Haim, S. and P. Ell (2009). "18F-FDG PET and PET/CT in the evaluation of cancer treatment response." J Nucl Med **50**(1): 88-99.

Berkers, C. R., O. D. Maddocks, E. C. Cheung, I. Mor and K. H. Vousden (2013). "Metabolic regulation by p53 family members." Cell Metab **18**(5): 617-633.

Briesemeister, S., J. Rahnenfuhrer and O. Kohlbacher (2010). "Going from where to why--interpretable prediction of protein subcellular localization." Bioinformatics **26**(9): 1232-1238.

Cairns, R. A., I. S. Harris and T. W. Mak (2011). "Regulation of cancer cell metabolism." Nat Rev Cancer **11**(2): 85-95.

Carretero, J., P. P. Medina, R. Blanco, L. Smit, M. Tang, G. Roncador, L. Maestre, E. Conde, F. Lopez-Rios, H. C. Clevers and M. Sanchez-Cespedes (2007). "Dysfunctional AMPK activity, signalling through mTOR and survival in response to energetic stress in LKB1-deficient lung cancer." Oncogene **26**(11): 1616-1625.

Chaneton, B. and E. Gottlieb (2012). "Rocking cell metabolism: revised functions of the key glycolytic regulator PKM2 in cancer." Trends in biochemical sciences **37**(8): 309-316.

Chaneton, B., P. Hillmann, L. Zheng, A. C. Martin, O. D. Maddocks, A. Chokkathukalam, J. E. Coyle, A. Jankevics, F. P. Holding, K. H. Vousden, C. Frezza, M. O'Reilly and E. Gottlieb (2012). "Serine is a natural ligand and allosteric activator of pyruvate kinase M2." Nature **491**(7424): 458-462.

Chen, J., J. Xie, Z. Jiang, B. Wang, Y. Wang and X. Hu (2011). "Shikonin and its analogs inhibit cancer cell glycolysis by targeting tumor pyruvate kinase-M2." Oncogene **30**(42): 4297-4306.

Chou, K. C. and H. B. Shen (2006). "Hum-PLoc: a novel ensemble classifier for predicting human protein subcellular localization." Biochem Biophys Res Commun **347**(1): 150-157.

Christofk, H. R., M. G. Vander Heiden, M. H. Harris, A. Ramanathan, R. E. Gerszten, R. Wei, M. D. Fleming, S. L. Schreiber and L. C. Cantley (2008). "The M2 splice isoform of pyruvate kinase is important for cancer metabolism and tumour growth." Nature **452**(7184): 230-233.

Christofk, H. R., M. G. Vander Heiden, N. Wu, J. M. Asara and L. C. Cantley (2008). "Pyruvate kinase M2 is a phosphotyrosine-binding protein." Nature **452**(7184): 181-186.

Chu, B., J. Wang, Y. Wang and G. Yang (2015). "Knockdown of PKM2 induces apoptosis and autophagy in human A549 alveolar adenocarcinoma cells." Mol Med Rep **12**(3): 4358-4363.

Clower, C. V., D. Chatterjee, Z. Wang, L. C. Cantley, M. G. Vander Heiden and A. R. Krainer (2010). "The alternative splicing repressors hnRNP A1/A2 and PTB influence pyruvate kinase isoform expression and cell metabolism." Proc Natl Acad Sci U S A **107**(5): 1894-1899.

Cortes-Cros, M., C. Hemmerlin, S. Ferretti, J. Zhang, J. S. Gounarides, H. Yin, A. Muller, A. Haberkorn, P. Chene, W. R. Sellers and F. Hofmann (2013). "M2 isoform of pyruvate kinase is dispensable for tumor maintenance and growth." Proc Natl Acad Sci U S A **110**(2): 489-494.
Cortés-Cros, M., C. Hemmerlin, S. Ferretti, J. Zhang, J. S. Gounarides, H. Yin, A. Muller, A. Haberkorn, P. Chene, W. R. Sellers and F. Hofmann (2013). "M2 isoform of pyruvate kinase is dispensable for tumor maintenance and growth." Proceedings of the National Academy of Sciences of the United States of America **110**(2): 489-494.
David, C. J., M. Chen, M. Assanah, P. Canoll and J. L. Manley (2010). "HnRNP proteins controlled by c-Myc deregulate pyruvate kinase mRNA splicing in cancer." Nature **463**(7279): 364-368.
David, C. J., M. Chen, M. Assanah, P. Canoll and J. L. Manley (2010). "HnRNP proteins controlled by c-Myc deregulate pyruvate kinase mRNA splicing in cancer." Nature **463**(7279): 364-368.
de Martel, C., J. Ferlay, S. Franceschi, J. Vignat, F. Bray, D. Forman and M. Plummer (2012). "Global burden of cancers attributable to infections in 2008: a review and synthetic analysis." Lancet Oncol **13**(6): 607-615.
DeBerardinis, R. J., J. J. Lum, G. Hatzivassiliou and C. B. Thompson (2008). "The biology of cancer: metabolic reprogramming fuels cell growth and proliferation." Cell Metab **7**(1): 11-20.
Dupuy, F., T. Griss, J. Blagih, G. Bridon, D. Avizonis, C. Ling, Z. Dong, D. R. Siwak, M. G. Annis, G. B. Mills, W. J. Muller, P. M. Siegel and R. G. Jones (2013). "LKB1 is a central regulator of tumor initiation and pro-growth metabolism in ErbB2-mediated breast cancer." Cancer Metab **1**(1): 18.
Egan, D. F., D. B. Shackelford, M. M. Mihaylova, S. Gelino, R. A. Kohnz, W. Mair, D. S. Vasquez, A. Joshi, D. M. Gwinn, R. Taylor, J. M. Asara, J. Fitzpatrick, A. Dillin, B. Viollet, M. Kundu, M. Hansen and R. J. Shaw (2011). "Phosphorylation of ULK1 (hATG1) by AMP-activated protein kinase connects energy sensing to mitophagy." Science **331**(6016): 456-461.
Fan, J., T. Hitosugi, T. W. Chung, J. Xie, Q. Ge, T. L. Gu, R. D. Polakiewicz, G. Z. Chen, T. J. Boggon, S. Lonial, F. R. Khuri, S. Kang and J. Chen (2011). "Tyrosine phosphorylation of lactate dehydrogenase A is important for NADH/NAD(+) redox homeostasis in cancer cells." Mol Cell Biol **31**(24): 4938-4950.
Fantin, V. R., J. St-Pierre and P. Leder (2006). "Attenuation of LDH-A expression uncovers a link between glycolysis, mitochondrial physiology, and tumor maintenance." Cancer Cell **9**(6): 425-434.
Faubert, B., E. E. Vincent, T. Griss, B. Samborska, S. Izreig, R. U. Svensson, O. A. Mamer, D. Avizonis, D. B. Shackelford, R. J. Shaw and R. G. Jones (2014). "Loss of the tumor suppressor LKB1 promotes metabolic reprogramming of cancer cells via HIF-1alpha." Proc Natl Acad Sci U S A **111**(7): 2554-2559.
Faubert, B., E. E. Vincent, M. C. Poffenberger and R. G. Jones (2015). "The AMP-activated protein kinase (AMPK) and cancer: many faces of a metabolic regulator." Cancer Lett **356**(2 Pt A): 165-170.
Ferrer, A., C. Caelles, N. Massot and F. G. Hegardt (1985). "Activation of rat liver cytosolic 3-hydroxy-3-methylglutaryl coenzyme A reductase kinase by adenosine 5'-monophosphate." Biochem Biophys Res Commun **132**(2): 497-504.
Frigo, D. E., M. K. Howe, B. M. Wittmann, A. M. Brunner, I. Cushman, Q. Wang, M. Brown, A. R. Means and D. P. McDonnell (2011). "CaM kinase kinase beta-mediated activation of the growth regulatory kinase AMPK is required for androgen-dependent migration of prostate cancer cells." Cancer Res **71**(2): 528-537.
Gao, X., H. Wang, J. J. Yang, X. Liu and Z. R. Liu (2012). "Pyruvate kinase M2 regulates gene transcription by acting as a protein kinase." Mol Cell **45**(5): 598-609.
Garg, A., M. Bhasin and G. P. Raghava (2005). "Support vector machine-based method for subcellular localization of human proteins using amino acid compositions, their order, and similarity search." J Biol Chem **280**(15): 14427-14432.
Goldberg, M. S. and P. A. Sharp (2012). "Pyruvate kinase M2-specific siRNA induces apoptosis and tumor regression." J Exp Med **209**(2): 217-224.

Goransson, O., A. McBride, S. A. Hawley, F. A. Ross, N. Shpiro, M. Foretz, B. Viollet, D. G. Hardie and K. Sakamoto (2007). "Mechanism of action of A-769662, a valuable tool for activation of AMP-activated protein kinase." J Biol Chem **282**(45): 32549-32560.
Grahame Hardie, D. (2016). "Regulation of AMP-activated protein kinase by natural and synthetic activators." Acta Pharm Sin B **6**(1): 1-19.
Greer, E. L. and A. Brunet (2009). "Different dietary restriction regimens extend lifespan by both independent and overlapping genetic pathways in C. elegans." Aging Cell **8**(2): 113-127.
Guertin, D. A. and D. M. Sabatini (2007). "Defining the role of mTOR in cancer." Cancer Cell **12**(1): 9-22.
Gupta, V. and R. N. Bamezai (2010). "Human pyruvate kinase M2: a multifunctional protein." Protein Sci **19**(11): 2031-2044.
Gupta, V., P. Kalaiarasan, M. Faheem, N. Singh, M. A. Iqbal and R. N. Bamezai (2010). "Dominant negative mutations affect oligomerization of human pyruvate kinase M2 isozyme and promote cellular growth and polyploidy." J Biol Chem **285**(22): 16864-16873.
Gupta, V., K. E. Wellen, S. Mazurek and R. N. Bamezai (2014). "Pyruvate kinase M2: regulatory circuits and potential for therapeutic intervention." Curr Pharm Des **20**(15): 2595-2606.
Hamabe, A., M. Konno, N. Tanuma, H. Shima, K. Tsunekuni, K. Kawamoto, N. Nishida, J. Koseki, K. Mimori, N. Gotoh, H. Yamamoto, Y. Doki, M. Mori and H. Ishii (2014). "Role of pyruvate kinase M2 in transcriptional regulation leading to epithelial-mesenchymal transition." Proc Natl Acad Sci U S A **111**(43): 15526-15531.
Hanahan, D. and R. A. Weinberg (2000). "The hallmarks of cancer." Cell **100**(1): 57-70.
Harada, K., S. Saheki, K. Wada and T. Tanaka (1978). "Purification of four pyruvate kinase isozymes of rats by affinity elution chromatography." Biochim Biophys Acta **524**(2): 327-339.
Hardie, D. G. and D. R. Alessi (2013). "LKB1 and AMPK and the cancer-metabolism link - ten years after." BMC Biol **11**: 36.
Hardie, D. G., D. Carling and N. Halford (1994). "Roles of the Snf1/Rkin1/AMP-activated protein kinase family in the response to environmental and nutritional stress." Semin Cell Biol **5**(6): 409-416.
Hardie, D. G., F. A. Ross and S. A. Hawley (2012). "AMPK: a nutrient and energy sensor that maintains energy homeostasis." Nat Rev Mol Cell Biol **13**(4): 251-262.
Hawley, S. A., M. D. Fullerton, F. A. Ross, J. D. Schertzer, C. Chevtzoff, K. J. Walker, M. W. Peggie, D. Zibrova, K. A. Green, K. J. Mustard, B. E. Kemp, K. Sakamoto, G. R. Steinberg and D. G. Hardie (2012). "The ancient drug salicylate directly activates AMP-activated protein kinase." Science **336**(6083): 918-922.
Hezel, A. F. and N. Bardeesy (2008). "LKB1; linking cell structure and tumor suppression." Oncogene **27**(55): 6908-6919.
Hitosugi, T., S. Kang, M. G. Vander Heiden, T. W. Chung, S. Elf, K. Lythgoe, S. Dong, S. Lonial, X. Wang, G. Z. Chen, J. Xie, T. L. Gu, R. D. Polakiewicz, J. L. Roesel, T. J. Boggon, F. R. Khuri, D. G. Gilliland, L. C. Cantley, J. Kaufman and J. Chen (2009). "Tyrosine phosphorylation inhibits PKM2 to promote the Warburg effect and tumor growth." Sci Signal **2**(97): ra73.
Hoshino, A., J. A. Hirst and H. Fujii (2007). "Regulation of cell proliferation by interleukin-3-induced nuclear translocation of pyruvate kinase." J Biol Chem **282**(24): 17706-17711.
Hsu, P. P. and D. M. Sabatini (2008). "Cancer cell metabolism: Warburg and beyond." Cell **134**(5): 703-707.
Hua, S. and Z. Sun (2001). "Support vector machine approach for protein subcellular localization prediction." Bioinformatics **17**(8): 721-728.
Inge, L. J., K. D. Coon, M. A. Smith and R. M. Bremner (2009). "Expression of LKB1 tumor suppressor in non-small cell lung cancer determines sensitivity to 2-deoxyglucose." J Thorac Cardiovasc Surg **137**(3): 580-586.
Iqbal, M. A. and R. N. Bamezai (2012). "Resveratrol inhibits cancer cell metabolism by down regulating pyruvate kinase M2 via inhibition of mammalian target of rapamycin." PLoS One **7**(5): e36764.
Iqbal, M. A., V. Gupta, P. Gopinath, S. Mazurek and R. N. Bamezai (2014). "Pyruvate kinase M2 and cancer: an updated assessment." FEBS Lett **588**(16): 2685-2692.

Iqbal, M. A., F. A. Siddiqui, V. Gupta, S. Chattopadhyay, P. Gopinath, B. Kumar, S. Manvati, N. Chaman and R. N. Bamezai (2013). "Insulin enhances metabolic capacities of cancer cells by dual regulation of glycolytic enzyme pyruvate kinase M2." Mol Cancer **12**: 72.
Israelsen, W. J., T. L. Dayton, S. M. Davidson, B. P. Fiske, A. M. Hosios, G. Bellinger, J. Li, Y. Yu, M. Sasaki, J. W. Horner, L. N. Burga, J. Xie, M. J. Jurczak, R. A. DePinho, C. B. Clish, T. Jacks, R. G. Kibbey, G. M. Wulf, D. Di Vizio, G. B. Mills, L. C. Cantley and M. G. Vander Heiden (2013). "PKM2 isoform-specific deletion reveals a differential requirement for pyruvate kinase in tumor cells." Cell **155**(2): 397-409.
Jeon, S. M., N. S. Chandel and N. Hay (2012). "AMPK regulates NADPH homeostasis to promote tumour cell survival during energy stress." Nature **485**(7400): 661-665.
Jeon, S. M. and N. Hay (2012). "The dark face of AMPK as an essential tumor promoter." Cell Logist **2**(4): 197-202.
Jeon, S. M. and N. Hay (2015). "The double-edged sword of AMPK signaling in cancer and its therapeutic implications." Arch Pharm Res **38**(3): 346-357.
Ji, H., M. R. Ramsey, D. N. Hayes, C. Fan, K. McNamara, P. Kozlowski, C. Torrice, M. C. Wu, T. Shimamura, S. A. Perera, M. C. Liang, D. Cai, G. N. Naumov, L. Bao, C. M. Contreras, D. Li, L. Chen, J. Krishnamurthy, J. Koivunen, L. R. Chirieac, R. F. Padera, R. T. Bronson, N. I. Lindeman, D. C. Christiani, X. Lin, G. I. Shapiro, P. A. Janne, B. E. Johnson, M. Meyerson, D. J. Kwiatkowski, D. H. Castrillon, N. Bardeesy, N. E. Sharpless and K. K. Wong (2007). "LKB1 modulates lung cancer differentiation and metastasis." Nature **448**(7155): 807-810.
Jiang, Y., X. Li, W. Yang, D. H. Hawke, Y. Zheng, Y. Xia, K. Aldape, C. Wei, F. Guo, Y. Chen and Z. Lu (2014). "PKM2 regulates chromosome segregation and mitosis progression of tumor cells." Mol Cell **53**(1): 75-87.
Jones, R. G., D. R. Plas, S. Kubek, M. Buzzai, J. Mu, Y. Xu, M. J. Birnbaum and C. B. Thompson (2005). "AMP-activated protein kinase induces a p53-dependent metabolic checkpoint." Mol Cell **18**(3): 283-293.
Jones, R. G. and C. B. Thompson (2009). "Tumor suppressors and cell metabolism: a recipe for cancer growth." Genes Dev **23**(5): 537-548.
Kahn, B. B., T. Alquier, D. Carling and D. G. Hardie (2005). "AMP-activated protein kinase: ancient energy gauge provides clues to modern understanding of metabolism." Cell Metab **1**(1): 15-25.
Kato, K., T. Ogura, A. Kishimoto, Y. Minegishi, N. Nakajima, M. Miyazaki and H. Esumi (2002). "Critical roles of AMP-activated protein kinase in constitutive tolerance of cancer cells to nutrient deprivation and tumor formation." Oncogene **21**(39): 6082-6090.
Keller, K. E., I. S. Tan and Y. S. Lee (2012). "SAICAR stimulates pyruvate kinase isoform M2 and promotes cancer cell survival in glucose-limited conditions." Science **338**(6110): 1069-1072.
Kumar, B. and R. N. Bamezai (2015). "Moderate DNA damage promotes metabolic flux into PPP via PKM2 Y-105 phosphorylation: a feature that favours cancer cells." Mol Biol Rep **42**(8): 1317-1321.
Lee, J., H. K. Kim, Y. M. Han and J. Kim (2008). "Pyruvate kinase isozyme type M2 (PKM2) interacts and cooperates with Oct-4 in regulating transcription." Int J Biochem Cell Biol **40**(5): 1043-1054.
Levy, P. and B. Bartosch (2016). "Metabolic reprogramming: a hallmark of viral oncogenesis." Oncogene **35**(32): 4155-4164.
Liang, J. and G. B. Mills (2013). "AMPK: a contextual oncogene or tumor suppressor?" Cancer Res **73**(10): 2929-2935.
Liu, L., J. Ulbrich, J. Muller, T. Wustefeld, L. Aeberhard, T. R. Kress, N. Muthalagu, L. Rycak, R. Rudalska, R. Moll, S. Kempa, L. Zender, M. Eilers and D. J. Murphy (2012). "Deregulated MYC expression induces dependence upon AMPK-related kinase 5." Nature **483**(7391): 608-612.
Lu, Z., X. Hu, Y. Li, L. Zheng, Y. Zhou, H. Jiang, T. Ning, Z. Basang, C. Zhang and Y. Ke (2004). "Human papillomavirus 16 E6 oncoprotein interferences with insulin signaling pathway by binding to tuberin." J Biol Chem **279**(34): 35664-35670.

Luo, W., H. Hu, R. Chang, J. Zhong, M. Knabel, R. O'Meally, R. N. Cole, A. Pandey and G. L. Semenza (2011). "Pyruvate kinase M2 is a PHD3-stimulated coactivator for hypoxia-inducible factor 1." Cell **145**(5): 732-744.
Lv, L., Y.-P. P. Xu, D. Zhao, F.-L. L. Li, W. Wang, N. Sasaki, Y. Jiang, X. Zhou, T.-T. T. Li, K.-L. L. Guan, Q.-Y. Y. Lei and Y. Xiong (2013). "Mitogenic and oncogenic stimulation of K433 acetylation promotes PKM2 protein kinase activity and nuclear localization." Molecular cell **52**(3): 340-352.
Marcus, A. I. and W. Zhou (2010). "LKB1 regulated pathways in lung cancer invasion and metastasis." J Thorac Oncol **5**(12): 1883-1886.
Marini, C., B. Salani, M. Massollo, A. Amaro, A. I. Esposito, A. M. Orengo, S. Capitanio, L. Emionite, M. Riondato, G. Bottoni, C. Massara, S. Boccardo, M. Fabbi, C. Campi, S. Ravera, G. Angelini, S. Morbelli, M. Cilli, R. Cordera, M. Truini, D. Maggi, U. Pfeffer and G. Sambuceti (2013). "Direct inhibition of hexokinase activity by metformin at least partially impairs glucose metabolism and tumor growth in experimental breast cancer." Cell Cycle **12**(22): 3490-3499.
Marsin, A. S., L. Bertrand, M. H. Rider, J. Deprez, C. Beauloye, M. F. Vincent, G. Van den Berghe, D. Carling and L. Hue (2000). "Phosphorylation and activation of heart PFK-2 by AMPK has a role in the stimulation of glycolysis during ischaemia." Curr Biol **10**(20): 1247-1255.
Marsin, A. S., C. Bouzin, L. Bertrand and L. Hue (2002). "The stimulation of glycolysis by hypoxia in activated monocytes is mediated by AMP-activated protein kinase and inducible 6-phosphofructo-2-kinase." J Biol Chem **277**(34): 30778-30783.
Massie, C. E., A. Lynch, A. Ramos-Montoya, J. Boren, R. Stark, L. Fazli, A. Warren, H. Scott, B. Madhu, N. Sharma, H. Bon, V. Zecchini, D. M. Smith, G. M. Denicola, N. Mathews, M. Osborne, J. Hadfield, S. Macarthur, B. Adryan, S. K. Lyons, K. M. Brindle, J. Griffiths, M. E. Gleave, P. S. Rennie, D. E. Neal and I. G. Mills (2011). "The androgen receptor fuels prostate cancer by regulating central metabolism and biosynthesis." EMBO J **30**(13): 2719-2733.
Mazurek, S. (2011). "Pyruvate kinase type M2: a key regulator of the metabolic budget system in tumor cells." The international journal of biochemistry & cell biology **43**(7): 969-980.
Mazurek, S. (2011). "Pyruvate kinase type M2: a key regulator of the metabolic budget system in tumor cells." Int J Biochem Cell Biol **43**(7): 969-980.
Mazurek, S., C. B. Boschek, F. Hugo and E. Eigenbrodt (2005). "Pyruvate kinase type M2 and its role in tumor growth and spreading." Semin Cancer Biol **15**(4): 300-308.
Menges, C. W., L. A. Baglia, R. Lapoint and D. J. McCance (2006). "Human papillomavirus type 16 E7 up-regulates AKT activity through the retinoblastoma protein." Cancer Res **66**(11): 5555-5559.
Mihaylova, M. M. and R. J. Shaw (2011). "The AMPK signalling pathway coordinates cell growth, autophagy and metabolism." Nature Cell Biology **13**(9): 1016-1023.
Mohseni, M., J. Sun, A. Lau, S. Curtis, J. Goldsmith, V. L. Fox, C. Wei, M. Frazier, O. Samson, K. K. Wong, C. Kim and F. D. Camargo (2014). "A genetic screen identifies an LKB1-MARK signalling axis controlling the Hippo-YAP pathway." Nat Cell Biol **16**(1): 108-117.
Moody, C. A. and L. A. Laimins (2010). "Human papillomavirus oncoproteins: pathways to transformation." Nat Rev Cancer **10**(8): 550-560.
Nafz, J., J. De-Castro Arce, V. Fleig, A. Patzelt, S. Mazurek and F. Rosl (2007). "Interference with energy metabolism by 5-aminoimidazole-4-carboxamide-1-beta-D-ribofuranoside induces HPV suppression in cervical carcinoma cells and apoptosis in the absence of LKB1." Biochem J **403**(3): 501-510.
Noch, E. and K. Khalili (2012). "Oncogenic viruses and tumor glucose metabolism: like kids in a candy store." Mol Cancer Ther **11**(1): 14-23.
Noguchi, T., H. Inoue and T. Tanaka (1986). "The M1- and M2-type isozymes of rat pyruvate kinase are produced from the same gene by alternative RNA splicing." The Journal of biological chemistry **261**(29): 13807-13812.

Noguchi, T., H. Inoue and T. Tanaka (1986). "The M1-and M2-type isozymes of rat pyruvate kinase are produced from the same gene by alternative RNA splicing." Journal of Biological Chemistry **261**(29): 13807-13812.
Noguchi, T., K. Yamada, H. Inoue, T. Matsuda and T. Tanaka (1987). "The L- and R-type isozymes of rat pyruvate kinase are produced from a single gene by use of different promoters." The Journal of biological chemistry **262**(29): 14366-14371.
Oakhill, J. S., R. Steel, Z. P. Chen, J. W. Scott, N. Ling, S. Tam and B. E. Kemp (2011). "AMPK is a direct adenylate charge-regulated protein kinase." Science **332**(6036): 1433-1435.
Onken, B. and M. Driscoll (2010). "Metformin induces a dietary restriction-like state and the oxidative stress response to extend C. elegans Healthspan via AMPK, LKB1, and SKN-1." PLoS One **5**(1): e8758.
Pal, R., S. Gochhait, S. Chattopadhyay, P. Gupta, N. Prakash, G. Agarwal, A. Chaturvedi, N. Husain, S. A. Husain and R. N. Bamezai (2011). "Functional implication of TRAIL -716 C/T promoter polymorphism on its in vitro and in vivo expression and the susceptibility to sporadic breast tumor." Breast Cancer Res Treat **126**(2): 333-343.
Pal, R., N. Srivastava, R. Chopra, S. Gochhait, P. Gupta, N. Prakash, G. Agarwal and R. N. Bamezai (2010). "Investigation of DNA damage response and apoptotic gene methylation pattern in sporadic breast tumors using high throughput quantitative DNA methylation analysis technology." Mol Cancer **9**: 303.
Pandita, A., B. Kumar, S. Manvati, S. Vaishnavi, S. K. Singh and R. N. Bamezai (2014). "Synergistic combination of gemcitabine and dietary molecule induces apoptosis in pancreatic cancer cells and down regulates PKM2 expression." PLoS One **9**(9): e107154.
Patra, K. C., Q. Wang, P. T. Bhaskar, L. Miller, Z. Wang, W. Wheaton, N. Chandel, M. Laakso, W. J. Muller, E. L. Allen, A. K. Jha, G. A. Smolen, M. F. Clasquin, R. B. Robey and N. Hay (2013). "Hexokinase 2 is required for tumor initiation and maintenance and its systemic deletion is therapeutic in mouse models of cancer." Cancer Cell **24**(2): 213-228.
Pierleoni, A., P. L. Martelli, P. Fariselli and R. Casadio (2006). "BaCelLo: a balanced subcellular localization predictor." Bioinformatics **22**(14): e408-416.
Qin, X., Y. Du, X. Chen, W. Li, J. Zhang and J. Yang (2014). "Activation of Akt protects cancer cells from growth inhibition induced by PKM2 knockdown." Cell Biosci **4**: 20.
Reznick, R. M. and G. I. Shulman (2006). "The role of AMP-activated protein kinase in mitochondrial biogenesis." J Physiol **574**(Pt 1): 33-39.
Rios, M., M. Foretz, B. Viollet, A. Prieto, M. Fraga, J. A. Costoya and R. Senaris (2013). "AMPK activation by oncogenesis is required to maintain cancer cell proliferation in astrocytic tumors." Cancer Res **73**(8): 2628-2638.
Roberts, D. J., V. P. Tan-Sah, J. M. Smith and S. Miyamoto (2013). "Akt phosphorylates HK-II at Thr-473 and increases mitochondrial HK-II association to protect cardiomyocytes." J Biol Chem **288**(33): 23798-23806.
Ross, F. A., C. MacKintosh and D. G. Hardie (2016). "AMP-activated protein kinase: a cellular energy sensor that comes in 12 flavours." FEBS J **283**(16): 2987-3001.
Ross, J. M., J. Oberg, S. Brene, G. Coppotelli, M. Terzioglu, K. Pernold, M. Goiny, R. Sitnikov, J. Kehr, A. Trifunovic, N. G. Larsson, B. J. Hoffer and L. Olson (2010). "High brain lactate is a hallmark of aging and caused by a shift in the lactate dehydrogenase A/B ratio." Proc Natl Acad Sci U S A **107**(46): 20087-20092.
Sanders, M. J., Z. S. Ali, B. D. Hegarty, R. Heath, M. A. Snowden and D. Carling (2007). "Defining the mechanism of activation of AMP-activated protein kinase by the small molecule A-769662, a member of the thienopyridone family." J Biol Chem **282**(45): 32539-32548.
Seyfried, T. N. and L. M. Shelton (2010). "Cancer as a metabolic disease." Nutr Metab (Lond) **7**: 7.
Shackelford, D. B., E. Abt, L. Gerken, D. S. Vasquez, A. Seki, M. Leblanc, L. Wei, M. C. Fishbein, J. Czernin, P. S. Mischel and R. J. Shaw (2013). "LKB1 inactivation dictates therapeutic response of non-small cell lung cancer to the metabolism drug phenformin." Cancer Cell **23**(2): 143-158.

Shackelford, D. B. and R. J. Shaw (2009). "The LKB1-AMPK pathway: metabolism and growth control in tumour suppression." Nat Rev Cancer **9**(8): 563-575.
Shaw, R. J. (2006). "Glucose metabolism and cancer." Curr Opin Cell Biol **18**(6): 598-608.
Shaw, R. J., M. Kosmatka, N. Bardeesy, R. L. Hurley, L. A. Witters, R. A. DePinho and L. C. Cantley (2004). "The tumor suppressor LKB1 kinase directly activates AMP-activated kinase and regulates apoptosis in response to energy stress." Proc Natl Acad Sci U S A **101**(10): 3329-3335.
Shen, Z., X. F. Wen, F. Lan, Z. Z. Shen and Z. M. Shao (2002). "The tumor suppressor gene LKB1 is associated with prognosis in human breast carcinoma." Clin Cancer Res **8**(7): 2085-2090.
Spangle, J. M. and K. Munger (2010). "The human papillomavirus type 16 E6 oncoprotein activates mTORC1 signaling and increases protein synthesis." J Virol **84**(18): 9398-9407.
Sun, H., A. Zhu, L. Zhang, J. Zhang, Z. Zhong and F. Wang (2015). "Knockdown of PKM2 Suppresses Tumor Growth and Invasion in Lung Adenocarcinoma." Int J Mol Sci **16**(10): 24574-24587.
Sun, Q., X. Chen, J. Ma, H. Peng, F. Wang, X. Zha, Y. Wang, Y. Jing, H. Yang, R. Chen, L. Chang, Y. Zhang, J. Goto, H. Onda, T. Chen, M. R. Wang, Y. Lu, H. You, D. Kwiatkowski and H. Zhang (2011). "Mammalian target of rapamycin up-regulation of pyruvate kinase isoenzyme type M2 is critical for aerobic glycolysis and tumor growth." Proc Natl Acad Sci U S A **108**(10): 4129-4134.
Tennakoon, J. B., Y. Shi, J. J. Han, E. Tsouko, M. A. White, A. R. Burns, A. Zhang, X. Xia, O. R. Ilkayeva, L. Xin, M. M. Ittmann, F. G. Rick, A. V. Schally and D. E. Frigo (2014). "Androgens regulate prostate cancer cell growth via an AMPK-PGC-1alpha-mediated metabolic switch." Oncogene **33**(45): 5251-5261.
Tiainen, M., A. Ylikorkala and T. P. Makela (1999). "Growth suppression by Lkb1 is mediated by a G(1) cell cycle arrest." Proc Natl Acad Sci U S A **96**(16): 9248-9251.
Vander Heiden, M. G., L. C. Cantley and C. B. Thompson (2009). "Understanding the Warburg effect: the metabolic requirements of cell proliferation." Science **324**(5930): 1029-1033.
Vousden, K. H. and K. M. Ryan (2009). "p53 and metabolism." Nat Rev Cancer **9**(10): 691-700.
Warburg, O. (1956). "On the origin of cancer cells." Science **123**(3191): 309-314.
Weber, W. A., M. Schwaiger and N. Avril (2000). "Quantitative assessment of tumor metabolism using FDG-PET imaging." Nucl Med Biol **27**(7): 683-687.
Whang, Y. M., S. I. Park, I. A. Trenary, R. A. Egnatchik, J. P. Fessel, J. M. Kaufman, D. P. Carbone and J. D. Young (2016). "LKB1 deficiency enhances sensitivity to energetic stress induced by erlotinib treatment in non-small-cell lung cancer (NSCLC) cells." Oncogene **35**(7): 856-866.
Wingo, S. N., T. D. Gallardo, E. A. Akbay, M. C. Liang, C. M. Contreras, T. Boren, T. Shimamura, D. S. Miller, N. E. Sharpless, N. Bardeesy, D. J. Kwiatkowski, J. O. Schorge, K. K. Wong and D. H. Castrillon (2009). "Somatic LKB1 mutations promote cervical cancer progression." PLoS One **4**(4): e5137.
Wong, N., D. Ojo, J. Yan and D. Tang (2015). "PKM2 contributes to cancer metabolism." Cancer Lett **356**(2 Pt A): 184-191.
Wu, C. A., Y. Chao, S. G. Shiah and W. W. Lin (2013). "Nutrient deprivation induces the Warburg effect through ROS/AMPK-dependent activation of pyruvate dehydrogenase kinase." Biochim Biophys Acta **1833**(5): 1147-1156.
Xia, L., X. R. Wang, X. L. Wang, S. H. Liu, X. W. Ding, G. Q. Chen and Y. Lu (2016). "A novel role for pyruvate Kinase M2 as a corepressor for P53 during the DNA damage response in human tumor cells." J Biol Chem.
Xiao, B., M. J. Sanders, E. Underwood, R. Heath, F. V. Mayer, D. Carmena, C. Jing, P. A. Walker, J. F. Eccleston, L. F. Haire, P. Saiu, S. A. Howell, R. Aasland, S. R. Martin, D. Carling and S. J. Gamblin (2011). "Structure of mammalian AMPK and its regulation by ADP." Nature **472**(7342): 230-233.
Yang, W., Y. Xia, D. Hawke, X. Li, J. Liang, D. Xing, K. Aldape, T. Hunter, W. K. Alfred Yung and Z. Lu (2012). "PKM2 phosphorylates histone H3 and promotes gene transcription and tumorigenesis." Cell **150**(4): 685-696.
Yang, W., Y. Xia, H. Ji, Y. Zheng, J. Liang, W. Huang, X. Gao, K. Aldape and Z. Lu (2011). "Nuclear PKM2 regulates beta-catenin transactivation upon EGFR activation." Nature **480**(7375): 118-122.

Yang, W., Y. Zheng, Y. Xia, H. Ji, X. Chen, F. Guo, C. A. Lyssiotis, K. Aldape, L. C. Cantley and Z. Lu (2012). "ERK1/2-dependent phosphorylation and nuclear translocation of PKM2 promotes the Warburg effect." Nature cell biology **14**(12): 1295-1304.
Yang, W., Y. Zheng, Y. Xia, H. Ji, X. Chen, F. Guo, C. A. Lyssiotis, K. Aldape, L. C. Cantley and Z. Lu (2012). "ERK1/2-dependent phosphorylation and nuclear translocation of PKM2 promotes the Warburg effect." Nat Cell Biol **14**(12): 1295-1304.
Yu, C. S., Y. C. Chen, C. H. Lu and J. K. Hwang (2006). "Prediction of protein subcellular localization." Proteins **64**(3): 643-651.
Zadra, G., J. L. Batista and M. Loda (2015). "Dissecting the Dual Role of AMPK in Cancer: From Experimental to Human Studies." Mol Cancer Res **13**(7): 1059-1072.
Zambo, V., M. Toth, K. Schlachter, P. Szelenyi, F. Sarnyai, G. Lotz, M. Csala and E. Kereszturi (2016). "Cytosolic localization of NADH cytochrome b(5) oxidoreductase (Ncb5or)." FEBS Lett **590**(5): 661-671.
Zeng, Q., J. Chen, Y. Li, K. D. Werle, R. X. Zhao, C. S. Quan, Y. S. Wang, Y. X. Zhai, J. W. Wang, M. Youssef, R. Cui, J. Liang, N. Genovese, L. T. Chow, Y. L. Li and Z. X. Xu (2016). "LKB1 inhibits HPV-associated cancer progression by targeting cellular metabolism." Oncogene.
Zheng, L., H. Ding, Z. Lu, Y. Li, Y. Pan, T. Ning and Y. Ke (2008). "E3 ubiquitin ligase E6AP-mediated TSC2 turnover in the presence and absence of HPV16 E6." Genes Cells **13**(3): 285-294.
zur Hausen, H. (2009). "Papillomaviruses in the causation of human cancers - a brief historical account." Virology **384**(2): 260-265.
Zwerschke, W., S. Mazurek, P. Massimi, L. Banks, E. Eigenbrodt and P. Jansen-Durr (1999). "Modulation of type M2 pyruvate kinase activity by the human papillomavirus type 16 E7 oncoprotein." Proc Natl Acad Sci U S A **96**(4): 1291-1296.

Appendix I

Appendix I

A.1 MAMMALIAN CELL CULTURE

A.1.1 10X PBS

Component	Concentration	Quantity in 1000 ml (10X)	Quantity in 1000 ml (1X)
NaCl	137 mM	80 gm	8.0 gm
KCl	2.7 mM	2 gm	0.2 gm
Na_2HPO_4	10 mM	14.4 gm	1.44 gm
KH_2PO_4	2 mM	2.4 gm	0.48 gm

Storage: 4°C

A.1.2 Incomplete cell culture Media recipe

Component	Quantity for 1000ml
DMEM (with high glucose)	13.7 gm
$NaHCO_3$	3.7 gm
Autoclaved Water	890ml

A.1.3 Complete media recipe

I. To 890ml of sterile filtered incomplete media in a 1000ml Duran screw-cap bottle.
II. 10ml of 100X Penicillin + Streptomycin cocktail was added.
III. Further, 100 ml of heat inactivated filtered fetal bovine serum was added to it.
IV. The resultant complete media was mixed well and the cap of bottle was sealed with paraffin and stored at 4°C.

A.1.4 Trypsin solution: 200 ml

Trypsin	500 mg
EDTA	40 mg
Glucose	200 mg
PBS	200 ml

A.1.5 Culture media preparation and filter sterilization

I. Two 1000ml Duran screw-cap bottles (one empty bottle and the other one with 890ml of double distilled water), and a filter unit fitted with 0.22µm filter membrane was autoclaved.
II. The constituents of mammalian cell culture media were weighed and dissolved in the autoclaved water.
III. The incomplete media was filtered sterilized and collected in a sterile empty Duran screw-cap bottle.
IV. To the sterile incomplete media, 1% of antibiotic (penicillin and streptomycin cocktail) and 10% of filter sterile FBS was added to obtain complete media; later it was sealed with parafilm and refrigerated.

A.1.6 Protocol for passaging of cells

i. Cells grown in the 60 mm culture dishes were regularly monitored under the microscope to take a note on their level of confluency.
ii. Upon attaining a sub-confluent level of around 75-80%, the culture media was removed gently without disturbing the monolayer of the cultured cells.
iii. The monolayer of the cells was washed twice with 1 ml of 1X PBS to remove toxic excretion from the cells.
iv. 500 µl of trypsin was added over the monolayer of cells and were spread evenly. The cells were then left in the cell culture incubator for 2 Min to allow trypsinization to occur.
v. Following the detachment of the cell from the dish, to stop further trypsinization, 2 ml of fresh complete medium was added to neutralize trypsin activity.
vi. To remove the trypsin, cell suspension was collected in 15ml falcon and centrifuged for 3 min at 1500 rpm and without further delay the supernatant was removed, leaving the cell pellet undisturbed.
vii. Further, to passage the cells, the pellet was resuspended in 1ml of fresh complete media and pipetted gently back and forth to obtain a uniform cell suspension.
viii. From the 1ml of cell suspension, 100 µl was pipetted out and re-seeded in a fresh culture dish added with 5 ml of fresh complete media.
ix. The exterior of the culture dish was wiped with spirit and then the cells were incubated in a CO_2- incubator at 37°C in presence of 5% CO_2.

A.1.7 Protocol for cell counting using hemocytometer

i. To calculate the exact number of mammalian cells in the known volume of cell suspension, 100 µl of cell suspension was pipetted out and diluted by adding an equal volume of trypan blue solution.
ii. The counting chamber and the dedicated cover slip of the hemocytometer was cleaned using 70% ethanol and was assembled and equipped for loading samples.
iii. Both of the counting chambers were loaded separately with 10 µl of a diluted mixture of trypan blue and cell suspension.
iv. The cells spread above the grid of hemocytometer counting chamber were visualized under a microscope with 10X magnification. The sum of cells that occupied all four corner squares ($1mm^2$) were counted and the exact no. of cells in the initial volume of cell suspension was calculated using the formula given below.
v. For calculating the total number of cells in the suspension the following formula was used:

Cells/ml= Average no. of cells in 4 corner box X 10,000 X 2 (dilution factor).

A.1.8 Protocol for cryopreservation

i. The cells harvested by trypsinization were washed twice with complete media and were spun down to pellet the cells and the media in the suspension was discarded.
ii. The cell pellet was re-suspended with 80% incomplete media without antibiotic, 10% FBS, and 10% of dimethyl sulfoxide (DMSO).
iii. The mixture was pipetted in cryovials as 1ml aliquots and were stored in -152°C deep freezer or alternatively in liquid nitrogen tanks.

A.1.9 Protocol for cell revival

i. The cryovials stored at -152°C were retrieved and thawed immediately by placing in a water bath pre-set at the temperature of 37°C.
ii. The cells from the cryovials were then transferred to a fresh 15ml falcon and to that 4 ml of fresh complete media was added.
iii. The falcon was centrifuged shortly to sediment the cells (1500 rpm for 3 min).

iv. After discarding the supernatant the cell pellet was resuspended in 5ml of fresh DMEM medium and was seeded in a 60mm culture dish and incubated in a CO_2-incubator for 24 hours.

v. Next day the media of the culture dish was replaced with a fresh media to remove the dead cells.

A.1.10 Transfection of mammalian cells using Lipofectamine™ 3000

i. 48 hours prior to transfection, a fresh 60 mM dish was seeded with $1X10^6$ cells; so that it attains required confluency (around 80-90%) on the day of transfection.

ii. On the day of transfection, 5 µg of DNA was diluted in 500 µl of Opti-MEM media in a fresh 1.5ml Eppendorf tube and 5µl of Lipofectamine 3000 reagent was added, mixed thoroughly and incubated for 5 min at RT.

iii. 10 µl of Lipofectamine 3000 transfection reagent was added to the above ingredients in the Eppendorf tube, mixed gently by pipetting and incubated for 30 min at RT.

iv. Prior to transfection, the media in the 60 mm dish was removed, and replaced with fresh media.

v. The transfection mixture was added on the top of the cell monolayer in a drop-wise manner.

vi. 60 mm dish was gently agitated and incubated in a CO_2 incubator for 24 hours; the media in the dish was replaced with fresh media.

vii. The cells were harvested in between 48 to 72 hours post transfection and utilized for downstream methods.

A.2 RNA Extraction and cDNA Preparation for Real-Time PCR

A.2.1 RNA isolation

i. The cultured cell pellets ($1 – 2\ X10^6$) were washed with ice-cold PBS, followed by addition of 1 ml of TRIZOL (TRI) reagent.

ii. The cells were pipetted vigorously to dissolve it with TRI reagent and allowed to stand for 10 min at RT

iii. 200 µl of chloroform was added to the samples and vortexed for 15 sec and incubated for 10 min at RT.

iv. The resultant mixtures were centrifuged at 12000 rpm for 15 min at 4°C, to obtain three distinct phases-
   A. proteins in the red organic phase
   B. DNA in the interphase
   C. RNA in the colorless upper aqueous phase

v. The aqueous phase was carefully collected in a fresh 1.5ml Eppendorf tube followed by the addition of 0.5 volume of isopropanol.

vi. The resultant mixture was vortexed for 15 sec, allowed to stand for 5 min at RT and then centrifuged at 12000 rpm for 15 min in a refrigerated condition.

vii. Without disturbing the RNA pellet that had formed on the bottom side of the microcentrifuge tube, the supernatant was discarded.

viii. To remove the contaminating salts, RNA pellet was washed with 1ml of 70% ethanol and centrifuged at 12000 rpm for 10 min at 4°C.

ix. Following centrifugation, the supernatant was decanted and the RNA pellet was air dried for 5 to 10 min.

x. The air dried RNA was dissolved in 20-30 µl of RNase-free water, 2 µl of RNA was resolved on 1% agarose gel to check its quality.

xi. RNA was quantified using NanoDrop and the remaining RNA was stored in -80°C, until further use.

A.2.2 cDNA preparation

A.2.2.1 DNase Treatment

i. DNase treatment was given by mixing 1 µl of reaction buffer, 2000ng of RNA and the mixture was made up to the volume of 7 µl by adding nuclease-free water.

ii. 1 µl of DNase enzyme was added to the mixture and incubated at 37°C for 30 min using a PCR machine.

iii. This was followed by addition of EDTA (Ethylenediaminetetraacetic acid) and kept at 62°C for 10 min, to stop further DNase activity.

Typical DNase treatment reaction

10X DNase buffer	1 µl
RNA	2000 ng
H_2O	7 µl (Makeup)
DNase Enzyme	1 µl

A.2.2.2 Single-stranded cDNA synthesis

RNA that was subjected to DNase treatment was used for cDNA conversion using random hexamer primers.

cDNA synthesis reaction mixture used

DNase-treated RNA (2000ng)	10 µl
5X Reverse Transcriptase Buffer	4 µl
DNTP's (10mM)	2 µl
Random Hexamer primers	2 µl
Reverse Transcriptase	1 µl
RNase free H_2O	1 µl

A.2.2.3 cDNA preparation conditions

Activation	25°C for 10 min
Reaction	37°C for 120 min
Denaturation of enzyme	85°C for 5 sec
Storage	4°C for α

A.2.2.4 PCR cycles (Real time)

i. 50°C – 2 min
ii. 95°C – 15 sec
iii. 60°C – 1 min
iv. 95°C – 10 min
40 Cycles of steps ii and iii were performed.

A.3 Confocal Microscopy

A.3.1 Seeding of cells on coverslips

i. Coverslips were cleaned by immersing in absolute alcohol and dried by bringing in contact with flame.
ii. Coverslips were then placed in the 6 well plates and 2 ml of complete cell culture medium was added to the wells.
iii. The required number of cells were then seeded over the cover slip, the culture plate was gently agitated to spread the cells evenly
iv. 6 well plates were then incubated in a CO_2 incubator for 24-48 hours.

A.3.2 Cell fixing and Immunostaining

i. Upon achieving the required confluency, the cells grown on the coverslips were washed twice with PBS and the cells on the coverslip were fixed by adding 3.7% of paraformaldehyde (PFA) solution for 20 min at RT.
ii. Cells were again washed twice with PBS, and then blocked and permeabilized by incubating in the blocking buffer contain Triton X-100 for 1 hour at RT.
iii. Following the above step, the coverslips were incubated in the primary antibodies of interest overnight at 4°C on a static platform.
iv. The slides were washed thrice at 10 min intervals by adding Tris Buffer Saline and Triton X-100 (TBST) and kept on a rocker.
v. The cells were then incubated with secondary antibodies conjugated with fluorophores (e.g. Alexa 488) for 1 hour at RT.
vi. Once again the cells are washed thrice with TBST and then subjected to mitochondrial and nuclear staining, using 4, 6-diamidino-2-phenylidone (DAPI) and MitoTracker-Red (1:500 dilution in PBS), and preventing it from light for 20 minutes at RT.

A.3.3 Mounting and visualization of microscopy slides

i. The glass slide was cleaned by wiping with absolute alcohol and labeled with experimental details.
ii. 20 µl of prolonged gold anti-fade agent was dropped on the middle of the slide
iii. The coverslips were placed exactly over the anti-fade droplet in an inverted position, avoiding trapping of air bubbles.
iv. Gentle pressure was exerted over the coverslip to remove the excessive anti-fade reagent using tissue paper ; and the square edges of the coverslip were sealed using nail polish (At this stage glass slides could be stored at -20°C for a week).
v. The slides prepared were visualized using inverted confocal microscope under oil immersion objective.

A.3.4 Tris Buffer Saline (TBS)

Ingredients	**Concentration**
Tris	A.05 gram
NaCl	8.76 gram
H_2O	Make up to 1000 ml
pH	7.6

A.3.5 Blocking and permeabilization solution

Ingredients	**Concentration**
BSA	5 gram
Triton X-100	0.1 %
TBS	Makeup to 100 ml

A.4 Plasmid Isolation

A.4.1 Luria Broth (100 ml)

Components	Concentration
Tryptone	1 gram
NaCl	500 mg
Yeast Extract	500 mg
Double Distilled Water	100 ml

A.4.2 Competent cell preparation

i. 5 ml of LB medium was inoculated with a fresh *E. coli* colony; and was grown overnight in an orbital shaker at 37ºC.

ii. From the overnight grown culture, 1 ml of medium was added to the pre-warmed broth of 100ml of LB and placed in orbital shaker at 37°C.

iii. The growth of bacteria was monitored periodically until it reached an optical density of 0.6 at the wavelength of 600 nm.

iv. Upon attaining required growth the bacterial culture was precooled in ice and then transferred to a sterile centrifuge tube which was subjected to centrifugation at 6,000 rpm for 8 minutes at 4 °C. Cells were collected and the supernatant was discarded.

v. Cells were re-suspended in 20 ml of ice-cold competent cell buffer [100 ml of competent cell buffer contained: 100 mM $CaCl_2$ (dihydrate), 70 mM $MnCl_2$, 40 mM $C_2H_3O_2Na$ pH 5.5, and 80% of Glycerol], incubated on ice for 20 minutes and then the cells were pelleted by centrifugation 6,000 rpm for 8 minutes at 4 °C.

vi. After discarding the supernatant, cell pellet was re-suspended gently in an aseptic condition by adding chilled 0.1 M $CaCl_2$ and 0.5 ml. The re-suspended, competent cells were distributed into aliquots of 50-100 microliters in microfuge tubes and snap frozen in liquid nitrogen and stored at -80ºC for later use.

A.4.3 Transformation

i. An aliquot of competent cells was taken out of -80°C and thawed on ice.
ii. 10 ng of plasmid DNA or ligation mixture was added into 50µL of competent cells and was gently mixed by tabbing a few times and the mixture was placed on ice for 20 min.
iii. Heat shock was given to the bacterial cells by placing the tubes into a 42°C water bath for 60-90 seconds and then back on the ice for 5 min.
iv. 500 µl to 800 µl of LB media (without antibiotic) was added and cells were incubated at 37°C for 45 min with vigorous shaking.
v. Agar plates (containing the appropriate antibiotic selection) were taken out from 4°C and pre-warmed to room temperature.
vi. The mixture was centrifuged at 2000 rpm for 3 min to pellet down the transformed bacterial cells, and the supernatant was discarded.
vii. The pellet was re-suspended in 100 µl of LB and was evenly spread on the agar plate containing selection antibiotic.
viii. Further, the plates were incubated at 37°C for 12 hour and positive colonies were confirmed by performing single colony PCR or plasmid isolation followed by restriction digestion to confirm the insert release.

A.4.4 Plasmid isolation (Alkaline lysis method)

A.4.4.1 Solution I 100 ml (Re-suspension solution)

50 mM Glucose	1.711gm
10 mM Tris pH-8	2.5 ml
pH-10 mM EDTA pH-8	2 ml
Double Distilled Water	Make up to 100 ml

Glucose solution was filtered sterilized, and solution I was stored at 4ºC.

A.4.4.2 Solution II (Lysis solution) 10 ml (freshly made)

10 N NaOH	0.2 ml (0.2M NaOH)
10% SDS	1 ml (1% SDS)

A.4.4.3 Solution III, 100 ml (Neutralization solution); Stored at 4°C

5M Potassium acetate	60 ml
Glacial acetic acid	11.5 ml
Water	28.5 ml

A.4.4.4 Protocol

i. A single colony of bacteria was inoculated in 5 ml of LB medium, with added selective antibiotic (Ampicillin or Kanamycin); and grown overnight at 37°C with vigorous shaking.
ii. Overnight culture was centrifuged at 8000 RPM for 5 min to pellet bacterial cells.
iii. 200µl of solution I and RNase was added to the cell pellet and mixed by vortexing and then kept on ice for 10 min.
iv. To this, 200 µl of the solution II (freshly prepared) was added and subjected to 6-10 invert mixing and left for 5 min at room temperature.
v. 400 µl of solution III was added and was invert mixed 6-10 times before keeping on ice for 10 min.
vi. The resultant mixture was centrifuged for 15 min at 12000 RPM at 4˚C and supernatant was carefully collected in a fresh 1.5 ml Eppendorf tube.
vii. 0.6 volume of isopropanol was added to the above supernatant, vortexed for 15 sec and centrifuged for 15 min at 12,000 RPM to precipitate plasmid DNA.
viii. Following this, the supernatant was discarded and the pellet was gently washed with 1ml of 70% ethanol by centrifuging at 12000 RPM for 15 min with subsequent removal of supernatant.
ix. The pellet was air dried and the isolated plasmid DNA was dissolved in 50 µl TE or nuclease free water.
x. To check the quality, 2 µl of plasmid DNA was loaded on an agarose gel and electrophoresed at 60V and visualized using U.V. trans-illuminator; further the concentration was quantified using Nanodrop.

Note: For transfections in mammalian cells, plasmid isolation was performed using Plasmid Midiprep kit (Qiagen) by following manufacturer's instructions.

A.5 Agarose Gel Electrophoresis

A.5.1. 10X TBE (Tris, Boric acid, EDTA)

Tris-base	80 mM
Boric acid	40 mM
EDTA (pH 8.0)	2 mM

A.5.2. Ethidium bromide

10 mg/ml; prepared in MilliQ water, wrapped in aluminum foil was kept in dark at RT.

A.5.3. 6X DNA loading buffer

Bromophenol blue	0.25% (w/v)
Xylene cyanol	0.25%
Glycerol	30% (v/v)

A.6. Glycolytic Enzyme Assay

A.6.1 Hexokinase Assay (Stock solution preparation)

Components	**MW (Da)**	**Stock Conc.**	**Working Conc.**	**Storage**
Tris-Cl pH 8	157.56.	1 M	100 mM	RT
$MgCl_2$	95.211	100 mM	5 mM	RT
Glucose	180.155	2 M	100 mM	-20°C
ATP	507.18	16 mM	0.8 mM	-20°C
NADP	744.41	20 mM	1 mM	-20°C
G6PD	133,000	----	2 units	-20°C
Total reaction volume (1 ml, makeup with Water)				

A.6.2 Pyruvate Kinase Assay (Stock solution preparation)

Components	**MW (Da)**	**Stock Conc.**	**Working Conc.**	**Storage**
Tris-Cl pH 7.4	157.56.	1.35 M	67.5 mM	RT
KCl	74.55	1.9 M	95 mM	RT
$MgCl_2$	95.21	0.135 M	6.75 mM	RT
PEP	267.2	34 mM	1.7 mM	-20°C
ADP	427.2	25 mM	1.25 mM	-20°C
NADH	709.4	2.8 mM	.14 mM	-20°C
LDH	14,000	2 mg/ml	2 µl	-20°C
Total reaction volume (1 ml, makeup with Water)				

A.6.3 Glycerol Gradient (To resolve and examine the oligomeric forms of Pyruvate kinase)

Required ingredients

i. 50 ml of 50 % glycerol was obtained by mixing 25 ml of 100% glycerol with 25 ml of 2X cell lysis buffer (250 mM Tris-cl pH 7.5, 300 mM NaCl and 2mM PMSF).
ii. 50 ml of 1x lysis buffer was used to make further dilutions

Final glycerol (%)	**50% Glycerol (µl)**	**1X Lysis buffer (µl)**
13	260	740
15	300	700
17	340	660
19	380	620
21	420	580
23	460	540
25	500	500
27	540	460

i. A step gradient 27% - 13% in a decreasing order from the bottom (27% to 13%) of glycerol solution (300 µl each) was loaded into the centrifugation tubes that were compatible with Beckman SW Ti55 rotor.

ii. 500 µg to 1000 µg of whole cell lysate were loaded on the top of the step gradient tubes; care was taken to balance the rotor.

iii. Tubes were placed in a centrifuge (Beckmann SWT55i rotor) and revolved at 50,000 rpm for 18 hrs.

iv. After completion of the spin, tubes were gently taken out from the rotor and 100 µl aliquots were collected in pre-chilled tubes

v. Relative pyruvate kinase activity for each fraction was examined as described earlier.

A.6.4 Lactate Dehydrogenase Assay (Stock solution preparation)

Components	**MW (Da)**	**Stock Conc.**	**Working Conc.**	**Storage**
Tris-Cl pH 7.3	157.56	1.35 M	200 mM	RT
Sodium Pyruvate	110	600 mM	30 mM	-20°C
NADH	709.4	132 mM	6.6 mM	-20°C
Total reaction volume (1 ml, makeup with Water)				

A.7 Protein isolation and quantification

A.7.1 Composition of cell lysis buffer (for protein isolation)

Components	**MW (Da)**	**Stock Conc.**	**5X Stock**
Tris-Cl pH 7.5	157.56.	1 M	250 mM
NaCl	58.44	5 M	750 mM
NP-40	---	----	5%
EDTA	372.24	500 mM	5 mM
EGTA	380.35	500 mM	5 mM
Lysis buffer was prepared in 5X concentration and stored in -80°C as 200µl aliquots, until further use			

To prepare 1X working lysis buffer, the 5X aliquot was thawed and added to the below mentioned protease and phosphatase inhibitors and further diluted by adding MilliQ water.

The whole cell protein lysate obtained by the above lysis method was quantified and used for downstream experimental processes such as glycolytic enzyme assay and Western blotting.

A.7.2 Protease and phosphatases used in protein isolation methods

Inhibitor	Protease/ phosphatase	Final concentration in lysis buffer	Stock Conc. and Storage
Leupeptin (2µg/µl)	Protease	5 µg / ml	-20°C*
Aprotinin (1µg/µl)	Protease	2 µg / ml	-20°C*
Pepstatin (1µg/µl)	Protease	1 µg / ml	-20°C*
100 mM PMSF	Protease	1 mM	-20°C*
Sodium Vanadate (NaV)	Phosphatase	1 mM	-20°C*
Sodium Fluoride (NaF)	Phosphatase	5 mM	-20°C*

(*) Multiple freeze-thaw cycle was avoided, and the stock was stored as aliquots, strictly following a single freeze-thaw cycle.

A.7.3 Protein Estimation Using BCA (Bicinchoninic Acid)

Principle

BCA Protein Assay is based on bicinchoninic acid (BCA) for the colorimetric detection and quantitation of total protein. This method involves reduction of Cu+2 to Cu+1 by protein in an alkaline medium (the biuret reaction) with the highly sensitive and selective colorimetric detection of the cuprous cation (Cu+1), using a unique reagent containing bicinchoninic acid. The purple-colored reaction product of this assay is formed by the chelation of two molecules of BCA with one cuprous ion. This water-soluble complex exhibits a strong absorbance at 562nm that is nearly linear with increasing protein concentration over a broad working range (20-2000µg/mL).

The macromolecular structure of protein, the number of peptide bonds and the presence of four particular amino acids (cysteine or cysteine, tryptophan, and tyrosine) are reported to be responsible for color formation with BCA.

Reagents

BCA Reagent A: Sodium carbonate, sodium bicarbonate, bicinchoninic acid and sodium tartrate in 0.1M sodium hydroxide

BCA Reagent B: 4% cupric sulfate

Albumin standard: Bovine serum albumin (BSA) at 2mg/mL in 0.9% saline and 0.05% Sodium azide.

Protocol

i. 200 µl of BCA reagent (50:4 ratio of reagent A: B) was added to the required number of wells of a 96 well plate.
ii. 10 wells were dedicated to BSA standard, 1 well for sample blank, 1 well for test blank and rest test sample wells as per the requirement.
iii. 20 µl of water was added to the first blank and 1 µl of 1X lysis buffer was added to the second blank, already containing 19 µl of water.
iv. Test samples were prepared as follows- T1: 200 µl BCA reagent + 19 µl PCR water + 1 µl test sample volume.
v. Standard Preparation: BSA (2 mg/ml) was diluted suitably to obtain concentrations ranging from 0.1-10 µg/ml and was added to the 10 wells allocated for the same.
vi. Samples were mixed properly by pipetting to ensure complex formation and air bubble creation avoided.
vii. The plate was incubated at 37°C for 30 minutes and then the absorbance was read at 562 nm in a microplate reader.
viii. Protein estimation was carried out using the absorbance and the standard curve obtained.
ix. Standard was made by using the OD of known BSA concentrations after subtracting B1 (BSA) blank O.D.
x. Test sample OD was also subtracted by B2 (Test) blank OD. Test sample OD was divided by the factor obtained from excel and further multiplied by the dilution factor of 20 in order to get the sample concentration (µg/µl).

A.8 Western Blotting

A.8.1 SDS-PAGE

A.8.1.130% Acrylamide solution preparation

To prepare 200 ml of 30% Acrylamide solution, 58 grams of acrylamide and 2 grams of bis-acrylamide was dissolved by adding 50 ml of water and kept overnight at RT in a light protective container, then the volume was made up to 100 ml and filtered using Whatman filter paper and stored at 4°C.

A.8.1.2 4X-SDS sample buffers

Tris-Cl (pH 6.8)	100 mM
SDS	4% w/v
Bromophenol blue	0.2% w/v
Glycerol	20% v/v
DTT or β-Mercaptoethanol	200 mM

A.8.1.3 5X SDS running buffer (for 500 ml) pH 8.3

Tris	15 grams
Glycine	72 grams
SDS	5 grams
Double Distilled Water	Makeup to 500 ml

A.8.1.4 Staining solution (Coomassie brilliant blue R-250, for 100 ml)

Coomassie brilliant blue R-250	0.25 gm
Glacial acetic acid	10 ml
Methanol	50 ml
Water	40 ml

A.8.1.5 Destaining solution (for 100 ml)

Methanol	50 ml
Glacial acetic acid	10 ml
Water	40 ml

A.8.1.6 Separating and stacking gel

Components	**% resolving gel (5 ml)**					**5% stacking gel (2 ml)**
	6	**8**	**10**	**12**	**15**	
H_2O	2.6	2.3	1.9	1.6	1.1	1.4
30% acrylamide	1.0	1.3	1.7	2.0	2.5	0.33
1.5 M Tris (pH 8.8)	1.3	1.3	1.3	1.3	1.3	-----
1 M Tris-Cl pH (6.8)	-----					0.25
10% SDS	0.05					0.02
10% APS*	0.05					0.02
TEMED	0.04					0.002

Running SDS-PAGE

i. Bio-Rad mini protean SDS-PAGE casting plates (1.5 mm thickness) were cleaned with spirit and then assembled using the plastic clamp and the lower portion was sealed using 1% agarose gel.
ii. 8 ml of 10% resolving gel was prepared and poured in-between the gel casting plates, and then 2 ml of water saturated butanol was added over resolving gel to remove air bubbles and to restrict air entry.
iii. To allow polymerization, the acrylamide gels were allowed to stand for 30 min at RT.
iv. The unpolymerized acrylamide and butanol overlay was discarded and washed twice with MilliQ water and the excessive water droplets were removed using tissue papers.
v. 5ml of 5% stacking gel was prepared and poured to fill the space in-between the glass plates; on top of the resolving gel layer.
vi. 10 well clean Teflon comb was inserted in between the glass plates following the addition of stacking gel solution, care was taken to avoid trapping of air bubbles and the gel allowed standing for another 30 min to polymerize.
vii. Meanwhile, the protein samples were prepared by mixing SDS gel loading dye with a required concentration of protein and cell lysis buffer to yield final 1X SDS gel loading dye concentration.
viii. Protein samples were kept in the boiling water bath (100°C) for 10 min to denature protein quaternary structure and to allow the binding of SDS to the protein.

ix. Following polymerization of the gel, Teflon comb was removed and the wells were washed with deionized water to remove unpolymerized separating gel solution.

x. The clamp holding the glass plates was removed and the gel was placed in the electrophoresis apparatus; and 1X SDS running buffer was added to submerge the acrylamide gel.

xi. Samples and the pre-stained protein molecular weight marker (ladder) were loaded in the wells in a predetermined order

xii. The apparatus was attached to a power pack and 80V of current was applied to the gels to resolve the proteins.

xiii. When the gel loading dye reached the bottom of separating gel layer, the power supply was terminated.

xiv. The gel in-between the glass plates was carefully removed and used for the downstream processing for Western blotting.

A.9 *Western blotting*

Reagents preparation

A.9.1 1X Transfer Buffer (1000ml)

Tris	25 mM
Glycine	192 mM
Methanol	20% (200 ml)
SDS	3.75 ml of 10% SDS
H2O MilliQ	Makeup to 1000 ml

A.9.2 Blocking Buffer (5% BSA)

2.5 grams of BSA was taken in a fresh 50 ml falcon, dissolved by adding TBS to the final volume of 50ml and stored at 4°C with 0.01% sodium azide.

A.9.3 Antibody dilution

The dilution of antibody was carried out as per manufacturers's suggestions in the above mentioned 5% blocking buffer.

A.9.4 Developer and Fixer

i. Developer (Kodak): A-3.2 gm+B-17.8 gm in 200 ml water

ii. Fixer (Kodak): 48.6 gm in 200 ml water.

A.9.5 ECL chemiluminescence kit

i. Luminata Forte from Millipore: 0.5-1.0 ml substrate solution was used as per the size of nitrocellulose membrane.

Protein transfer to Nitrocellulose membrane, Membrane Blocking and developing the blot

i. Nitrocellulose (NC) membrane and the Whatman filter papers were cut equal to the dimension of the gel.
ii. Gel and NC-membrane were incubated and equilibrated with pre-chilled transfer buffer.
iii. A sandwich of filter paper/NC-membrane/SDS-Gel were placed in Bio-Rad transfer apparatus cassettes.
iv. Further, the transfer cassettes were placed into the apparatus and then placed directly between positive and negative electrodes.
v. The apparatus was further, filled with pre-chilled transfer buffer, leaving a magnetic bead at the bottom of the tank to maintain even buffer temperature and ion distribution in the tank.
vi. 125 mA was passed through the gel and NC-membrane sandwich for 4 hours at 4°C.
vii. At the end of the protein transfer, the membrane was removed from the sandwich, washed once using TBST and then incubated in 5% blocking solution for 1 hour at RT.
viii. After blocking, the membrane was incubated overnight with appropriate primary antibody for 12-15 hrs at 4˚C with gentle agitation on the rocker.
ix. Following this step, the membrane was washed thrice with TBST at 10 minutes interval each and then incubated in appropriate secondary antibody conjugated with horseradish peroxidase for 1 hour at RT.
x. Once again, the membrane was washed thrice with TBST at 10 minutes interval each.
xi. The membrane was developed using Luminata Forte® ECL chemiluminescence in a dark room.
xii. Briefly, the membrane was removed from wash buffer, air dried and kept in the middle of the saran-wrap.
xiii. 1 ml of Luminata Forte® substrate solution was gently added over the membrane, the saran-wrap was folded and sealed, to prevent leakage of ECL substrate and kept inside the X-ray cassette.

xiv. The luminescence signals that emerged from the protein of interest in the membrane were captured on X-ray film and then immersed sequentially in the developer, water, and fixer to capture and record the signal in the X-ray film.

A.10 Vector Maps and DNA Sequences

A.10.1 pcDNA 3.1 (Invitrogen, USA)

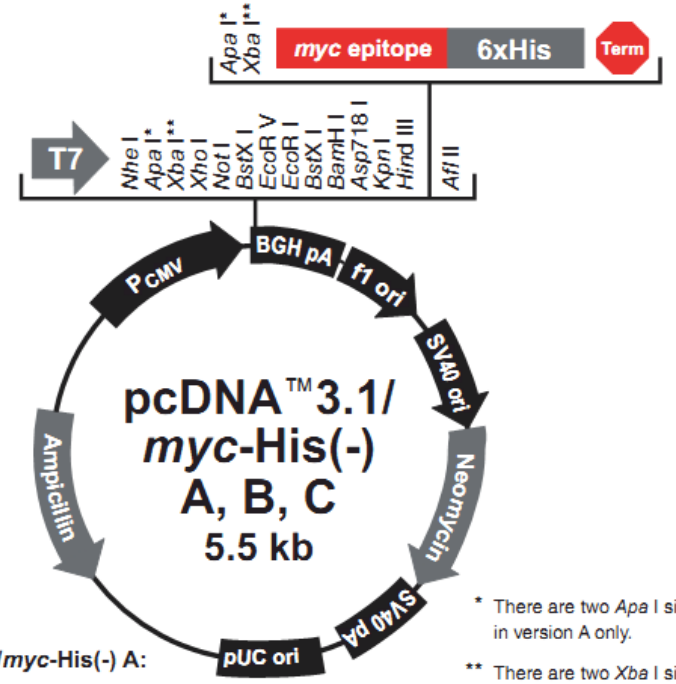

* There are two *Apa* I sites in version A only.

** There are two *Xba* I sites in version B only.

Comments for pcDNA™3.1/*myc*-His(-) A: 5522 nucleotides

CMV promoter: bases 209-863
T7 promoter/priming site: bases 863-882
Multiple cloning site: bases 895-1006
myc epitope: bases 1007-1036
Polyhistidine tag: bases 1052-1069
BGH reverse priming site: bases 1113-1130
BGH polyadenylation signal: bases 1116-1343
f1 origin: bases 1389-1817
SV40 promoter and origin: bases 1844-2152
Neomycin resistance gene: bases 2227-3021
SV40 polyadenylation signal: bases 3195-3325
pUC origin: bases 3708-4381
Ampicillin resistance gene: bases 4526-5386 (complementary strand)

Source: *www.invitrogen.com*

A.10.2 pGEX-4T-1 (GE Healthcare Life Sciences)

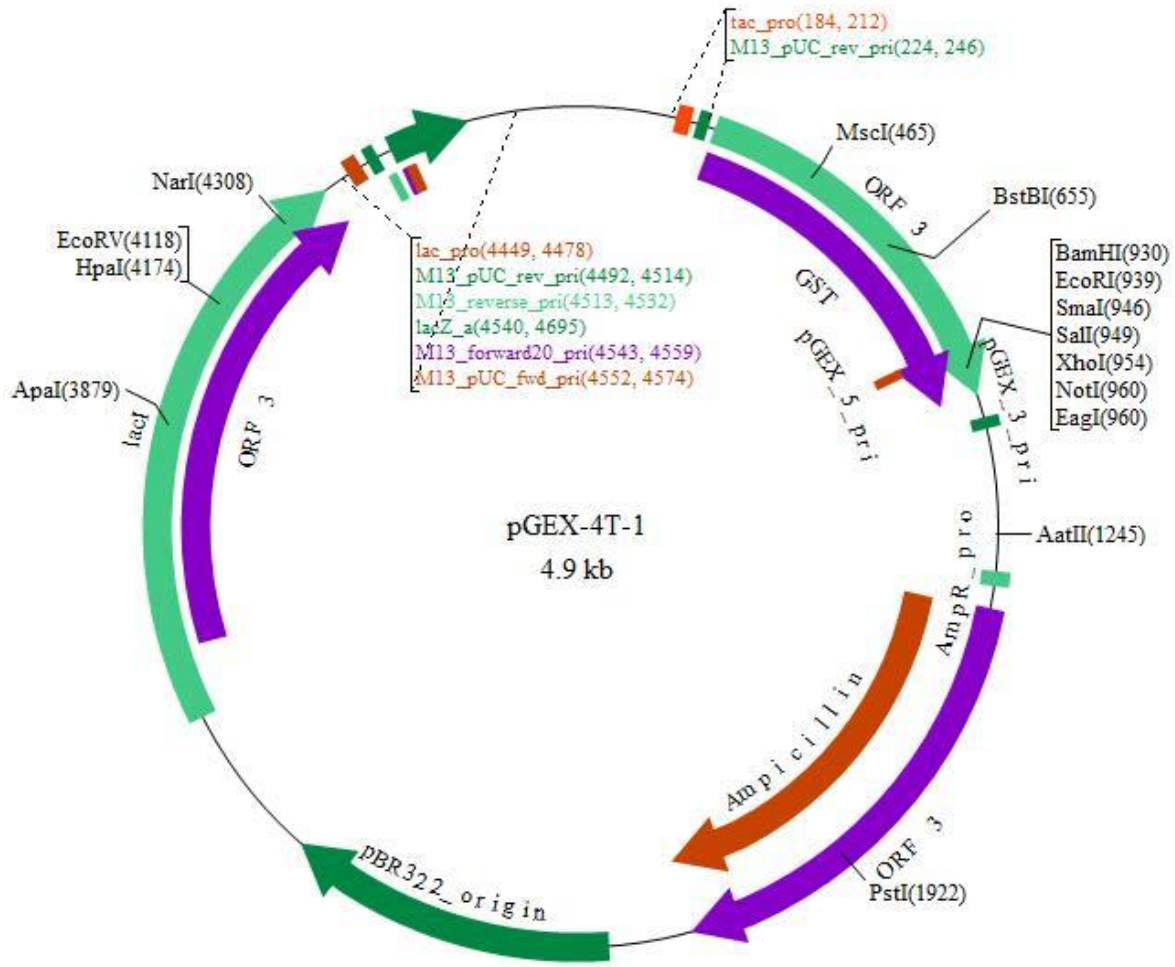

Source: www.gelifesciences.com

A.10.3 pGIPZ (Open Biosystems, USA)

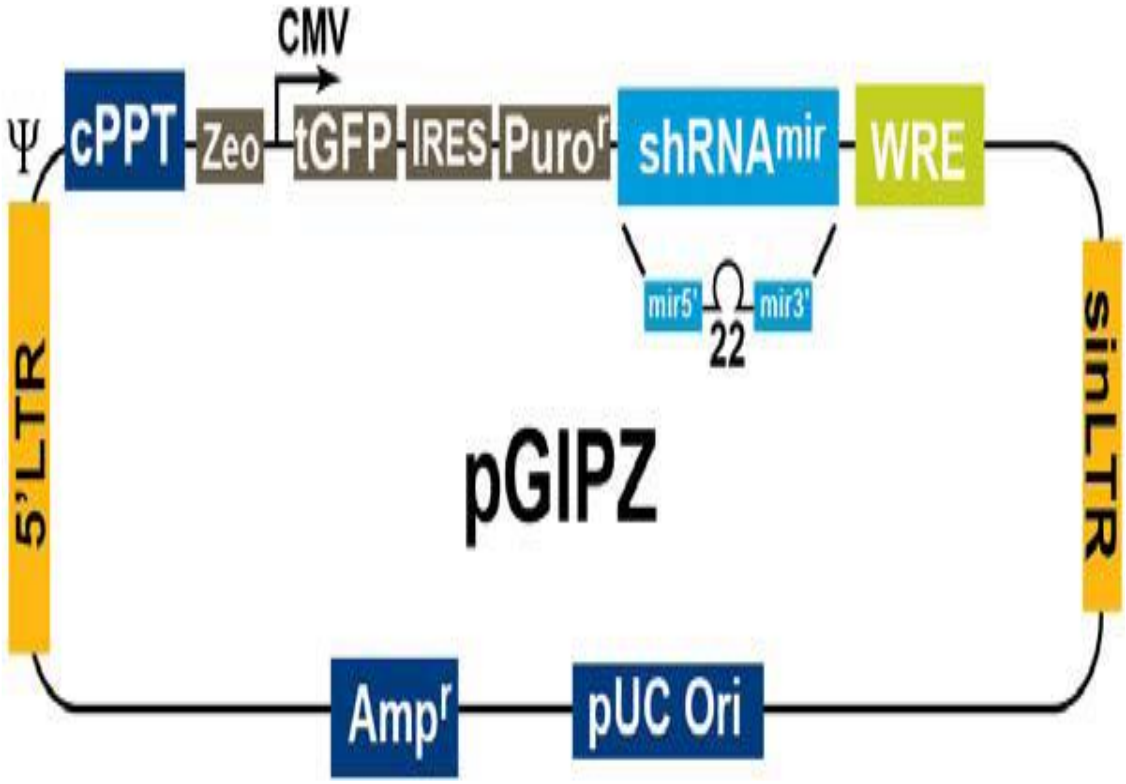

Vector Element	Utility
CMV Promoter	RNA Polymerase II promoter
cPPT	Central Polypurine tract helps translocation into the nucleus of non-dividing cells
WRE	Enhances the stability and translation of transcripts
TurboGFP	Marker to track shRNAmir expression
IRES-puro resistance	Mammalian selectable marker
Amp resistance	Ampicillin (carbenicillin) bacterial selectable marker
5'LTR	5' long terminal repeat
pUC ori	High copy replication and maintenance of plasmid in *E. coli*
SIN-LTR	3' self inactivating long terminal repeat (Shimada, et al. 1995)
RRE	Rev response element
Zeo resistance	Bacterial selectable marker

Source: *Open Biosystems manual at www.openbiosystems.com*

A.10.4 pLKO.1 *(Sigma-Aldrich)*

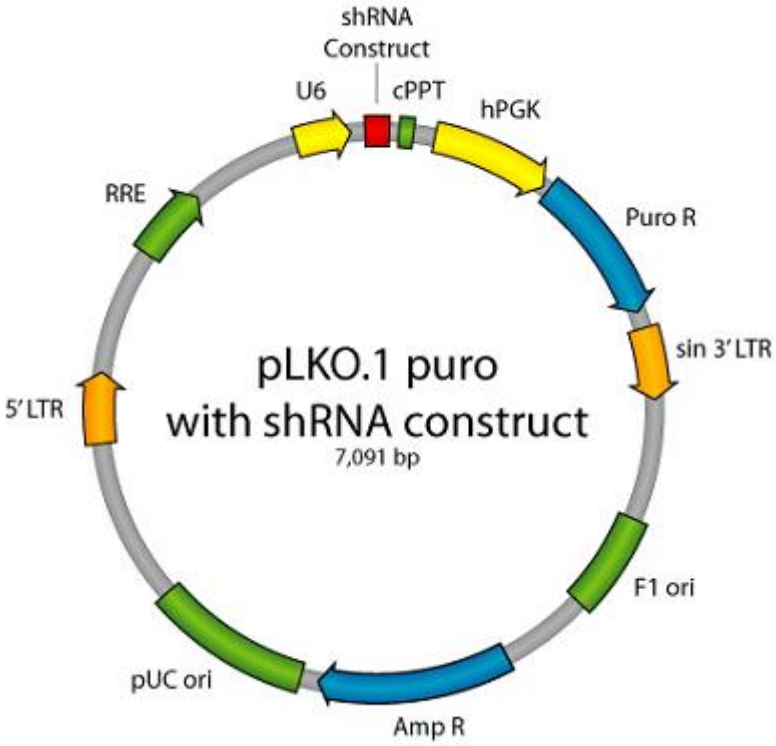

Source: *MISSION® shRNA Vector - Sigma-Aldrich*

*16.5 Human PKM1 cDNA sequence (NCBI Reference Sequence: **NM_002654.3**)*

ATGTCGAAGCCCCATAGTGAAGCCGGGACTGCCTTCATTCAGACCCAGCAGCTGCACGCAGCCA
TGGCTGACACATTCCTGGAGCACATGTGCCGCCTGGACATTGATTCACCACCCATCACAGCCCGG
AACACTGGCATCATCTGTACCATTGGCCCAGCTTCCCGATCAGTGGAGACGTTGAAGGAGATGA
TTAAGTCTGGAATGAATGTGGCTCGTCTGAACTTCTCTCATGGAACTCATGAGTACCATGCGGAG
ACCATCAAGAATGTGCGCACAGCCACGGAAAGCTTTGCTTCTGACCCCATCCTCTACCGGCCCGT
TGCTGTGGCTCTAGACACTAAAGGACCTGAGATCCGAACTGGGCTCATCAAGGGCAGCGGCACT
GCAGAGGTGGAGCTGAAGAAGGGAGCCACTCTCAAAATCACGCTGGATAACGCCTACATGGAA
AAGTGTGACGAGAACATCCTGTGGCTGGACTACAAGAACATCTGCAAGGTGGTGGAAGTGGGC
AGCAAGATCTACGTGGATGATGGGCTTATTTCTCTCCAGGTGAAGCAGAAAGGTGCCGACTTCCT
GGTGACGGAGGTGGAAAATGGTGGCTCCTTGGGCAGCAAGAAGGGTGTGAACCTTCCTGGGGCT
GCTGTGGACTTGCCTGCTGTGTCGGAGAAGGACATCCAGGATCTGAAGTTTGGGGTCGAGCAGG
ATGTTGATATGGTGTTTGCGTCATTCATCCGCAAGGCATCTGATGTCCATGAAGTTAGGAAGGTC
CTGGGAGAGAAGGGAAAGAACATCAAGATTATCAGCAAAATCGAGAATCATGAGGGGGTTCGG
AGGTTTGATGAAATCCTGGAGGCCAGTGATGGGATCATGGTGGCTCGTGGTGATCTAGGCATTGA
GATTCCTGCAGAGAAGGTCTTCCTTGCTCAGAAGATGATGATTGGACGGTGCAACCGAGCTGGG
AAGCCTGTCATCTGTGCTACTCAGATGCTGGAGAGCATGATCAAGAAGCCCCGCCCCACTCGGG
CTGAAGGCAGTGATGTGGCCAATGCAGTCCTGGATGGAGCCGACTGCATCATGCTGTCTGGAGA
AACAGCCAAAGGGGACTATCCTCTGGAGGCTGTGCGCATGCAGCACCTGATAGCTCGTGAGGCT
GAGGCAGCCATGTTCCACCGCAAGCTGTTTGAAGAACTTGTGCGAGCCTCAAGTCACTCCACAG
ACCTCATGGAAGCCATGGCCATGGGCAGCGTGGAGGCTTCTTATAAGTGTTTAGCAGCAGCTTTG
ATAGTTCTGACGGAGTCTGGCAGGTCTGCTCACCAGGTGGCCAGATACCGCCCACGTGCCCCCAT
CATTGCTGTGACCCGGAATCCCCAGACAGCTCGTCAGGCCCACCTGTACCGTGGCATCTTCCCTG
TGCTGTGCAAGGACCCAGTCCAGGAGGCCTGGGCTGAGGACGTGGACCTCCGGGTGAACTTTGC
CATGAATGTTGGCAAGGCCCGAGGCTTCTTCAAGAAGGGAGATGTGGTCATTGTGCTGACCGGA
TGGCGCCCTGGCTCCGGCTTCACCAACACCATGCGTGTTGTTCCTGTGCCGTGA ...1596

16.6 Human PKM1 proteins sequence:

MSKPHSEAGTAFIQTQQLHAAMADTFLEHMCRLDIDSPPITARNTGIICTIGPASRSVETLKEMIKSGMN
VARLNFSHGTHEYHAETIKNVRTATESFASDPILYRPVAVALDTKGPEIRTGLIKGSGTAEVELKKGATL
KITLDNAYMEKCDENILWLDYKNICKVVEVGSKIYVDDGLISLQVKQKGADFLVTEVENGGSLGSKKG
VNLPGAAVDLPAVSEKDIQDLKFGVEQDVDMVFASFIRKASDVHEVRKVLGEKGKNIKIISKIENHEGV
RRFDEILEASDGIMVARGDLGIEIPAEKVFLAQKMMIGRCNRAGKPVICATQMLESMIKKPRPTRAEGS
DVANAVLDGADCIMLSGETAKGDYPLEAVRMQHLIAREAEAAMFHRKLFEELVRASSHSTDLMEAM
AMGSVEASYKCLAAALIVLTESGRSAHQVARYRPRAPIIAVTRNPQTARQAHLYRGIFPVLCKDPVQEA
WAEDVDLRVNFAMNVGKARGFFKKGDVVIVLTGWRPGSGFTNTMRVVPVP
….531

*16.5 Human PKM2 cDNA sequence (NCBI Reference Sequence: **NM_002654.3**)*

ATGTCGAAGCCCCATAGTGAAGCCGGGACTGCCTTCATTCAGACCCAGCAGCTGCACGCAGCCA
TGGCTGACACATTCCTGGAGCACATGTGCCGCCTGGACATTGATTCACCACCCATCACAGCCCGG
AACACTGGCATCATCTGTACCATTGGCCCAGCTTCCCGATCAGTGGAGACGTTGAAGGAGATGA
TTAAGTCTGGAATGAATGTGGCTCGTCTGAACTTCTCTCATGGAACTCATGAGTACCATGCGGAG
ACCATCAAGAATGTGCGCACAGCCACGGAAAGCTTTGCTTCTGACCCCATCCTCTACCGGCCCGT
TGCTGTGGCTCTAGACACTAAAGGACCTGAGATCCGAACTGGGCTCATCAAGGGCAGCGGCACT
GCAGAGGTGGAGCTGAAGAAGGGAGCCACTCTCAAAATCACGCTGGATAACGCCTACATGGAA
AAGTGTGACGAGAACATCCTGTGGCTGGACTACAAGAACATCTGCAAGGTGGTGGAAGTGGGC
AGCAAGATCTACGTGGATGATGGGCTTATTTCTCTCCAGGTGAAGCAGAAAGGTGCCGACTTCCT
GGTGACGGAGGTGGAAAATGGTGGCTCCTTGGGCAGCAAGAAGGGTGTGAACCTTCCTGGGGCT
GCTGTGGACTTGCCTGCTGTGTCGGAGAAGGACATCCAGGATCTGAAGTTTGGGGTCGAGCAGG
ATGTTGATATGGTGTTTGCGTCATTCATCCGCAAGGCATCTGATGTCCATGAAGTTAGGAAGGTC
CTGGGAGAGAAGGGAAAGAACATCAAGATTATCAGCAAAATCGAGAATCATGAGGGGGTTCGG
AGGTTTGATGAAATCCTGGAGGCCAGTGATGGGATCATGGTGGCTCGTGGTGATCTAGGCATTGA
GATTCCTGCAGAGAAGGTCTTCCTTGCTCAGAAGATGATGATTGGACGGTGCAACCGAGCTGGG
AAGCCTGTCATCTGTGCTACTCAGATGCTGGAGAGCATGATCAAGAAGCCCCGCCCCACTCGGG
CTGAAGGCAGTGATGTGGCCAATGCAGTCCTGGATGGAGCCGACTGCATCATGCTGTCTGGAGA
AACAGCCAAAGGGGACTATCCTCTGGAGGCTGTGCGCATGCAGCACCTGATTGCCCGTGAGGCA
GAGGCTGCCATCTACCACTTGCAATTATTTGAGGAACTCCGCCGCCTGGCGCCCATTACCAGCGA
CCCCACAGAAGCCACCGCCGTGGGTGCCGTGGAGGCCTCCTTCAAGTGCTGCAGTGGGGCCATA
ATCGTCCTCACCAAGTCTGGCAGGTCTGCTCACCAGGTGGCCAGATACCGCCCACGTGCCCCCAT
CATTGCTGTGACCCGGAATCCCCAGACAGCTCGTCAGGCCCACCTGTACCGTGGCATCTTCCCTG
TGCTGTGCAAGGACCCAGTCCAGGAGGCCTGGGCTGAGGACGTGGACCTCCGGGTGAACTTTGC
CATGAATGTTGGCAAGGCCCGAGGCTTCTTCAAGAAGGGAGATGTGGTCATTGTGCTGACCGGA
TGGCGCCCTGGCTCCGGCTTCACCAACACCATGCGTGTTGTTCCTGTGCCGTGA ...1596

16.6 Human PKM2 proteins sequence:

MSKPHSEAGTAFIQTQQLHAAMADTFLEHMCRLDIDSPPITARNTGIICTIGPASRSVETLKEMIKSGMN
VARLNFSHGTHEYHAETIKNVRTATESFASDPILYRPVAVALDTKGPEIRTGLIKGSGTAEVELKKGATL
KITLDNAYMEKCDENILWLDYKNICKVVEVGSKIYVDDGLISLQVKQKGADFLVTEVENGGSLGSKKG
VNLPGAAVDLPAVSEKDIQDLKFGVEQDVDMVFASFIRKASDVHEVRKVLGEKGKNIKIISKIENHEGV
RRFDEILEASDGIMVARGDLGIEIPAEKVFLAQKMMIGRCNRAGKPVICATQMLESMIKKPRPTRAEGS
DVANAVLDGADCIMLSGETAKGDYPLEAVRMQHLIAREAEAAIYHLQLFEELRRLAPITSDPTEATAV
GAVEASFKCCSGAIIVLTKSGRSAHQVARYRPRAPIIAVTRNPQTRQAHLYRGIFPVLCKDPVQEAWAE
DVDLRVNFAMNVGKARGFFKKGDVVIVLTGWRPGSGFTNTMRVVPVP
….531

*16.5 Human AMPKa2 cDNA sequence (NCBI Reference Sequence: **NM_002654.3**)*

ATGGCTGAGAAGCAGAAGCACGACGGGCGGGTGAAGATCGGACACTACGTGCTGGGCGACACG
CTGGGCGTCGGCACCTTCGGCAAAGTGAAGATTGGAGAACATCAATTAACAGGCCATAAAGTGG
CAGTTAAAATCTTAAATAGACAGAAGATTCGCAGTTTAGATGTTGTTGGAAAAATAAAACGAGA
AATTCAAAATCTAAAACTCTTTCGTCATCCTCATATTATCAAACTATACCAGGTGATCAGCACTC
CAACAGATTTTTTTATGGTAATGGAATATGTGTCTGGAGGTGAATTATTTGACTACATCTGTAAGC
ATGGACGGGTTGAAGAGATGGAAGCCAGGCGGCTCTTTCAGCAGATTCTGTCTGCTGTGGATTAC
TGTCATAGGCATATGGTTGTTCATCGAGACCTGAAACCAGAGAATGTCCTGTTGGATGCACACAT
GAATGCCAAGATAGCCGATTTCGGATTATCTAATATGATGTCAGATGGTGAATTTCTGAGAACTA
GTTGCGGATCTCCAAATTATGCAGCACCTGAAGTCATCTCAGGCAGATTGTATGCAGGTCCTGAA
GTTGATATCTGGAGCTGTGGTGTTATCTTGTATGCTCTTCTTTGTGGCACCCTCCCATTTGATGATG
AGCATGTACCTACGTTATTTAAGAAGATCCGAGGGGGTGTCTTTTATATCCCAGAATATCTCAAT
CGTTCTGTCGCCACTCTCCTGATGCATATGCTGCAGGTTGACCCACTGAAACGAGCAACTATCAA
AGACATAAGAGAGCATGAATGGTTTAAACAAGATTTGCCCAGTTACTTATTTCCTGAAGACCCTT
CCTATGATGCTAACGTCATTGATGATGAGGCTGTGAAAGAAGTGTGTGAAAAATTTGAATGTACA
GAATCAGAAGTAATGAACAGTTTATATAGTGGTGACCCTCAAGACCAGCTTGCAGTGGCTTATCA
TCTTATCATTGACAATCGGAGAATAATGAACCAAGCCAGTGAGTTCTACCTCGCCTCTAGTCCTC
CATCTGGTTCTTTTATGGATGATAGTGCCATGCATATTCCCCCAGGCCTGAAACCTCATCCAGAA
AGGATGCCACCTCTTATAGCAGACAGCCCCAAAGCAAGATGTCCATTGGATGCACTGAATACGA
CTAAGCCCAAATCTTTAGCTGTGAAAAAAGCCAAGTGGCATCTTGGAATCCGAAGTCAGAGCAA
ACCGTATGACATTATGGCTGAAGTTTACCGAGCTATGAAGCAGCTGGATTTTGAATGGAAGGTAG
TGAATGCATACCATCTTCGTGTAAGAAGAAAAAATCCAGTGACTGGCAATTACGTGAAAATGAG
CTTACAACTTTACCTGGTTGATAACAGGAGCTATCTTTTGGACTTTAAAAGCATTGATGATGAAGT
AGTGGAGCAGAGATCTGGTTCCTCAACACCTCAGCGTTCCTGTTCTGCTGCTGGCTTACACAGAC
CAAGATCAAGTTTTGATTCCACAACTGCAGAGAGCCATTCACTTTCTGGCTCTCTCACTGGCTCTT
TGACCGGAAGCACATTGTCTTCAGTTTCACCTCGCCTGGGCAGTCACACCATGGATTTTTTTGAAA
TGTGTGCCAGTCTGATTACTACTTTAGCCCGTTGA ...1659

16.6 Human *AMPKa2* proteins sequence:

MAEKQKHDGRVKIGHYVLGDTLGVGTFGKVKIGEHQLTGHKVAVKILNRQKIRSLDVVGKIKREIQNL
KLFRHPHIIKLYQVISTPTDFFMVMEYVSGGELFDYICKHGRVEEMEARRLFQQILSAVDYCHRHMVVH
RDLKPENVLLDAHMNAKIADFGLSNMMSDGEFLRTSCGSPNYAAPEVISGRLYAGPEVDIWSCGVILY
ALLCGTLPFDDEHVPTLFKKIRGGVFYIPEYLNRSVATLLMHMLQVDPLKRATIKDIREHEWFKQDLPS
YLFPEDPSYDANVIDDEAVKEVCEKFECTESEVMNSLYSGDPQDQLAVAYHLIIDNRRIMNQASEFYLA
SSPPSGSFMDDSAMHIPPGLKPHPERMPPLIADSPKARCPLDALNTTKPKSLAVKKAKWHLGIRSQSKP
YDIMAEVYRAMKQLDFEWKVVNAYHLRVRRKNPVTGNYVKMSLQLYLVDNRSYLLDFKSIDDEVVE
QRSGSSTPQRSCSAAGLHRPRSSFDSTTAESHSLSGSLTGSLTGSTLSSVSPRLGSHTMDFFEMCASLITTL

*16.5 Human AMPKa2 T172D cDNA sequence (NCBI Reference Sequence: **NM_002654.3**)*

ATGGCTGAGAAGCAGAAGCACGACGGGCGGGTGAAGATCGGACACTACGTGCTGGGCGACACG
CTGGGCGTCGGCACCTTCGGCAAAGTGAAGATTGGAGAACATCAATTAACAGGCCATAAAGTGG
CAGTTAAAATCTTAAATAGACAGAAGATTCGCAGTTTAGATGTTGTTGGAAAAATAAAACGAGA
AATTCAAAATCTAAAACTCTTTCGTCATCCTCATATTATCAAACTATACCAGGTGATCAGCACTC
CAACAGATTTTTTTATGGTAATGGAATATGTGTCTGGAGGTGAATTATTTGACTACATCTGTAAGC
ATGGACGGGTTGAAGAGATGGAAGCCAGGCGGCTCTTTCAGCAGATTCTGTCTGCTGTGGATTAC
TGTCATAGGCATATGGTTGTTCATCGAGACCTGAAACCAGAGAATGTCCTGTTGGATGCACACAT
GAATGCCAAGATAGCCGATTTCGGATTATCTAATATGATGTCAGATGGTGAATTTCTGAGAACTA
GTTGCGGATCTCCAAATTATGCAGCACCTGAAGTCATCTCAGGCAGATTGTATGCAGGTCCTGAA
GTTGATATCTGGAGCTGTGGTGTTATCTTGTATGCTCTTCTTTGTGGCACCCTCCCATTTGATGATG
AGCATGTACCTACGTTATTTAAGAAGATCCGAGGGGGTGTCTTTTATATCCCAGAATATCTCAAT
CGTTCTGTCGCCACTCTCCTGATGCATATGCTGCAGGTTGACCCACTGAAACGAGCAACTATCAA
AGACATAAGAGAGCATGAATGGTTTAAACAAGATTTGCCCAGTTACTTATTTCCTGAAGACCCTT
CCTATGATGCTAACGTCATTGATGATGAGGCTGTGAAAGAAGTGTGTGAAAAATTTGAATGTACA
GAATCAGAAGTAATGAACAGTTTATAT ...936

16.6 Human *AMPKa2 T172D consecutive active protein* proteins sequence:

MAEKQKHDGRVKIGHYVLGDTLGVGTFGKVKIGEHQLTGHKVAVKILNRQKIRSLDVVGKIKREIQNL
KLFRHPHIIKLYQVISTPTDFFMVMEYVSGGELFDYICKHGRVEEMEARRLFQQILSAVDYCHRHMVVH
RDLKPENVLLDAHMNAKIADFGLSNMMSDGEFLRDSCGSPNYAAPEVISGRLYAGPEVDIWSCGVILY
ALLCGTLPFDDEHVPTLFKKIRGGVFYIPEYLNRSVATLLMHMLQVDPLKRATIKDIREHEWFKQDLPS
YLFPEDPSYDANVIDDEAVKEVCEKFECTESEVMNSLY ….531

*16.5 Human C-Myc cDNA sequence (NCBI Reference Sequence: **NM_002654.3**)*

ATGCCCCTCAACGTTAGCTTCACCAACAGGAACTATGACCTCGACTACGACTCGGTGCAGCCGTA
TTTCTACTGCGACGAGGAGGAGAACTTCTACCAGCAGCAGCAGCAGAGCGAGCTGCAGCCCCCG
GCGCCCAGCGAGGATATCTGGAAGAAATTCGAGCTGCTGCCCACCCCGCCCCTGTCCCCTAGCC
GCCGCTCCGGGCTCTGCTCGCCCTCCTACGTTGCGGTCACACCCTTCTCCCTTCGGGGAGACAAC
GACGGCGGTGGCGGGAGCTTCTCCACGGCCGACCAGCTGGAGATGGTGACCGAGCTGCTGGGAG
GAGACATGGTGAACCAGAGTTTCATCTGCGACCCGGACGACGAGACCTTCATCAAAAACATCAT
CATCCAGGACTGTATGTGGAGCGGCTTCTCGGCCGCCGCCAAGCTCGTCTCAGAGAAGCTGGCCT
CCTACCAGGCTGCGCGCAAAGACAGCGGCAGCCCGAACCCCGCCCGCGGCCACAGCGTCTGCTC
CACCTCCAGCTTGTACCTGCAGGATCTGAGCGCCGCCGCCTCAGAGTGCATCGACCCCTCGGTGG
TCTTCCCCTACCCTCTCAACGACAGCAGCTCGCCCAAGTCCTGCGCCTCGCAAGACTCCAGCGCC
TTCTCTCCGTCCTCGGATTCTCTGCTCTCCTCGACGGAGTCCTCCCCGCAGGGCAGCCCCGAGCCC
CTGGTGCTCCATGAGGAGACACCGCCCACCACCAGCAGCGACTCTGAGGAGGAACAAGAAGAT
GAGGAAGAAATCGATGTTGTTTCTGTGGAAAAGAGGCAGGCTCCTGGCAAAAGGTCAGAGTCTG
GATCACCTTCTGCTGGAGGCCACAGCAAACCTCCTCACAGCCCACTGGTCCTCAAGAGGTGCCA
CGTCTCCACACATCAGCACAACTACGCAGCGCCTCCCTCCACTCGGAAGGACTATCCTGCTGCCA
AGAGGGTCAAGTTGGACAGTGTCAGAGTCCTGAGACAGATCAGCAACAACCGAAAATGCACCA
GCCCCAGGTCCTCGGACACCGAGGAGAATGTCAAGAGGCGAACACACAACGTCTTGGAGCGCC
AGAGGAGGAACGAGCTAAAACGGAGCTTTTTTGCCCTGCGTGACCAGATCCCGGAGTTGGAAAA
CAATGAAAAGGCCCCCAAGGTAGTTATCCTTAAAAAAGCCACAGCATACATCCTGTCCGTCCAA
GCAGAGGAGCAAAAGCTCATTTCTGAAGAGGACTTGTTGCGGAAACGACGAGAACAGTTGAAA
CACAAACTTGAACAGCTACGGAACTCTTGTGCGTAA ...1320

16.6 Human c-Myc proteins sequence:

MPLNVSFTNRNYDLDYDSVQPYFYCDEEENFYQQQQQSELQPPAPSEDIWKKFELLPTPPLSPSRRSGLC
SPSYVAVTPFSLRGDNDGGGGSFSTADQLEMVTELLGGDMVNQSFICDPDDETFIKNIIIQDCMWSGFS
AAAKLVSEKLASYQAARKDSGSPNPARGHSVCSTSSLYLQDLSAAASECIDPSVVFPYPLNDSSSPKSCA
SQDSSAFSPSSDSLLSSTESSPQGSPEPLVLHEETPPTTSSDSEEEQEDEEEIDVVSVEKRQAPGKRSESGSPS
AGGHSKPPHSPLVLKRCHVSTHQHNYAAPPSTRKDYPAAKRVKLDSVRVLRQISNNRKCTSPRSSDTE
ENVKRRTHNVLERQRRNELKRSFFALRDQIPELENNEKAPKVVILKKATAYILSVQAEEQKLISEEDLLR
KRREQLKHKLEQLRNSCA ….439

Appendix II

Appendix II

I. Publications

- Chaman, N., M. A. Iqbal, F. A. Siddiqui, **P. Gopinath** and R. N. Bamezai (2015). "ERK2-Pyruvate Kinase Axis Permits Phorbol 12-Myristate 13-Acetate-induced Megakaryocyte Differentiation in K562 Cells." J Biol Chem **290**(39): 23803-23815. ISSN/ISBN 1083-351X.
- Iqbal, M. A., V. Gupta, **P. Gopinath**, S. Mazurek and R. N. Bamezai (2014). "Pyruvate kinase M2 and cancer: an updated assessment." FEBS Lett **588**(16): 2685-2692. ISSN/ISBN 1873-3468.
- Iqbal, M. A., F. A. Siddiqui, N. Chaman, V. Gupta, B. Kumar, **P. Gopinath** and R. N. Bamezai (2014). "Missense mutations in pyruvate kinase M2 promote cancer metabolism, oxidative endurance, anchorage independence, and tumor growth in a dominant negative manner." J Biol Chem **289**(12): 8098-8105. ISSN/ISBN 1083-351X.
- Iqbal, M. A., F. A. Siddiqui, V. Gupta, S. Chattopadhyay, **P. Gopinath**, B. Kumar, S. Manvati, N. Chaman and R. N. Bamezai (2013). "Insulin enhances metabolic capacities of cancer cells by dual regulation of glycolytic enzyme pyruvate kinase M2." Mol Cancer **12**: 72. ISSN/ISBN 1476-4598.
- Vibhor Gupta, **P. Gopinath**, Mohd Askandar Iqbal, Sybille Mazurek, Kathryn E. Wellen and Rameshwar N. K. Bamezai (2014). "Interplay between epigenetics & cancer metabolism." Curr Pharm Des. **20**(11): 1706-1714. ISSN/ISBN 1873-4286.

- **P. Gopinath**, Mohd Askandar Iqbal et al., Knockdown of PKM isoforms in cancer cells activates AMPK signaling to reprogram energy metabolism by stimulating mitochondrial biogenesis and autophagy for cell survival (Manuscript under Review).

II. Abstracts Published in peer-reviewed international journals

- **Gopinath Prakasam** and Rameshwar N.K. Bamezai, LKB1-AMPK axis regulates the switch of Pyruvate Kinase M isoforms to tolerate nutritional stress. Molecular Cancer Research. DOI: 10.1158/1557-3125.METCA15-B19 Published January 2016.

III. International and National, conference, workshop, and presentation.

- Attended, an international conference "Metabolism and Cancer", an 'American Association for Cancer Research (AACR) Conference event, held at Hyatt Regency, Bellevue Washington, USA in June 2015 and presented a poster on the topic of "LKB1-AMPK axis regulates the switch of Pyruvate Kinase M isoforms to tolerate nutritional stress*".*
- Attended, an international symposium "Frontiers in Metabolism: From Molecular Physiology to systems Medicine", an 'EMBO/EMBL symposia event, held at Heidelberg, Germany in November 2014 and presented a poster on the topic of "*AMPK regulates pyruvate Kinase M gene isoform switching and reverts Warburg effect in cancer cell lines".*
- Attended, 9th National Research Scholar Meet in Life Sciences -2013, held at Advance Centre for Treatment, Research and Education in Cancer, Navi Mumbai on December 2013 and delivered an oral presentation on the topic of "Insulin enhances metabolic capacities of cancer cells by dual regulation of glycolytic enzyme pyruvate kinase M2'.

- Attended, BioCamp 2013 – Novartis Biotechnology Leadership Camp, Hyderabad, India on July 8 -10, 2013.

IV. Awards

- Won a "Best team award" and cash price of Rs. 5000 from BioCamp 2013 – Novartis Biotechnology Leadership Camp, Hyderabad, India on July 8 -10, 2013
- *Awarded Corpus Fund* by Jawaharlal Nehru University, New Delhi, India.
- *Awarded Travel Grant* by Department of Science and Technology (DST), Govt. of India.
- *Awarded Travel Grant* by Indian Council for Medical Research (ICMR), Govt. of India
- *Awarded Travel Grant* by Council for Scientific and Industrial Research (CSIR), Govt. of India
- *Awarded Travel Grant* by Immunology foundation of India (G.P. Talwar Foundation).
- *Awarded travel grant* by organizers of "Frontiers in Metabolism: From Molecular Physiology to systems Medicine", an 'EMBO/EMBL symposia event, held at Heidelberg, Germany in November 2014.

Plagiarism Check